PETROLOGY AND GEOCHEMISTRY
OF ULTRAMAFIC-GABBROIC INTRUSIONS
IN ABITIBI AREA, ONTARIO

PETROLOGY AND GEOCHEMISTRY OF ULTRAMAFIC-GABBROIC INTRUSIONS IN ABITIBI AREA, ONTARIO

By

NEIL DONALD MACRAE, M.Sc.

A thesis

Submitted to the Faculty of Graduate Studies

in Partial Fulfilment of the Requirements

for the Degree

Doctor of Philosophy

McMaster University

September, 1965

DOCTOR OF PHILOSOPHY (1965)
(Geology)

McMaster University
Hamilton, Ontario

TITLE: Petrology and Geochemistry of Ultramafic-Gabbroic Intrusions in the Abitibi Area, Ontario

AUTHOR: Neil Donald MacRae, M.Sc. (McMaster University)

SUPERVISOR: Professor Denis M. Shaw

NUMBER OF PAGES: x, 163

SCOPE AND CONTENTS: A brief review of the general geology of the peridotite belt south of Lake Abitibi is presented. The petrography and geochemistry of each major intrusion is discussed in detail and mineral and element variation diagrams are drawn for a number of cross sections. The degree of differentiation of the initial magmas is discussed and illustrated by comparison with a hypothetical model. On the assumption that all ultramafic-gabbroic intrusions in the area are related, a model for the physical evolution of the assemblage is suggested. The criteria of classification of ultramafic rocks are examined with particular reference to the analysed rocks. In this relationship, a brief statement of the origin of basaltic magmas is presented.

ACKNOWLEDGMENTS

Supervision of the project was provided by Drs. D.M. Shaw and H.P. Schwarcz of the Department of Geology, McMaster University. General discussions with Drs. Ford and Bik of the Department of Geography helped to define many of the problems during progress of the work. Throughout the course of the investigation, I have relied heavily on the critical judgment and advice of T.N. Irvine, Geological Survey of Canada, Ottawa. Initial work on the Centre Hill section was begun under the supervision of Dr. Irvine while he was at McMaster University.

Field work was carried out in the summers of 1963 and 1964 with considerable aid from Canadian Johns-Manville Co. Ltd. Without their generous financial and technical assistance the scope of the investigation would have been seriously curtailed. During the 1964 season, Steve Burnie acted as field assistant and diamond drill assistant; particularly in the latter capacity, his help was invaluable. Stanford Katambala, an undergraduate student at McMaster University, worked as field assistant for the 1963 season, and his generous and capable help were sincerely appreciated. Mr. Katambala's tragic death in the late summer of 1964 was a sad loss to all who knew and worked with him.

Grants from the National Research Council and the Geological Survey of Canada covered the cost of most laboratory research. Thin sections were prepared by H.D. Falkiner, and rapid chemical analyses were done by J.R. Muysson, both of the Department of Geology, McMaster University.

J.G. Payne assisted with spectrographic work; D.W. Otterman contributed by colouring maps; and various members of the graduate class promoted valuable discussion on a number of problems.

ABSTRACT

A number of ultramafic-gabbroic intrusions of variable characteristics constitute the Abitibi Peridotite Belt. A field and laboratory petrographic and geochemical study along complete or partial sections across several of those masses along the southern side of Lake Abitibi demonstrate their degree of differentiation, the relationships between sections, and the mode of emplacement of the bodies. Geochemical data are obtained by both spectrographic analysis of numerous whole-rock samples and rapid silicate analysis of selected samples from the major intrusions.

The intrusions fall into three general types: (1) well-differentiated sills varying from peridotite to quartz-gabbro with cyclic repetition particularly in the ultramafic zone of layer sequences; (2) similarly differentiated bodies but lacking cyclic repetition; (3) isolated wholly ultramafic or wholly gabbroic bodies showing negligible differentiation.

The first type is illustrated by the Munro Lake sill, a 1500 to 3500 foot-wide sheet bent into a west-plunging east-west syncline and exposed in three principal areas over a strike length of approximately 7 miles. The Ghost Range intrusion in the eastern part of the belt best illustrates the second type of body. Intrusions of the third type are spatially distributed close to the Munro Lake sill and commonly overlie it.

The physical model proposed to cover the genesis of all intrusions assumes a common origin and employs a periodically active volcanic system. Cyclic repetition of layer sequences in the Munro Lake sill reflect magma pulses through a main volcanic channelway; wholly gabbroic bodies resulted from solidification of expelled residual liquids into fractures overlying the Munro Lake chamber; wholly ultramafic bodies resulted from intrusion of the crystal mush developed on or above the chamber floor; and plutons of simple ultramafic-gabbroic sequence developed from uninterrupted fractional differentiation of magma in chambers isolated from the main channelways.

Chill phases were examined in several localities, but in only the Garrison sill is the composition of the chill phase roughly equivalent to the calculated composition of the original basaltic liquid. Obvious contamination and destruction of the original chill zones by stoping of the wall rocks are largely responsible for the lack of representative chill phases.

Serpentinization of all the ultramafic rocks has been extensive, and in only rare instances may remnants of fresh minerals be located. Asbestos serpentine of commercial quality is found locally and invariably is associated with talc and magnesium carbonate.

TABLE OF CONTENTS

ILLUSTRATIONS

TABLES

APPENDICES

I. INTRODUCTION

A series of ultramafic-gabbroic intrusions extending in a rough belt approximately 2 to 6 miles wide from near Timmins, Ontario, extends past the south end of Lake Abitibi to the Ontario-Quebec border. This southwesterly trending belt extends approximately 80 miles and has been referred to as the Abitibi Peridotite Belt (Hewitt and Satterly, 1953). In view of the present intensive interest in ultramafic rocks, a detailed petrographic and chemical study of this belt has been undertaken. A 30-mile section at the south end of Lake Abitibi (Fig. 1) was selected for study because exposure was fairly good and base maps were most complete. It is the principal purpose of this thesis to demonstrate the degree of differentiation and mode of emplacement of the ultramafic-gabbroic bodies in this area.

Previous research on various aspects of petrology in the region has been conducted by workers from both industry and academic institutions. Of the latter, two M.Sc. theses by Reeves (1950) and MacRae (1963) along with two Ph.D. theses by Taylor (1955) and Naldrett (1964) are the most significant. Various officers of the Ontario Department of Mines have mapped and described the gross features from many of the intrusions along the belt. Their work forms the basis for succeeding research.

FIGURE 1

Abitibi Peridotite Belt, Matheson Section

Locality abbreviations for Figure 1 and succeeding illustrations:

CH	Centre Hill	GR	Ghost Range
W-M	Warden-Munro	W-MH	west McCool Hill
MH	McCool Hill	Mc	McCool general
GS	Garrison Sill	M	Munro general

Fig. 1.

ABITIBI PERIDOTITE BELT

MATHESON SECTION

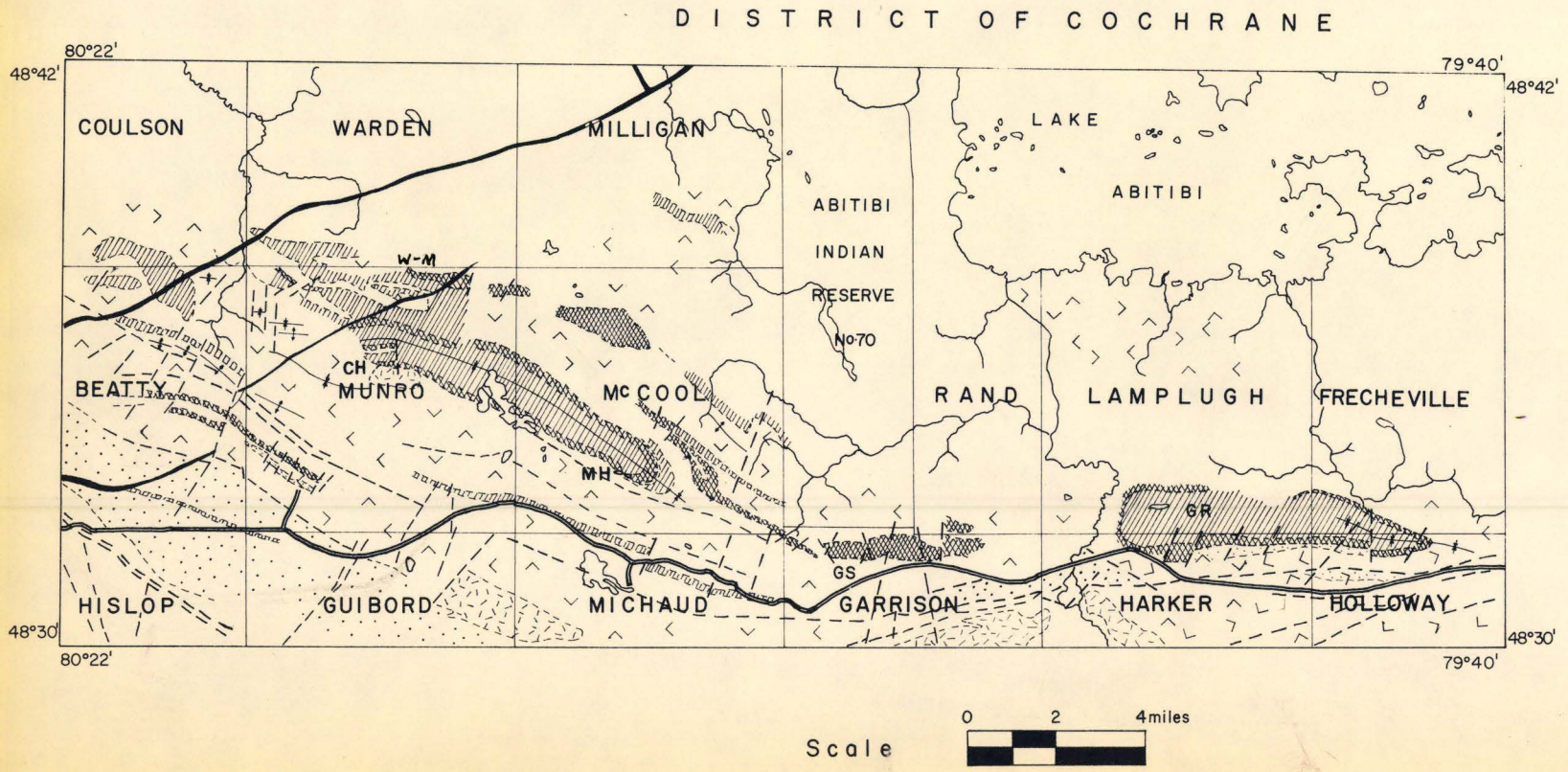

LEGEND

PRECAMBRIAN

Proterozoic

Keweenawan and Matachewan

Diabase

INTRUSIVE CONTACT

Archean

Acid Intrusive Rocks

Granite, syenite, porphyries

Mafic and Ultramafic Intrusive Rocks

Gabbro, diorite, diabase

Pyroxenite, peridotite, dunite

INTRUSIVE CONTACT

Sedimentary Rocks

Conglomerate, greywacke, argillite

UNCONFORMITY

Basic Volcanic Rocks

Andesite, basalt

Acid and Intermediate Volcanic Rocks

Rhyolite, trachyte

SYMBOLS

Synclinal axis

Anticlinal axis

Fault

Note Modified after south-central portion of Ont. Dept. Mines map no. P 140.

II. REGIONAL GEOLOGY

All bedrock in that part of the belt south of Lake Abitibi is Precambrian and locally is overlain by deposits of Pleistocene and Recent sand, gravel, and clay. Extending along the southwestern part of the belt is the Destor-Porcupine fault, between whose branches are sedimentary rock slices of argillite, conglomerate, and tuff. Outside this fault zone sedimentary rocks are scarce. Prest (1951) notes that the extensive volcanic rock sequence lying to the north of the fault zone overlies, in general, the sedimentary rock sequence. Basic volcanic flows and pillowed lavas comprise the major part of the volcanic rocks. At various horizons are conformable thin layers of rhyolitic volcanic rocks and chert which are especially notable because they commonly fringe the ultramafic-gabbroic intrusions. Many of the intrusions are sill-like and it is probable that the acid volcanic rocks and chert afforded horizons of weakness that permitted emplacement of the intrusions. A period of extensive folding and faulting followed solidification of the ultramafic-gabbroic rocks, during which time a number of granitic plutons were intruded. Low grade regional metamorphism and locally extensive hydrothermal alteration accompanied this activity. The youngest rocks are two series of diabase dikes. The older of the two swarms, usually termed the Matachewan diabase, trends roughly north-south; the younger, called the Keweenawan diabase, trends northeast. Fahrig and Wanless (1963) dated these two dike swarms at 2485 and 1230 million years respectively.

While regional metamorphism is typically of the greenschist facies, zones of amphibolite facies about the ultramafic-gabbroic intrusions are common. Along some fault zones, particularly those showing strike-slip movement, the rocks are altered to talc-chlorite and talc-carbonate schists. The ultramafic rocks are extensively serpentinized; as a result, asbestos of commercial grade has been mined at two localities. Uralitization of the pyroxenes and saussuritization of feldspar are also pronounced.

III. GENERAL FEATURES OF THE ULTRAMAFIC-GABBROIC INTRUSIONS

A. STRUCTURE

The ultramafic-gabbroic intrusions are commonly sill-like in form and vary in thickness from 200 feet to approximately 3000 feet. Total lengths are difficult to estimate due to the extensive deformation which affected the area after their solidification. Major faulting and folding have tended to isolate sections of intrusions and an attempt has been made to correlate as many of the exposed segments as possible simply by detailed mapping and sampling of stratigraphic sections across them. Ontario Department of Mines aeromagnetic maps and data made available by the Exploration Division of Canadian Johns-Manville Co. have been of considerable help in this effort (c.f. reports by Satterly et al).

Several of the intrusions show major layering from peridotite through pyroxenite to gabbro. Such phase layering (Hess, 1960) may alternate or repeat several times in a single cross section over one sill. Individual layers commonly have a fairly wide range in thickness. Local irregularities of layering are believed to be due to magmatic currents before solidification had been completed. Some of these structures, such as cross lamination, are of aid in determining tops of the sill. For certain small zones it is reasonable to assume that the order of accumulation of minerals was the same as their order of crystallization, thus the stratigraphic order of appearance of cumulus minerals is a good indicator of tops. In addition, top determinations on the surrounding volcanic rocks are readily available.

B. PETROGRAPHY

Dunite-Peridotite

The major rock types are defined graphically in Appendix 7. In this presentation, the term "peridotite" is used in its broadest sense. In both dunite and peridotite, textural evidence suggests a cumulus origin for olivine and chromite. Following the terminology proposed by Wager et al (1960), a primary crystal phase which grew in and settled from a liquid is a cumulus phase, and those minerals which crystallized between the cumulus crystals in their place of rest are the intercumulus or interstitial phases.

In the field, rocks bearing a high proportion of olivine tend to weather grey to brown and show vague layering. Unfortunately, the degree of serpentinization is very high in the Abitibi peridotite and small shear zones commonly have destroyed much primary texture or even grossly accentuated such features as layering.

In thin section, olivine and chromite are found to be the two common cumulus minerals, with clinopyroxene, orthopyroxene, and plagioclase as interstitial phases.[1] Clinopyroxene, the most important of the intercumulus phases, is present in amounts up to 45 per cent of the total rock. Plagioclase is commonly interstitial to poikilitic clinopyroxene and may constitute up to 25 per cent of the rock. Orthopyroxene, which occurs as large poikilitic grains, was noted from only one locality.

---

1. In most cases, neither fresh plagioclase nor orthopyroxene remain in the rocks, thus their identification is based on the texture and mineralogy of secondary components. The practice of estimating original mineralogy and volume per cent of each phase is maintained throughout this thesis.

Where peridotitic rocks have been extensively altered, poikilitic clinopyroxene grains weather with high relief (Fig. 2) and always appear roughly prismatic. Grains occasionally measure over one inch in diameter, but the average size is approximately one-half inch. No compositional zoning was noted for clinopyroxene grains. The orientation of the grains was not studied, but qualitatively there appears to be no preferential orientation.

Olivine grains show a wide variation in grain size particularly near the base of each layer; away from the base their size becomes slightly larger and more uniform. Some resorption of individual grains commonly shows as general rounding of primary euhedral faces, although there is no noticeable embayment by interstitial material. A reaction between olivine and clinopyroxene is suggested by a significant reduction in the average grain size of olivine within poikilitic clinopyroxene; as opposed to the size of those surrounded by a different matrix material (Fig. 3). No preferential orientation of olivine was noted except along a fairly narrow horizon in one sill. In most cases, olivine grains were too severely altered to determine if zoning were present; no zoning was found in those grains which were relatively unaltered.

Alteration of olivine has taken place in two steps. The first process of serpentinization is widespread and appears to have been an equal volume process since there is little evidence of small-scale structural deformation. Characteristically, much secondary magnetite has been released by this process and appears now as fracture and cleavage-filling material in olivine and intercumulus phases, as rims around the olivine pseudomorphs, or as magnetite "dust" within the olivine pseudo-

morphs. A later alteration of the serpentine to light green amphibole and chlorite is less widespread. Where this latter process is most advanced there is little secondary magnetite, suggesting that part of the iron released during serpentinization has been resorbed in the later process. Plagioclase has been completely altered to medium green, fine-grained aggregates of chlorite and amphibole fibers. The very diffuse contacts between plagioclase and its more mafic neighbours suggests a reaction between the two phases during late-stage metamorphism. Clinopyroxene is the least altered material in the peridotitic rocks. Where general alteration is pronounced, clinopyroxene shows transition to a light green amphibole (Fig. 4). Orthopyroxene, where present, is completely altered to serpentine and chlorite. In some areas talc and magnesite are common secondary minerals. It has been found that where such is the case, ore grade asbestos is more likely to occur than elsewhere. This type of alteration is superimposed on general serpentinization and is distinct from it.

Chromite, as small, single octahedral crystals approximately 0.5 to 1.5 mm in diameter, forms no more than 5 per cent of the rock volume. Small rims of secondary magnetite (Fig. 5) generally make identification of chromite in either hand specimen or thin section difficult, but polished sections clearly reveal the relationship.

Clinopyroxenite

Clinopyroxenite, composed essentially of cumulus clinopyroxene and inter-cumulus plagioclase, commonly occurs in a layer intermediate to peridotite and gabbro. In outcrop these layers weather a dark reddish brown and appear to be homogenous. Igneous lamination (the preferential

Fig. 2. Poikilitic texture of peridotite; Warden-Munro

Fig. 3. Photomicrograph: poikilitic peridotite. Crossed nicols; clinopyroxene-light grey, altered plagioclase-dark. X 45

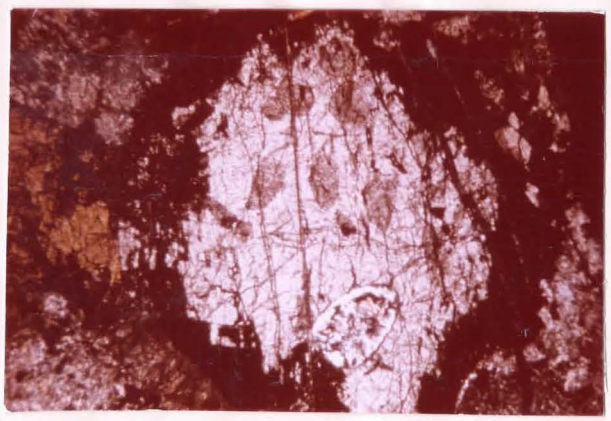

Fig. 4. Photomicrograph: clinopyroxene partially altered to amphibole. Clinopyroxene-light grey, amphibole rim-at extinction. Small included olivine grain (serpentinized). X 45.Peridotite

Fig. 5. Photomicrograph: rims of secondary magnetite on cumulus chromite. Polished section; X.180 ·Peridotite

orientation of platy cumulus crystals) is a common feature of clinopyroxenite. Modal analyses indicate a range of 55 to 97 per cent by volume clinopyroxene with the remainder made up of plagioclase, orthopyroxene, and locally, an oxide phase. A few scattered olivine grains are generally included, particularly near the contacts with peridotite.

It is apparent that the cumulus clinopyroxene grains continued to grow after they settled to the floor of the chamber because the "adcumulus" rims (Wager et al, 1960) on the crystals in some cases are so extensive as to interfere with those of adjacent crystals (Fig. 6). Some compositional zoning was noted on the adcumulus material but none in the cumulus cores. Very narrow essentially continuous lamellae were noted in a number of clinopyroxene grains but their origin could not be satisfactorily determined by optical methods; they may be either exsolution lamellae or simply twin lamellae. Commonly, clinopyroxene grains in the clinopyroxenite samples show simple twinning along the (100) plane.

Olivine is a minor cumulus phase in some clinopyroxenite layers, particularly near the contacts with peridotite layers (Fig. 7). In general, the olivine in these layers is much less altered than that in the peridotitic rocks.

Plagioclase is the most abundant interstitial mineral, occurring in amounts from 5 to 45 per cent. Where the plagioclase content increases above 25 per cent, cumulus laths may be expected and do indeed occur. Plagioclase is generally completely altered to either saussurite or a very fine-grained aggregate of chlorite and amphibole.

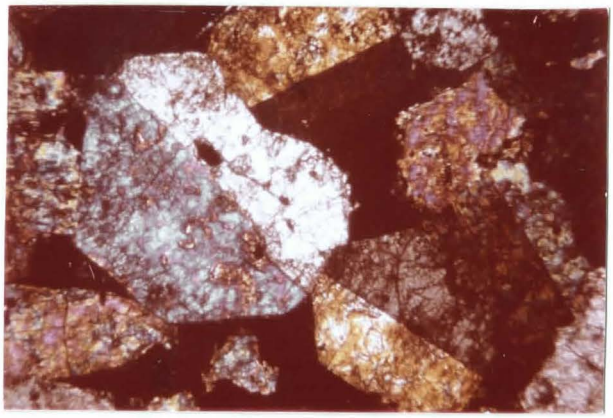

Fig. 6. Photomicrograph: cumulus clinopyroxene grains in clinopyroxenite, showing interference of adcumulus rims. X 45

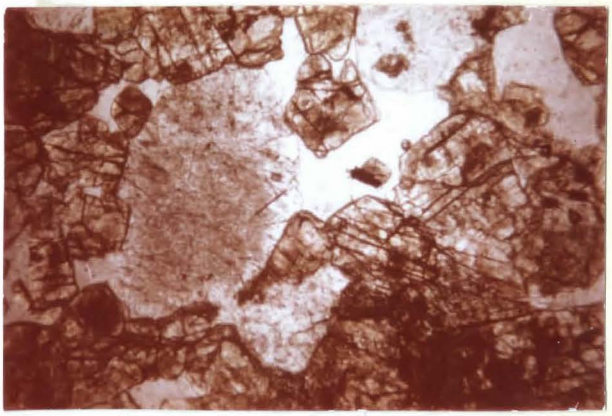

Fig. 7a. Photomicrograph: feldspathic clinopyroxenite, one included serpentinized olivine grain. Plagioclase-white to light grey, olivine-greyish green. Plane light. X 45

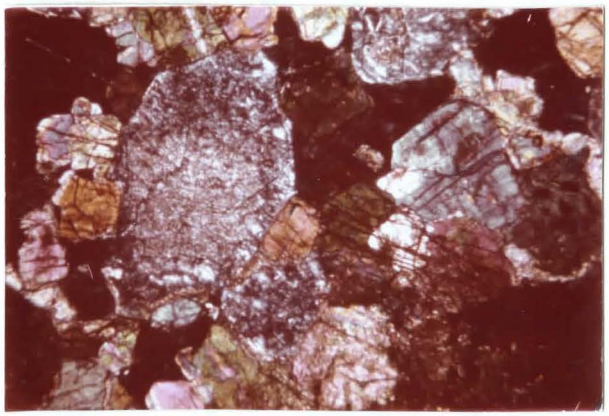

Fig. 7b. Same as 7a but crossed nicols.

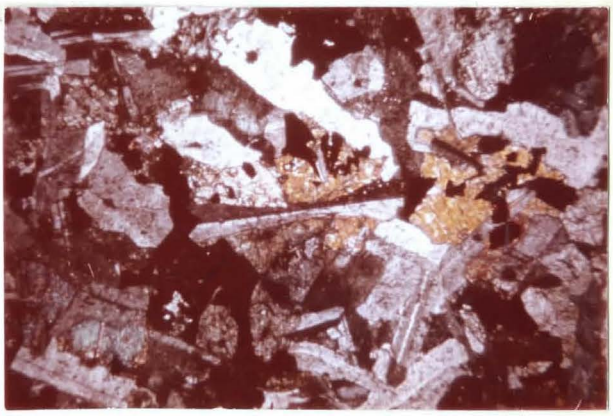

Fig. 8. Photomicrograph: diabasic gabbro, showing rim addition from pore liquid to original plagioclase lath (central "bow-tie" shaped grain). Crossed nicols. X 45

A second interstitial phase is commonly present and is represented now by a distinctive reddish brown chlorite with intermixed amphibole fibers. This material is assumed to be the alteration product of primary orthopyroxene mainly because of its mode of occurrence in the sequence, although no fresh orthopyroxene was noted in any clinopyroxenite sample. Minor amounts of interstitial oxide phases - either magnetite or ilmenomagnetite - have been noted. Locally, the oxide phase has altered to limonite with associated leucoxene.

Gabbroic Rocks

Gabbroic rocks include those rocks in which plagioclase and pyroxene are present in approximately equal amounts, and are the principal phases. Plagioclase is predominantly a euhedral phase with considerable rim addition evident on many laths (Fig. 8). Zoning of plagioclase is not extensive but in some cases the adcumulus growths exhibit fairly good zoning to less calcic borders. Twinning of plagioclase on the albite law is usual and most extensive where the bulk rock composition is quite acidic. In some layers clinopyroxene appears as extensive ophitic grains, and those plagioclase crystals enclosed in clinopyroxene are somewhat smaller than average and more euhedral - suggesting clinopyroxene and plagioclase began crystallizing at approximately the same time in these rocks. Clinopyroxene is chiefly interstitial to plagioclase but in several samples there is evident a cumulus core to the grains. Where quartz is a significant component, the texture is more diabasic; plagioclase laths tend to be more elongate and the interstitial phases are generally strongly ophitic. Micrographic intergrowth of plagioclase

and quartz (granophyric texture) is commonly an interstitial phase of the quartz gabbros. Oxides, commonly magnetite or ilmenomagnetite, occur as both interstitial and primary crystalline phases, but there is generally one particular horizon in each gabbroic zone of the major layered bodies where magnetite in the cumulus phase is fairly abundant. With the exception of the various oxide phases, apatite is the most common accessory mineral.

Scattered rounded areas of chlorite and amphibole with minor serpentine and magnetite are common at certain horizons throughout gabbroic layers. Textural relationships suggest that the centers of these aggregates were a cumulus mineral which reacted upon settling to a second mineral, the rim reaction being almost complete. Regional alteration then was responsible for the destruction of both primary centre and reaction phase and formation of the present secondary assemblage. Analogous phenomena have been described by Naldrett (1964) as representing the reaction between interstitial liquid and cumulus olivine, yielding orthopyroxene rims: this explanation suitably describes the present aggregates.

Rhythmic layering (Hess, 1960) is the variation in proportion of component minerals in adjacent layers; it is commonly developed at various horizons in gabbroic rocks of the major layered intrusions. In the intrusions of the Abitibi area, rhythmic layering is most pronounced near the borders of the gabbroic layers. Here and elsewhere where there has been magmatic disturbance during the formation of a gabbroic layer, igneous lamination of plagioclase laths is also a common feature.

Alteration is generally severe enough to prohibit determination of composition of plagioclase and clinopyroxene. Only in rare instances were reliable data obtained. Saussuritization of plagioclase and uralitization of mafic silicates were the most common alteration processes.

Pegmatitic Schlieren

A number of very coarse grained rocks in lenses and pods, some 2 or 3 feet in width and 10 to 15 feet in length, occur infrequently at various horizons and approximately parallel to the layer contacts in many of the intrusions examined. Invariably, the composition of the pod is slightly less mafic than the host rock, the texture is hypidiomorphic-granular, and grain size is large. These pods represent local segregation, possibly by a mechanism of filter pressing, of pore-space liquid.

Clinopyroxene-Grossularite Xenoliths

At three different localities clinopyroxene-hydrogrossular xenoliths have been identified. In the ultramafic zone of the Warden-Munro section, particularly in layer 5, the xenoliths measure six inches to two feet wide by five feet to more than 50 feet in length; their third dimension is unknown. Contacts are sharp but somewhat uneven, and their orientation is approximately parallel to layer contacts.

Similar xenoliths occur toward the top of the ultramafic zone in the Garrison sill, but here their lengths are apparently little more than 25 to 30 feet while widths range from one to 15 feet. Overburden and post-solidification structural deformation make it difficult to trace their extent.

Approximately 250 feet below the top of the peridotite layer of the Ghost Range body, pyroxene-garnet xenoliths are common. Each xenolith is approximately 5 to 6 feet in width but may be 100 feet or more in length. Several drill holes through this general zone indicate that at least two of the xenoliths do not extend more than 25 feet below the surface. Orientation is approximately parallel to the layer contacts, but deviations of 10 to 20 degrees are not uncommon. The xenoliths have a white weathered surface and show in sharp contrast to the red-brown peridotite. Partial remobilization of the smaller xenoliths is pronounced, as seen in Fig. 9.

In thin section, the xenoliths are composed essentially of medium to coarse grained, anhedral clinopyroxene and hydrogrossular (Fig. 10); clinopyroxene is largely altered to chlorite and amphibole. The form of the hydrogrossular suggests that it is an alteration product of feldspar. Texture and chemistry of the rock are too altered to be of much use in suggesting the composition of the original rock, however. Presumably the xenoliths originated from wall rock loosened by the intruding magma.

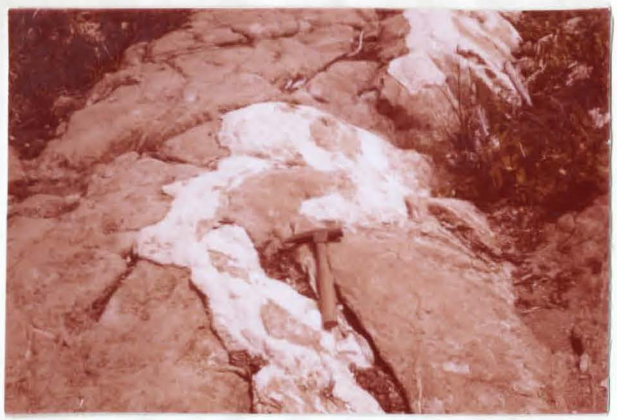

Fig. 9. Clinopyroxene-hydrogrossular xenolith in peridotite. Ghost Range.

Fig. 10. Photomicrograph: clinopyroxene-hydrogrossular assemblage. Hydrogrossular black. Crossed nicols. X 45

Fig. 13. Interbanded normal gabbro (light coloured) and melanogabbro; Centre Hill

Fig. 17. Harrisitic layers in clinopyroxenite; Warden-Munro

IV. DESCRIPTION OF INDIVIDUAL INTRUSIONS

A study of the various outcrop areas suggests that the intrusions are of three basic types. The first, represented by the Munro Lake sill, consists of a relatively large number of conformable phase layers showing cyclic repetition of rock type but also a clear division into ultramafic and gabbroic zones. The second type is best exemplified by the Ghost Range intrusion, which shows a single cycle from peridotitic to gabbroic rocks. Those intrusions which are wholly gabbroic (Perry Lake sill) or wholly ultramafic (western tip of Centre Hill) are grouped together as the third type. It is interesting to note that of this last type, all the ultramafic bodies and most of the gabbroic ones are closely associated spatially with the Munro Lake sill, and, in fact, appear to stratigraphically overlie the sill.

The major intrusions and areas of intrusion are described below.

A. MUNRO LAKE SILL

Three areas of similarly layered gabbroic-ultramafic rock are exposed at Centre Hill in Munro township, along the boundary between Munro and Warden townships, and at McCool Hill in McCool township (Fig. 1). Interpretation of aeromagnetic maps and the general similarity of layering indicate that the three exposures are part of a generally continuous body, here named the Munro Lake sill. The sill is a grossly layered body approximately 7 miles in length and 1500 to 3500 feet in thickness. It is folded into a major east-west syncline with near vertical limbs and is complexly broken by both longitudinal and cross faults.

FIGURE 11

Geological map of Centre Hill area

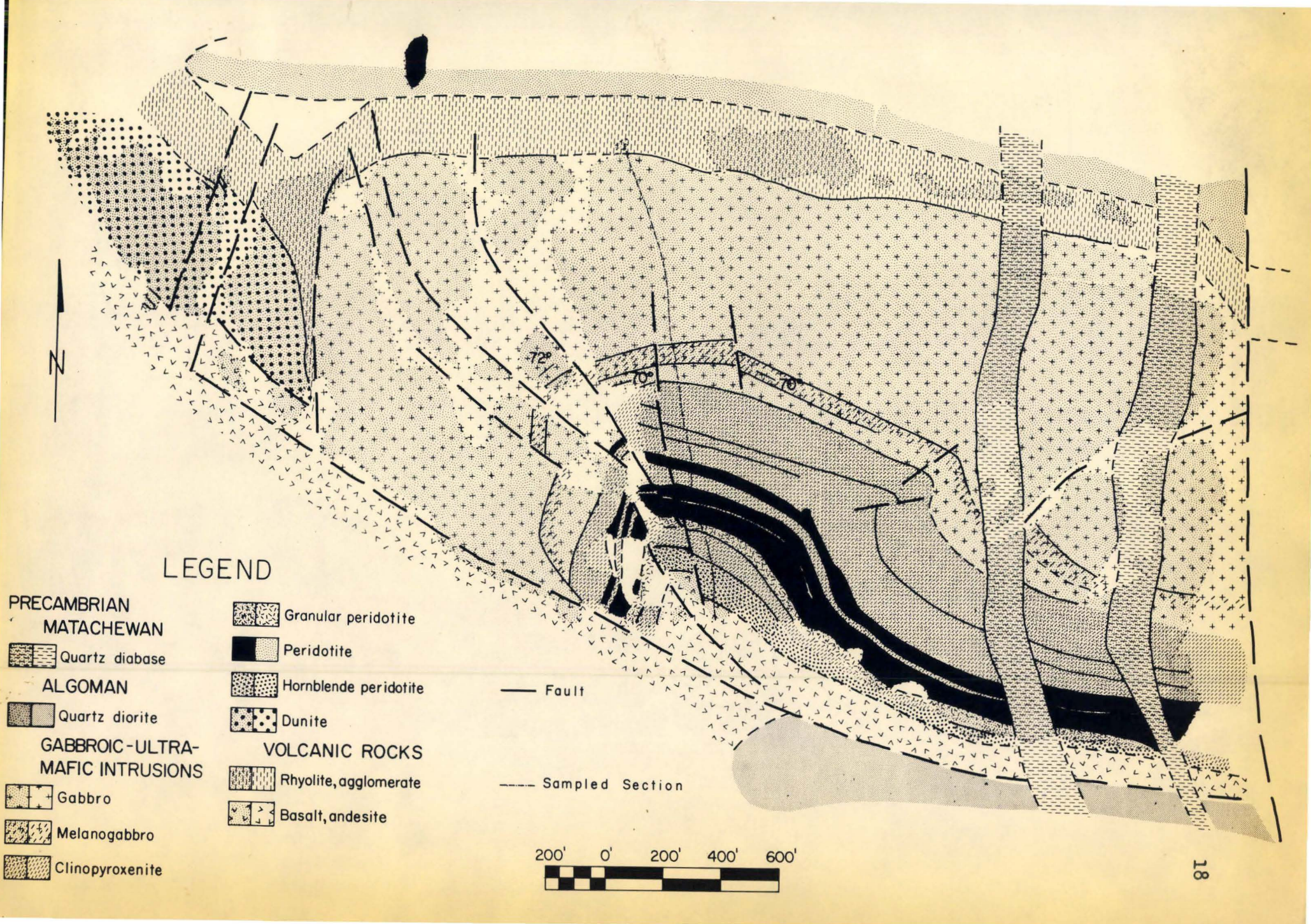
N
72°
70°
70°
LEGEND
PRECAMBRIAN
MATACHEWAN
Quartz diabase
ALGOMAN
Quartz diorite
GABBROIC-ULTRA-
MAFIC INTRUSIONS
Gabbro
Melanogabbro
Clinopyroxenite
Granular peridotite
Peridotite
Hornblende peridotite
Dunite
VOLCANIC ROCKS
Rhyolite, agglomerate
Basalt, andesite
Fault
Sampled Section
200' 0' 200' 400' 600'

For the purpose of correlation from section to section, detailed mapping and sampling were carried out at the three principal localities. Textural, mineralogical, and chemical variations are set out below for each of the three sections.

Centre Hill Section

The detailed petrography and geochemistry of the Centre Hill section have been previously reported (MacRae, 1963), thus only a summary is required here.

Within the exposure area at Centre Hill, the sill is essentially vertical with east-west strike but sharply folded southward at its west end against the Centre Hill fault (Fig. 11). Both northern and southern contacts with volcanic rocks are exposed; the northern rocks are rhyolite agglomerate and the southern, basalt. The contacts are sharp though somewhat uneven and generally show much iron staining. The lower or southern basalts have been metamorphosed to amphibolite immediately adjacent to the sills. Chill phases representative of original liquid are not apparent at the intrusive contacts.

1. Stratigraphy

The outcrop area may be divided into the following units: a lower marginal zone, a layered series, and a western tip of dunite. The western tip of dunite is faulted from the rest of the body and is isolated by a slice of rhyolitic roof rock. It appears to be a fault slice of a peripheral body rather than an integral part of the Munro Lake sill. It will be described in more detail in a later section. Seven cyclic units similar to those established for the Stillwater complex (Jackson, 1963) and the Muskox intrusion (Irvine and Smith, 1965) have been outlined in the Centre

TABLE I. Summary of Petrographic Features of Centre Hill Section

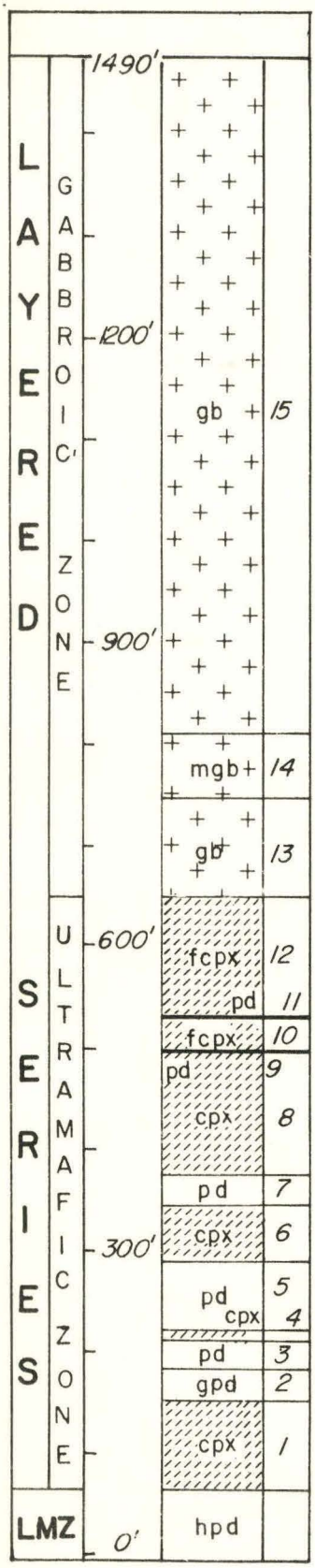

Zone of fine grained gabbro

Minor, poorly developed rhythmic layering

Zone in which interstitial granophyre is particularly abundant

Plagioclase shows prominent igneous lamination. Rhythmic layering well developed
Cumulus magnetite

Igneous lamination less pronounced

Poikilitic texture

Poikilitic texture. Rhythmic layering near base

Poikilitic texture

Granular texture. Rock shows rhythmic layering

Minor cumulus olivine

Fig. 12. Modal Variation Diagram for Centre Hill Section. Rock type abbreviations: pd-peridotite, hpd-hornblende peridotite, gpd-granular peridotite, cpx-clinopyroxenite, fcpx-feldspathic clinopyroxenite, gb-gabbro, mgb-melanogabbro

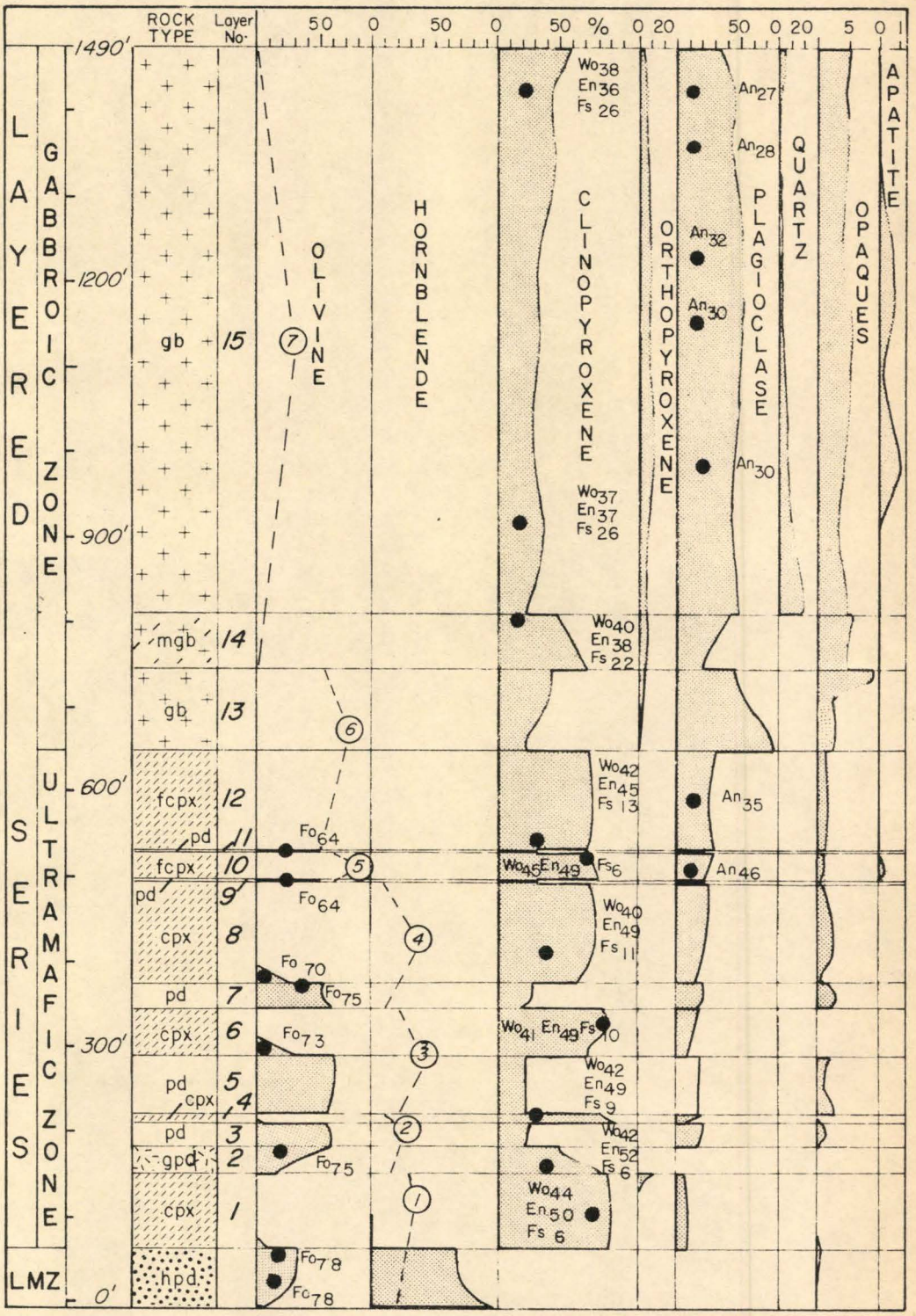

Hill section (Fig. 12). In the ultramafic zone they consist of repetitions of successive phase layers of peridotite and clinopyroxenite, and in the gabbroic zone of melanogabbro and normal gabbro. Marking the top of the sixth cyclic unit and the base of the seventh is a two to three foot zone of narrow interbands of normal gabbro and melanogabbro (Fig. 13).

2. Lower Marginal Zone

The lower marginal zone consists of peridotite, distinguished by red-brown poikilitic plates of hornblende which enclose very small olivine grains. The zone is relatively uniform and free of minor layering.

3. Ultramafic Zone

The ultramafic zone, the lower part of the layered series, is 660 feet wide and consists of an alternation of peridotite and clinopyroxenite with sharply defined boundaries. The clinopyroxenite, which is massive and medium to fine grained, becomes more feldspathic toward the top of the zone. The peridotite typically contains poikilitic plates of clinopyroxene and less abundant interstitial plagioclase. Olivine grains are generally well rounded and commonly serpentinized.

4. Gabbroic Zone

Gabbroic rocks make up the top 830 feet of the layered series. The gabbros show considerable minor layering and subtle mineralogical and chemical variations, the important ones of which are summarized in Table I and Fig. 12.

Warden-Munro Section

The Warden-Munro section of the Munro Lake sill covers a broad area of outcrop along the boundary between Munro and Warden townships (Figs. 1,14).

Due particularly to the relative erosive resistance of a series of north-south diabase dikes which cut the area, outcrop is fairly abundant. Access is provided to the south end of the section by a gravel road which leads to the Potterdoal property. Warden township has never been geologically mapped in detail, but Satterly records in his report of Munro township (1951) a partial section of the Warden-Munro rock sequence. Here he notes the close similarity of lithology to the exposures mapped at Centre Hill. Figure 15 is a composite of Satterly's Munro map and sketches from air photographs of that part of the section included within Warden township. Detail in the following description holds particularly for the narrow section sampled, this section being marked by lines AB, B'C on Fig. 15; the rest of the outcrop area was examined in a more general fashion.

The gabbroic-ultramafic rocks occur as a steeply dipping sill with a general east-west trend. The western end of the exposure shows some intense folding and faulting, and geophysical data indicate that the sill is much narrowed by deformation at this point. The sill is well exposed over a length of 1200 feet and a width of 2500 feet. Determination of top direction from pillows and flow breccias of adjacent volcanic rocks is readily established as being to the south. The northern contact of the sill is not exposed and no drill information is readily available. The southern area, however, is well exposed. Here, gabbroic rocks are in contact with a band of thinly laminated chert. Abundant evidence of magma stoping is apparent at this contact; many tongues of gabbroic material project into the chert and chert blocks of various sizes are scattered within the fine-grained gabbroic border for more than 50 feet. Discontinuous thin bands of chert characterize a zone approximately 750 feet north of

FIGURE 15

Geological map of Warden-Munro area.
Section line indicated by ABB'C

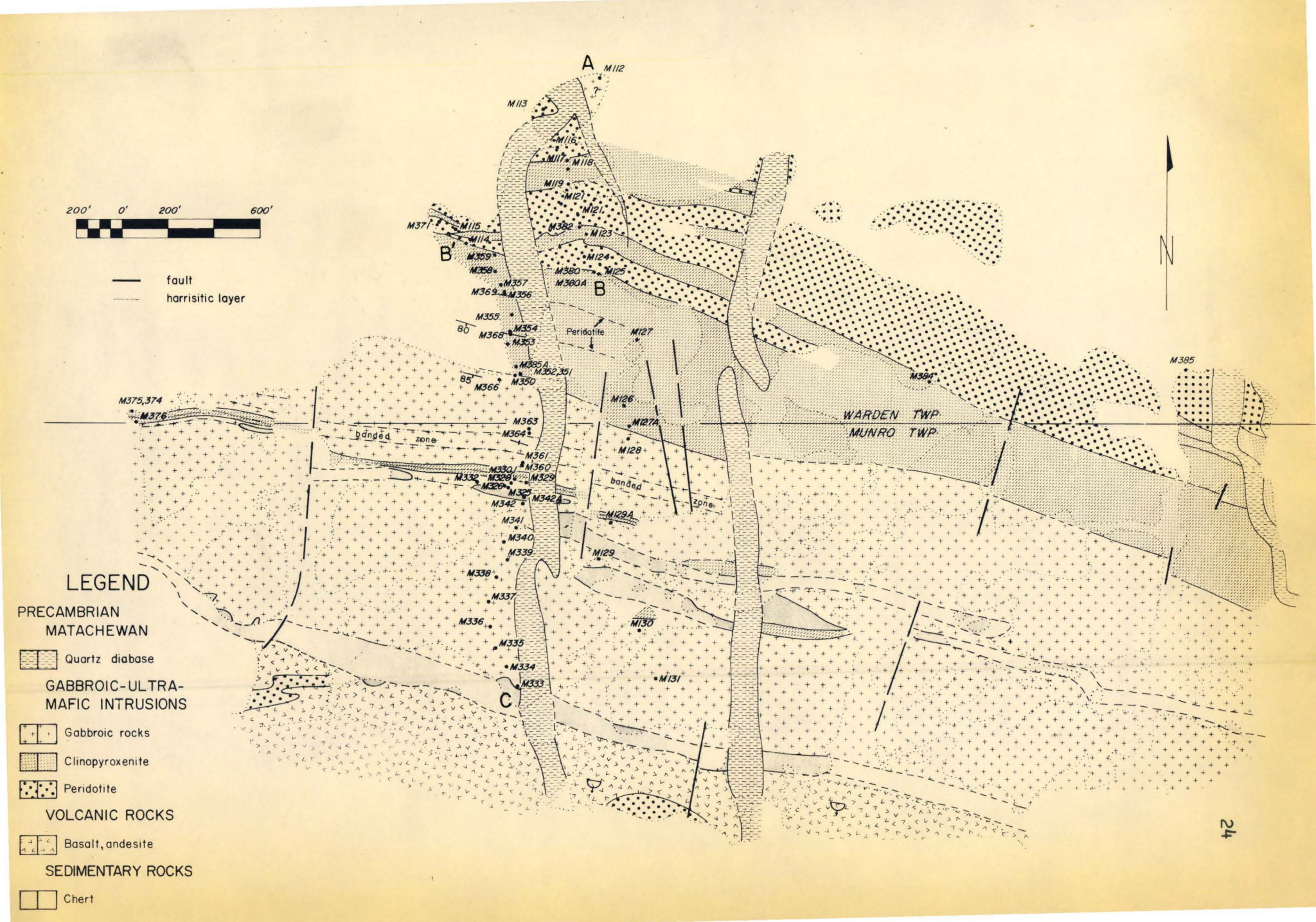
200' 0' 200' 600'
fault
harrisitic layer
A
A'
B
B'
C
C'
N
WARDEN TWP
MUNRO TWP
Peridotite
banded zone
banded zone
M112
M113
M116
M117
M118
M119
M121
M121.
M382
M123
M124
M125
M380
M360A
M127
M126
M127A
M128
M129A
M129
M130
M131
M385
M384
M385A
M352,351
M350
M366
M375,374
M376
M363
M364
M361
M360
M330
M332
M328
M329
M325
M342A
M342
M341
M340
M339
M338
M337
M336
M335
M334
M333
M371
M115
M114
M359
M358
M357
M369
M356
M355
M354
M368
M353
80
85
LEGEND
PRECAMBRIAN
MATACHEWAN
Quartz diabase
GABBROIC-ULTRA-MAFIC INTRUSIONS
Gabbroic rocks
Clinopyroxenite
Peridotite
VOLCANIC ROCKS
Basalt, andesite
SEDIMENTARY ROCKS
Chert
24

the main contact. It is suggested that these are blocks or slabs stoped from the roof during injection of the magma. It is of interest to note that the density of the chert is 2.64 g/cc. If chert blocks sank through the magma, the density of the latter must have been less than that of the chert. In this regard, it is noted that the density of the original magma for the Stillwater complex, by comparison, is estimated at 2.65 g/cc at 1125°C, and its density after separation of the ultramafic rocks at 2.58 g/cc for the same temperature (Hess, 1960).

1. Stratigraphy

Since the lower or northern contact of the Munro Lake sill is not exposed at Warden-Munro, there is no indication of a lower marginal zone as at Centre Hill. The total exposed section belongs to the layered series and may be subdivided into an ultramafic northern zone and a gabbroic southern zone. Table 2 summarizes petrographic features with respect to stratigraphic position in the sampled section and Fig. 16 is a modal variation diagram through the section. The ultramafic zone consists of a series of interbanded peridotite and clinopyroxenite layers with generally sharp contacts. As at Centre Hill, the layers appear as cyclic repetitions. Six such cyclic units are exposed, five of which are in the ultramafic zone. The gabbroic zone, which is in contact with chert on the south, has a very fine-grained upper border for approximately 150 feet north of the contact. Where grain size becomes larger, the texture is seen to be diabasic.

TABLE II. Summary of Petrographic Features of Warden-Munro Section

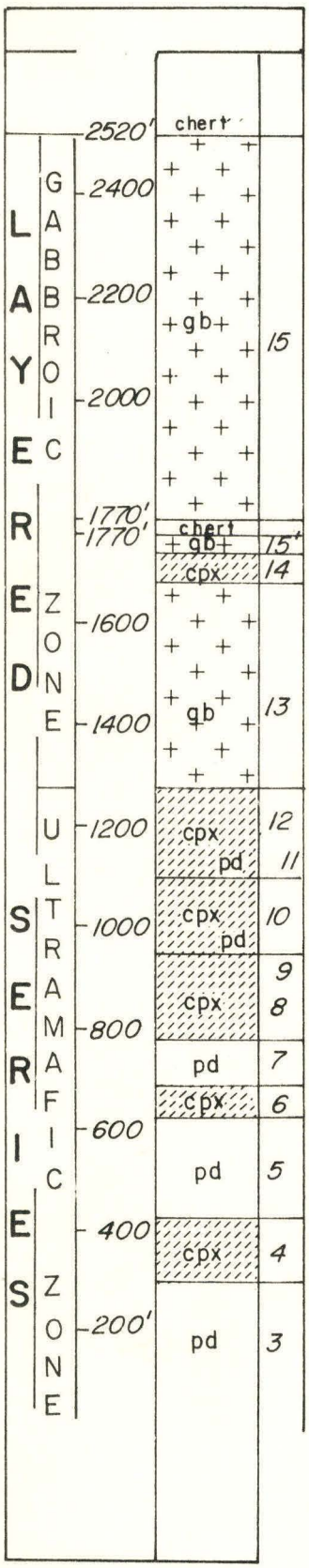

150' chill zone. Numerous chert inclusions for 50'
Chlorite aggregates pseudomorphous after orthopyroxene

Granophyric texture

Chlorite aggregates pseudomorphous after orthopyroxene

Poikilitic quartz grains

8' chill zone

16' chill zone. Numerous small chert inclusions. Small rounded grains pyrite
Granophyric texture. Cumulus magnetite

Zone of harrisitic layering
Vague rhythmic layering
Igneous discontinuity, branching structures on lower side

Banded zone

'Spotted' texture

Local pods of clinopyroxenite

Gabbro blocks surrounded by clinopyroxenite
Feldspathic
Fair igneous lamination

2" peridotite

6" peridotite

6-8" shear zone

Poikilitic texture

Slight igneous lamination
2" shear zone

Poikilitic texture

Scattered olivine grains throughout

30' shear zone

Poikilitic texture

Fig. 16. Modal Variation Diagram for Warden-Munro Section.

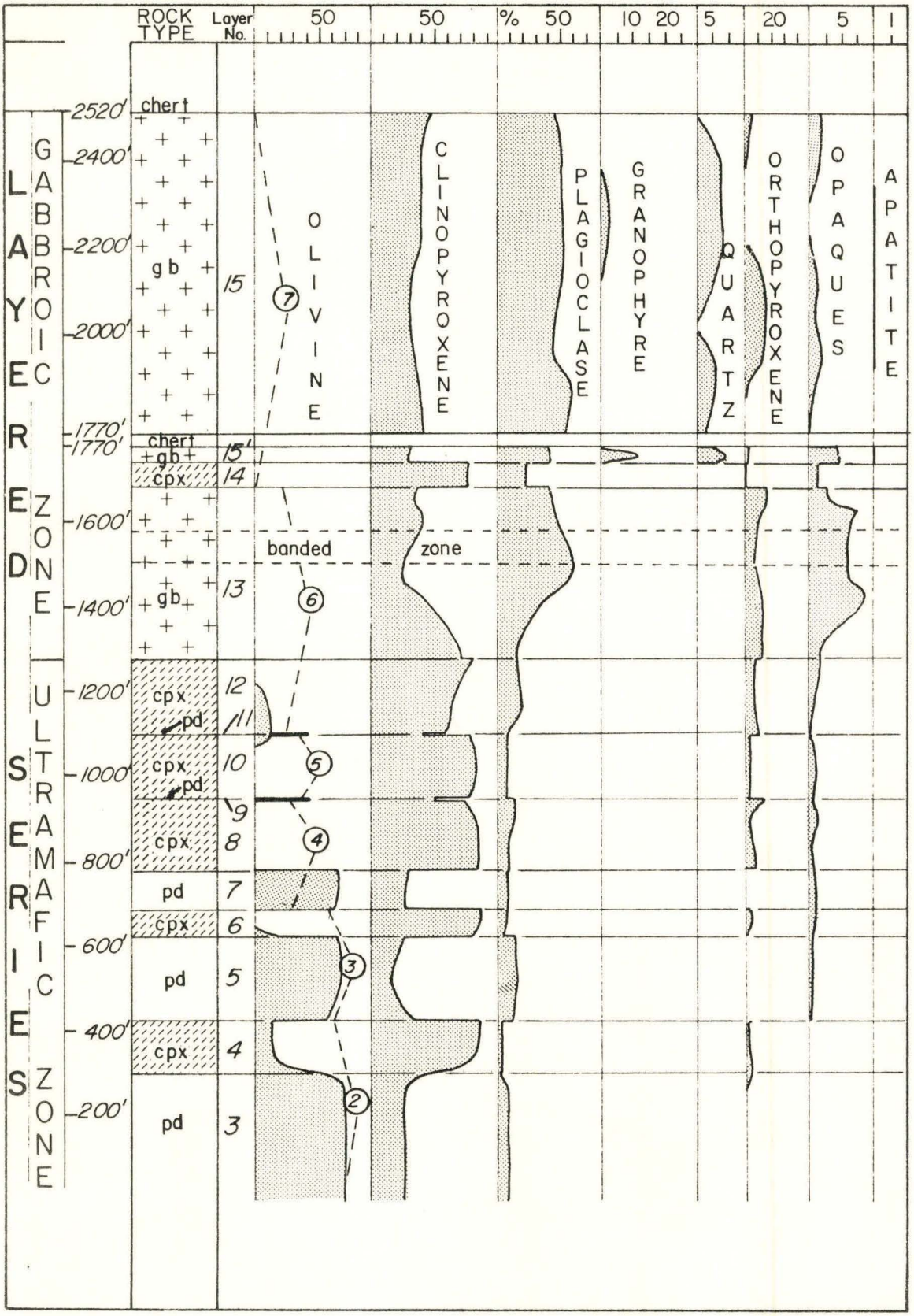

2. Ultramafic Zone

All layers exposed in the ultramafic zone of the layered series are either peridotite or clinopyroxenite. Peridotite layers are composed of cumulus olivine and chromite - the latter in relatively small amounts - with intercumulus plagioclase and poikilitic clinopyroxene. Serpentinization of the peridotite has been severe and no fresh olivine remains for analysis. Plagioclase in the peridotite layers and in the lower clinopyroxenite layers is now altered to dense aggregates of chlorite. Higher in the layered series, plagioclase has been saussuritized such that at no place in the Warden-Munro section can a reliable plagioclase composition be determined by ordinary optical methods. Clinopyroxene is generally not severely altered, and fresh flakes were obtained for composition determinations (Table X) except from the more severely altered peridotites, where clinopyroxene is largely altered to light green amphibole.

The upper portion of the ultramafic zone is made up essentially of clinopyroxenite. Two thin layers of 2 to 6 inches each of peridotite split the clinopyroxenite into three layers of approximately 170 feet each. Several of the peridotite-clinopyroxenite contacts show intense shearing which is probably associated with late-stage deformation. Clinopyroxenite of the ultramafic zone is typically medium to fine-grained, shows fair to poor igneous lamination of the cumulus pyroxene laths, and has plagioclase as the chief intercumulus phase. Particularly near the base of the clinopyroxenite layers, scattered cumulus olivine grains are common, and some olivine composition determinations were possible (Table X).

3. Gabbroic Zone

The gabbroic zone consists of one complete cycle and the top layer of a second (Fig. 16). The uppermost unit is composed of a 65 foot wide layer of feldspathic clinopyroxenite topped by 790 feet of gabbro[1]. Grano-

[1] The gabbroic zone is described from the top down rather than the reverse for convenience of description of certain features.

phyric texture and fairly abundant quartz characterize a zone in the upper one third to one half of the top layer, layer 15 (Fig. 16, Table II). In the lower half of the layer local small to medium sized aggregates of chlorite, assumed to be pseudomorphous after orthopyroxene, increase in amount from nil to approximately 18 per cent and then fall off again to a negligible amount, all over a width of 350 feet. In the same general area but over a wider zone, quartz shows the opposite trend, such that in the centre of the zone quartz is absent but increases to approximately 12 per cent at either end. At the northern end of the top gabbro, quartz grains appear as small to medium sized poikilitic grains.

The base of layer 15 is marked by a narrow horizon along which are numerous thin slabs of chert. The chert slabs have a chill border of melanogabbro approximately 8 feet wide on their upper side and 16 feet wide on their lower side. The 40 foot-wide layer of gabbro north of the chert horizon, layer 15', closely resembles in mineralogy and texture the granophyric zones of the upper gabbro. The outstanding distinguishing feature of this gabbroic rock is the habit of opaque oxides; south of the chert horizon the chief opaque oxide is ilmenomagnetite, which occurs either as an interstitial phase or as cumulus grains with wide adcumulus

rims. In layer 15' the predominant opaque mineral is cumulus magnetite, in amounts up to 5 per cent of the total rock volume. This is the only horizon in the section at which cumulus magnetite has been identified. Within the melanogabbro chill phase and the lower gabbro, scattered poikilitic grains weather in high relief in outcrop. Thin sections of these grains show them to be composed of quartz, magnetite, chlorite, and a little amphibole. This assemblage is taken to represent reaction products of orthopyroxene. At the northern edge of the melanogabbro chill phase rounded globules of pyrite are common over a very narrow horizon.

A 2 to 3 inch gradational contact separates layer 15' from a 65 foot-wide layer of feldspathic clinopyroxenite to the north. The clinopyroxenite layer is made up of approximately 75 per cent cumulus clinopyroxene with interstitial plagioclase and ilmenomagnetite. Particularly toward the top of the layer are scattered poikilitic grains presumably of the same origin as those described as orthopyroxene in layer 15'. Within two to five feet of the lower or northern contact is a zone of harrisitic layering[1] (Fig. 17), in which clinopyroxene crystals have grown to a maximum length of 6 inches. The lower contact of clinopyroxenite with gabbro is very sharp; this contact marks the transition from one cyclic unit to a second.

The first 2 to 3 feet of gabbro in layer 13 show vague rhythmic layering but no igneous lamination. In the same width clinopyroxene grains consist of cumulus cores with heavy adcumulus rims, but lower in the layer clinopyroxene is completely intercumulus and forms medium to large ophitic grains. Plagioclase laths are commonly small to medium with narrow adcumulus rims. Texture in general is diabasic, although not as strongly as in layer 15.

[1] Chemical growth of crystals upward from chamber floor during period of non-deposition of crystals.

Approximately 100 feet north of the top contact of layer 13 is a sharp igneous disconformity (Table II) probably caused by magmatic currents sweeping the chamber floor. For approximately one half inch above this horizon there is excellent igneous lamination of plagioclase laths; below, gabbro appears homogenous with semi-diabasic texture. Spreading northward (downward) from the igneous disconformity are numerous branching structures (Fig. 18) measuring up to 3 feet in width. The pattern is caused by medium to large amphibole crystals which have grown to fill apparent fractures in the lower gabbro. Presumably the fractures developed after at least partial solidification of the gabbro beneath the igneous disconformity but prior to formation of the upper.

From 110 feet to 175 feet north of the clinopyroxenite-gabbro contact and 15 feet north of the igneous disconformity is a zone of interbanded melanogabbro and normal gabbro, henceforth referred to as the "banded zone". Below and above the banded zone contacts between layers show no evidence of disturbance, but within the zone there is much irregularity and cross lamination (Fig. 19,20). It is reasonable to conclude that the disturbance, whether due to local slumping of the body or an earthquake, disrupted the crystal mush on the floor of the chamber by current activity. Immediately prior to the disturbance slight and regular variations of the current in the magma produced vague rhythmic layering, but the effect was much pronounced by the stronger currents. Upon prolonged disruption the rhythmic layers deformed plastically, resulting in some cross lamination - structures somewhat similar to the cross bedding of sedimentary sequences. Analogous features are described by Hess (1960) in the Norite Zone of the Stillwater complex.

Fig. 18. Branching structures below igneous disconformity; Warden-Munro

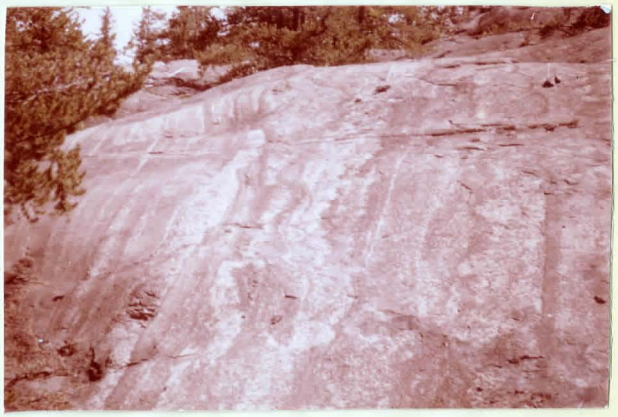

Fig. 19. Banded zone-normal gabbro and melanogabbro; Warden-Munro

Fig. 20. Igneous cross lamination in banded zone; Warden-Munro

Fig. 21. Pod of clinopyroxenite in gabbro; Warden-Munro

Below the banded zone the gabbro has a spotted appearance due largely to local large skeletal opaque oxides, and partly to aggregation of mafic silicates. Particularly from the banded zone northward textures cease to be diabasic and become more granular. The lower 50 to 100 feet of gabbro show some intermixing of clinopyroxenite and gabbro. In the southern part of the zone of intermixing, feldspathic clinopyroxenite occurs in small pods, up to 5 feet in length, containing medium to large clinopyroxene grains (Fig. 21). Textures within the pods are not cumulus; the pyroxene grains are elongate and bear some similarities to those of the harrisitic layers of the upper clinopyroxenite. Texture in the gabbroic rocks surrounding the pods is much distorted, such that there is a strong parallelism of plagioclase to the pod contacts. In the northern part of the zone feldspathic clinopyroxenite appears as the matrix material between large blocks of gabbro. Gabbro blocks measure up to several tens of feet in length and 5 to 10 feet in width. The attitude of igneous lamination of feldspars on adjacent blocks may differ by as much as 10 degrees, indicating that there has been slight tilting of the blocks. The pattern of deformation within this zone suggests that part way through the formation of the gabbroic layer a structural deformation of the chamber caused lower clinopyroxenite - which was, apparently, still not completely solidified - to be squeezed upward into 'fractures' and recrystallized.

The northern extent of gabbro blocks marks the lower limit of the gabbroic zone.

Diorite Dykes

Layer 12 of the Warden-Munro section is cut by several diorite dykes which strike roughly parallel to the layer contacts and dip nearly

vertically. Locally, the dykes cut the plane of igneous lamination by 2 to 5 degrees. The dykes range in width from 1 foot to 5 feet and are continuous along strike for the extent of the outcrop area (Fig. 22), although they commonly are displaced several times by small cross faults.

All dykes show coarse grained borders in which the crystals have a more or less random orientation. Textural features within the dykes apparently depend on width. Narrow dykes, i.e. those under 2½ feet in width, have fairly wide border zones, followed by a much finer grained inner zone (Fig. 23) in which there is a significant parallelism of plagioclase crystals to the strike of the dyke. The wider dykes have a more complex central zoning; inward from the coarse grained border zones are two narrow zones similar to the central region of the narrow dykes. Here, parallelism of plagioclase is well developed. The central-most zone contains medium to coarse grains, again in a more or less random orientation. Mineralogic proportions are constant in all zones except those showing strong plagioclase orientation, where plagioclase is present in greater than average abundance. Mineral proportions on the average are plagioclase 70: clinopyroxene 26: opaques 3: apatite 1.

The zonal arrangement of both types of dykes suggests that they were emplaced as a partly crystalline mush and flow of material was responsible for parallelism of laths near the walls. The country rock, clinopyroxenite, while solid, was still hot when the dykes were emplaced, promoting growth of crystals in the border zones. Presumably the material derived from differentiation of the same magma that gave rise to the layered series.

Fig. 22. Diorite dyke cutting clinopyroxenite; Warden-Munro

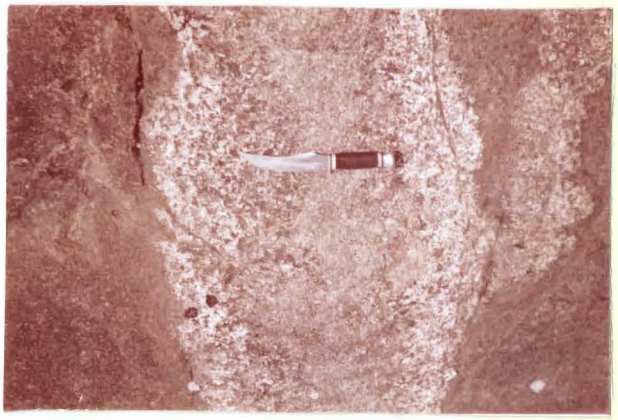

Fig. 23. Coarse grained border zones of diorite dykes.

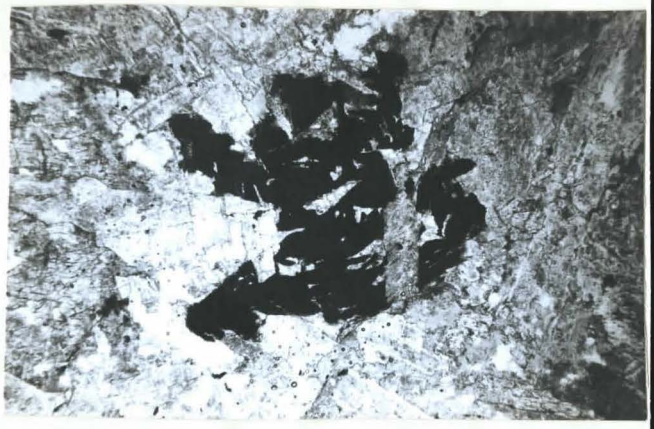

Fig. 26. Photomicrograph: skeletal opaque oxide in gabbro. Plane light. X 45

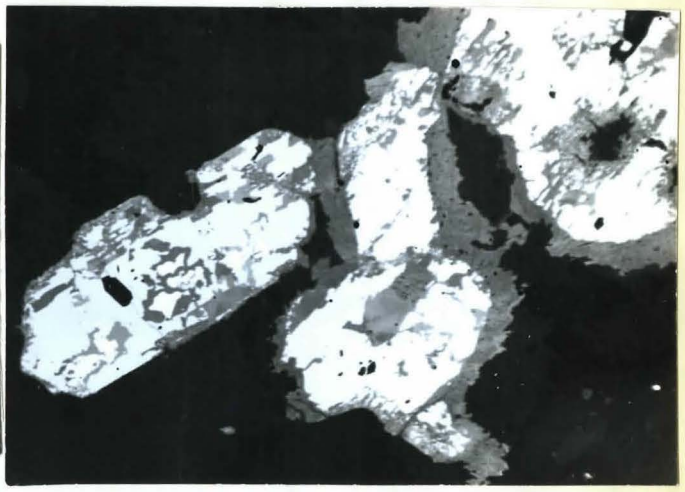

Fig. 27. Photomicrograph: ilmenite-magnetite intergrowth; ilmenite-light grey, magnetite-dark grey, hematite-white. Polished section. Centre Hill. X 180. Gabbro

Comparison of Layers from Centre Hill to Warden-Munro

While all three sections of the Munro Lake sill have gross similarities of petrography and chemistry, only the Warden-Munro and Centre Hill sections are sufficiently well exposed that a detailed comparison is justified. As can be seen in Figure 24, correlation of strata between the two sections is good. Particularly in the ultramafic zone, phase layer thicknesses in the Warden-Munro section are somewhat greater than in the Centre Hill section. This may be a reflection of either the shape of the chamber or the direction of inflow of magma. The banded zone of Warden-Munro is in the middle of layer 13, while at Centre Hill it is at the top of the layer. Layer 14 at Centre Hill is a melanogabbro - essentially a mixture of clinopyroxene and plagioclase both with wide adcumulus rims - but at Warden-Munro the same layer is more properly termed feldspathic clinopyroxenite since plagioclase is largely intercumulus. Within this layer at Warden-Munro harrisitic layering of clinopyroxene occurs; no similar feature appears in layer 14 of the Centre Hill section.

McCool Hill Section

McCool Hill is one of the few areas of high ground in McCool township. The high ground is apparently caused by the relative resistance to erosion of the underlying gabbroic rocks. Exposure is not good on the hill, but sufficient diamond drilling and geophysical work have been done in the past to outline the general geology. The center of the monadnock consists of gabbroic rocks which mark the nose of a west-northwest plunging sycline (Figure 25). Ultramafic rocks have been traced around the eastern side of the hill and along both northern and southern slopes. The syncline, which plunges at approximately 45°,

Fig. 24. Diagrammatic Comparison of Centre Hill and Warden-Munro Strata

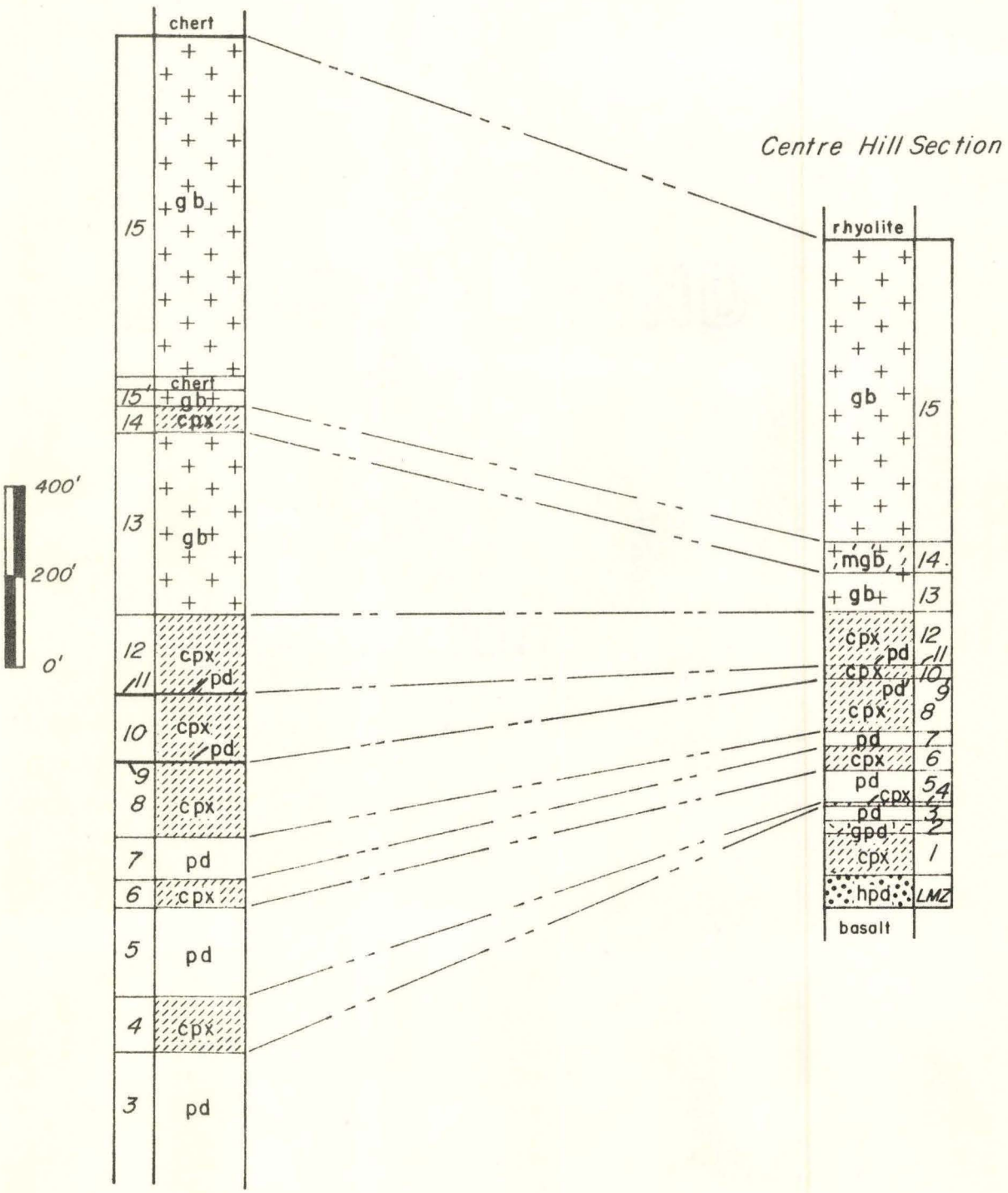

is nearly isoclinal with dips on the northern limb (70-75°) approximately 5 to 10° shallower than those on the southern limb. Total distance across the fold at the west end of McCool Hill from both volcanic-ultramafic rock contacts is one mile. Scattered exposure and geophysical data trace the ultramafic-gabbroic rock series northwest to the McCool-Munro township boundary. The intrusion is generally conformable to the adjacent volcanic rocks and it is mainly from attitudes of the volcanic rocks that the regional structure has been outlined.

1. Stratigraphy

The intrusion can be broadly divided into an ultramafic zone and a gabbroic zone (Table III). The ultramafic zone shows the cyclical units typical of the Centre Hill and Warden-Munro sections. Exposure is not good enough to permit detailed mapping of the cycles or even to determine their exact number, but logs of a few diamond drill holes near the nose of the fold (from the files of Canadian Johns-Manville Co. Ltd.) record at least three repetitions of the peridotite-clinopyroxenite sequence. Where any contacts between layers are exposed, they are generally sharp, show no evidence of chill, and locally may be marked by narrow shear zones. No volcanic rock-intrusion contacts are exposed, thus no statement can be made regarding either the metamorphic condition of the volcanic rocks or textural relations of the intrusion at the contacts. An attempt was made to drill for the basal contact with the aid of a portable diamond drill (see Appendix 5), but a combination of mechanical difficulties and a shortage of time necessitated stopping the hole at 44 feet. The hole was drilled at the north end of Monahan Lake (Figure 25) where base was estimated at 60-70 feet.

Table III. Summary of petrographic features of McCool Hill generalized section

GABBROIC ZONE	Gabbro	1200'+	Upper part of zone not visible Diabasic texture
ULTRAMAFIC ZONE	Clinopyroxenite	400'	Cumulus magnetite Rhythmic layering and igneous lamination of plagioclase General increase in size of cumulus clinopyroxene upward Adcumulus rims on clinopyroxene Vague igneous lamination Scattered aggregates of chlorite+ amphibole
	Peridotite	300'	Poikilitic texture 3-6 inch shear zone
	Clinopyroxenite	50'	Very little interstitial plagioclase Wide adcumulus rims of clinopyroxene Scattered aggregates of chlorite+ amphibole
	Peridotite	200'+	Poikilitic texture Up to 3 per cent chromite
			Lower part of zone not exposed

2. Ultramafic Zone

The ultramafic zone consists of a series of peridotite and clinopyroxenite phase layers. Two cyclic units of the sequence peridotite-clinopyroxenite are exposed. The peridotite is essentially cumulus olivine in small to medium sized grains surrounded by medium to large poikilitic grains of clinopyroxene and interstitial plagioclase. Cumulus chromite is a common accessory mineral. Alteration of olivine and plagioclase has been generally complete - olivine to serpentine, magnetite, and chlorite and plagioclase to chlorite. Clinopyroxene is mildly altered to amphibole.

Clinopyroxenite phase layers are composed of cumulus clinopyroxene grains and lesser amounts of interstitial plagioclase. Scattered olivine grains are fairly common, particularly near the layer contact. Igneous lamination of clinopyroxene laths is evident throughout this rock type. Commonly, clinopyroxene is not severely altered, but alteration of olivine and plagioclase is generally complete.

3. Gabbroic Zone

The upper part of the zone is not visible, and discontinuous exposure of the lower part permits only a general description. The base of the gabbroic zone is marked by a sharp contact with clinopyroxenite. Igneous lamination of plagioclase is pronounced for several feet within the gabbro (Table III) and a zone of rhythmic layering occurs at approximately 50 feet from the base. Cumulus texture rapidly fades out upward to diabasic texture. At several horizons within the diabasic section are scattered lenses of pegmatitic gabbro. Opaque oxides are interstitial ex-

cept at a narrow horizon about 200 feet above the lower contact where magnetite occurs as small euhedral grains. Scattered aggregates of chlorite plus amphibole are taken to be alteration products of orthopyroxene and olivine.

Opaque Oxides and Sulphides in Gabbroic Rocks

Within the gabbroic rocks opaque oxides are important constituents. Early formed gabbros generally contain scattered interstitial opaque oxides in medium sized skeletal forms (Fig. 26). In polished section the grains are found to be irregular aggregates or intergrowths of ilmenite and magnetite (Fig. 27). Minor hematite has been detected in some of the grains. At a higher stratigraphic horizon and over a fairly narrow width, medium to small crystals of cumulus magnetite commonly occur (Fig. 28). In the latest formed gabbroic and granophyric rocks opaque oxides take several forms. Magnetite continued to crystallize as a primary form at first, but the addition of wide rims resulted in irregular shaped grains. Individual small grains of ilmenite also formed (Fig. 29) and may or may not have served as nuclei for additional growth. Finally, apparently wholly interstitial grains of titaniferous magnetite are readily distinguished by their exsolution texture. In the latter grains trellis intergrowths of thin ilmenite lamellae stand out sharply in polished section (Fig. 30).

According to Buddington and Lindsley (1964) it is to be expected that primary ilmenite should crystallize contemporaneously with titaniferous magnetite from most magmas. Also, the development of trellis pattern ilmenite-magnetite is typical of lower temperature crystallization than the

Fig. 28. Photomicrograph: cumulus magnetite in gabbro. Centre Hill. X 45

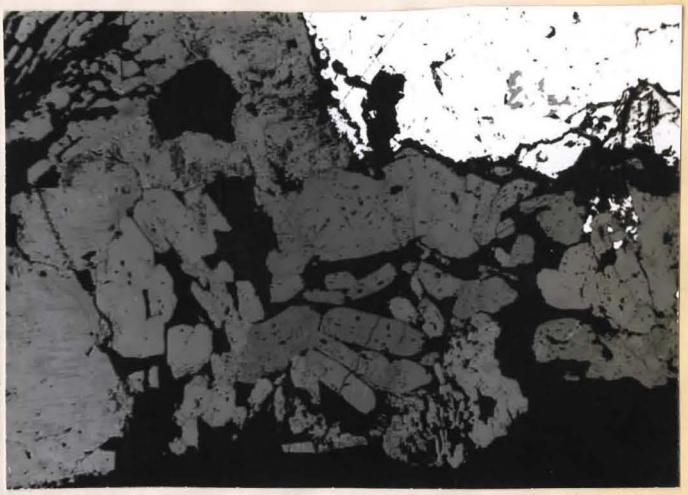

Fig. 29. Photomicrograph: individual ilmenite crystals with grains titaniferous magnetite (lower left corner) and pyrite (upper right corner). Polished section. Centre Hill. X 180 Gabbro

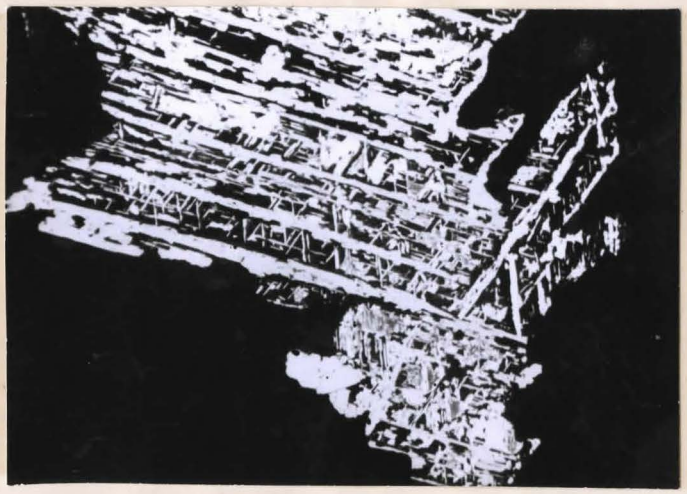

Fig. 30. Photomicrograph: trellis pattern of altered exsolved titaniferous magnetite; ilmenite-white. Polished section. Centre Hill. X 180 Gabbro

Fig. 31. Photomicrograph: intergrowth of pyrite (light grey) and chalcopyrite (medium grey). Polished section. Centre Hill. X 180 Gabbro

development of irregular intergrowths or aggregates. Buddington and Lindsley further state that there is only negligible solubility of ilmenite in magnetite, and the primary crystallized grains were solid solutions of magnetite and ulvospinel which 'exsolved' to ilmenite and magnetite upon lower temperature and oxidation.

Sulphides are uncommon in any of the rock types, but sporadic occurrences were noted in gabbroic rocks in particular. Some correlation of the occurrences with stratigraphy were noted at Centre Hill and again at Warden-Munro. At both locations sulphide grains are somewhat concentrated near the base of the gabbroic rocks along a narrow horizon where normal gabbro and melanogabbro are interbanded. A second horizon of sulphide occurrence at Warden-Munro is within the lower granophyric gabbro in its chill phase against chert blocks. Pyrite and chalcopyrite are the most common sulphides, however pyrrhotite aggregates have been observed in some gabbroic rocks. Chalcopyrite appears as small anhedral grains, usually intimately associated with pyrite (Fig. 31). It is doubtful that any of the texture represent exsolution, however, since in this event pyrite could not be a primary phase but a low temperature reaction from pyrrhotite. The pyrite grains commonly have one or two faces of cubic cleavage, thus are assumed to be primary and not reaction phases. During crystallization of the gabbroic rocks great differences in temperature are not to be expected and, in fact, are not indicated by mineralogic or chemical data. It is difficult, therefore, to understand why pyrite and chalcopyrite would form in one gabbroic rock while in an apparently identical rock the sulphides are pyrrhotite and chalcopyrite.

A similar problem was noted by Wager, Vincent and Smales (1957) for the upper granophyric zone of the Skaergaard intrusion, but a satisfactory answer is not yet available.

B. GHOST RANGE INTRUSION

The Ghost Range body is an ultramafic-gabbroic intrusion at the far east end of the area outlined in Fig. 1. It stretches east-west along a 7 mile by 1 mile ridge as an apparently doubly plunging synclinal trough. Attitudes both outside the intrusion on conformable volcanic rocks and on internal contacts indicate very steep dips on the southern limb. Although topography is high relative to the surrounding area, soil cover is extensive and rock exposure is poor to fair. Much of the structure of the intrusion has been outlined by interpretation of aeromagnetic maps. The area of outcrop includes part of Harker, Holloway, Lamplugh, and Frecheville townships, of which only the former two have been mapped in detail (Satterly, 1951; 1953). Fig. 32 is a compilation of Satterly's mapping, my own reconnaissance of the area, and data made available by the exploration division of Canadian Johns-Manville Co. Ltd. Reeves (1950) did some preliminary research on the southern half of the Ghost Range, but later information obtained by various exploration companies necessitates revision of his conclusions.

The southern contact with acidic volcanic rocks, although not exposed, can be defined approximately between outcrops of volcanic and intrusive rock as little as 150 feet apart. The volcanic rocks show very little evidence of alteration or deformation by the intrusive rock. Exposure on the northern limb is practically non-existent, the only un-

covered contact zone being at Lightning Mountain where the country rock is basalt flow breccia. Here, the intrusive rock is intensely sheared over a width of 10 to 15 feet.

Within the centre of the syncline a few outcrops of rhyolitic rocks are found near the east end of the body, but there is too little outcrop to yield any information about the condition of the top contact.

Stratigraphy

Gabbroic rocks occupy the centre of the trough and ultramafic rocks the periphery. No cyclical layering as within the Munro Lake sill is evident, rather a simple sequence from peridotite to gabbroic rocks exists. Since outcrop per cent is not particularly good, an attempt has been made to group all the mapped partial sections into one generalized cross section of the body. A number of common petrographic features were noted to recur along strike at specific horizons and these were used to position the various partial sections. The generalized section, with only approximate layer thicknesses, is illustrated in Fig. 33 and the petrographic features are summarized in Table IV.

Ultramafic Zone

Exposure is generally poor in the peridotite layers but much overburden has been stripped off small sections on the southwest end to permit detailed mapping of asbestos showings. In outcrop, the peridotitic rocks appear reddish brown. One quarter to half inch diameter orthopyroxene grains, now completely altered to serpentine and chlorite, give the weathered surface a stucco-like appearance. The average orthopyroxene content is estimated to have been 25 per cent. In thin section, altered

Fig. 33. Modal Variation Diagram for Generalized Section of Ghost Range Intrusion

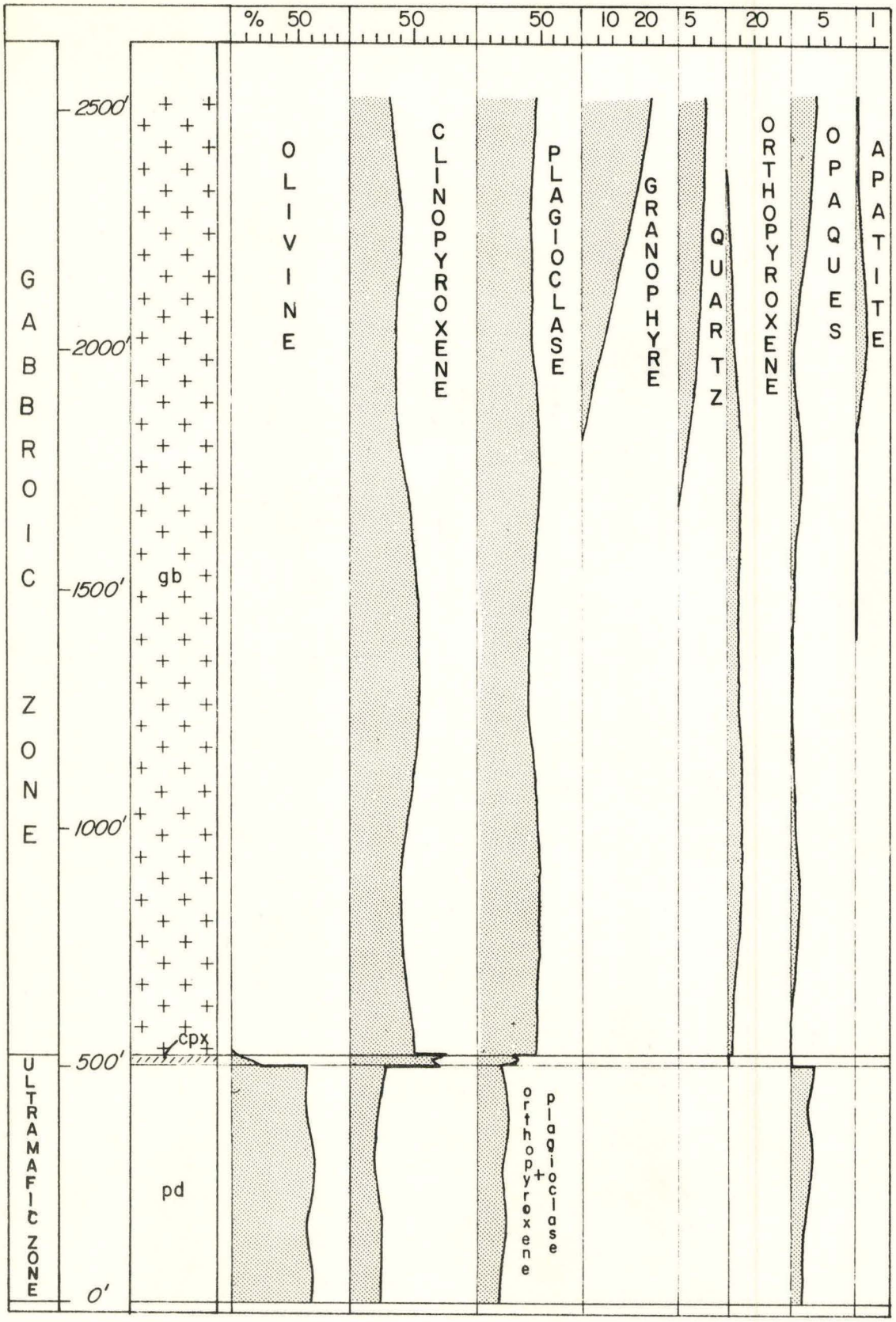

TABLE IV. Summary of Petrographic Feature of Ghost Range Intrusion

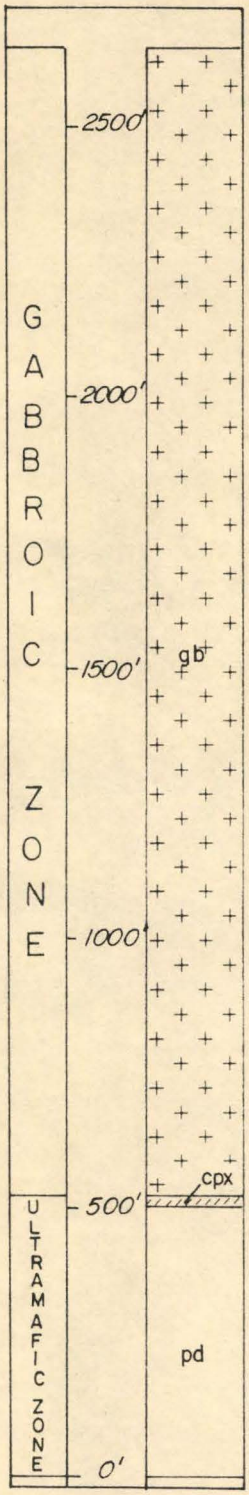

Granophyric texture

Diabasic texture

Cumulus magnetite

Orthopyroxene altered to chlorite

Igneous lamination of plagioclase laths

Scattered cumulus olivine. No igneous lamination

Clinopyroxene - hydrogrossular xenoliths

Poikilitic clinopyroxene. Estimated 25% of matrix is orthopyroxene but not distinguishable from altered plagioclase in thin section

ophitic orthopyroxene cannot be distinguished from altered interstitial plagioclase. Both original phases have altered to very fine grained nearly isotropic material - serpentine and chlorite from orthopyroxene and chlorite from plagioclase. The intercumulus phase is approximately divided between isotropic material and medium to large poikilitic grains of clinopyroxene. Rounded olivine grains show a significant increase in size sorting upward through the layer as well as a slight increase in average grain size. Euhedral chromite is common in small amounts throughout the layer.

Intermediate to the gabbroic and peridotitic rocks is a 5 to 20 foot layer of clinopyroxenite. The upper contact with gabbroic rocks is sharp and there is no evidence of chilling. Scattered cumulus olivine grains are common throughout the layer. Plagioclase is the only major interstitial phase. Locally, particularly where very thin, the clinopyroxenite layer is highly feldspathic and may readily be mistaken in outcrop for melanogabbro. The lower contact with peridotite locally shows intense shearing over 1 or 2 feet.

Gabbroic Zone

A granophyric intergrowth of plagioclase and quartz is an abundant interstitial material of the gabbroic rocks in the centre of the syncline - the uppermost exposed rocks. Discrete grains of quartz are also present up to 13 per cent. Toward the base of the granophyric zone rounded magnetite occurs along a narrow horizon (Table IV). Below this horizon opaque oxides appear as an interstitial phase; above it, the cores of grains may be primary crystals, but there is much rim addition. Scattered chlorite

plus amphibole aggregates which are common in the lower half of the exposed gabbroic zone are assumed to represent alteration of orthopyroxene and olivine. Igneous lamination of feldspar is well developed near the base of the gabbroic zone.

C. GARRISON SILL

Southeast of McCool township, in the northwest portion of Garrison township, is a band of ultramafic-gabbroic rocks known as the Garrison sill (Figs. 1, 34 . The body is an apparently conformable intrusion trending east-west and exposed along a 1½ mile-long ridge. Dips are approximately 60-75° northwest. Total exposed apparent thickness of the intrusion is 800 feet, but from extensive geophysical exploration and diamond drilling the total apparent width is estimated to be 2500 feet. The northern contact rocks are andesite and basaltic pillowed lavas; tops on the latter are indicated to be northward. Metamorphism of the country rocks to the north has transformed them to amphibolite. Gabbroic rocks, which are on the northern side of the intrusion, have a chill phase of at least 10 feet. The composition of this chill zone (see Table XVI) is more acidic than the composition that would be obtained by weighting average peridotite, clinopyroxenite, and gabbro analyses by their respective thicknesses in the section and combining the results. It is possible that the exposed and examined area represents a side section of the original chamber at which the slope of the roof is such as to cut out most of the gabbroic zone.

Stratigraphy

As at the Ghost Range, the Garrison sill appears to be a simple sequence from dunitic or peridotitic to gabbroic rocks with no cyclic repetitions. Since only a small portion of the ultramafic zone is exposed, however, it is possible that cyclic repetitions of ultramafic rocks may occur. Only very detailed sampling and analysis of drill core could solve the problem, and such detail was not attempted for the present study. Table V gives a summary of petrographic features.

Ultramafic Zone

Cumulus olivine, poikilitic clinopyroxene, and interstitial plagioclase and orthopyroxene are the chief mineral phases of peridotite in the Garrison sill. The top 5 to 10 feet of peridotite commonly show preferential orientation of olivine parallel to the contact (Fig. 35). Some of the alignment is due to secondary shearing, as outlined by magnetite-filled fractures in the grains. However, since the preferential orientation persists even where shearing is a minimum, primary magmatic currents are held partly responsible. There is a noticeable increase in total volume per cent of olivine away from the upper contact such that the southernmost peridotite contains only 20 per cent interstitial material.

All rocks are very severely altered throughout the exposed part of the sill, but particularly at the western end. Talc, magnesium carbonate, and serpentine are common secondary minerals. Canadian Johns-Manville Co. Ltd. are exploring the possibilities of commercial grade asbestos in the altered peridotite and have recently done considerable diamond drilling and mapping. The type of alteration is similar to that des-

Table V. Summary of petrographic feature of Garrison sill

GABBROIC ZONE	Gabbro	approx. 300'	Top contact with intermediate volcanic rocks. Chill phase approx. 10 feet wide. 5-6% quartz Texture diabasic throughout Scattered pods clinopyroxenite near base - local garnetiferous rocks -
ULTRAMAFIC ZONE	Clinopyroxenite Peridotite	approx.10' approx. 2200'	Fine to medium grained Upper shear zone less than 1 foot wide Strong preferential orientation of olivine Increase downward in olivine/matrix ratio (Lower part of zone not visible)

cribed by Satterly (1950) and others at the Munro Mine on the Barton Creek sill.

At its widest point the clinopyroxenite layer which separates gabbroic from peridotitic rocks is 50 feet but it averages about 10 feet in width. Cumulus clinopyroxene grains are fine to medium in size; along scattered discontinuous horizons, grain size is very coarse. Plagioclase is the only major intercumulus mineral. On its lower side, the clinopyroxenite layer is in contact with peridotite across a 2-3 inch shear zone.

Gabbroic Zone

The gabbroic layer has a generally diabasic texture with no indication of cumulus features. Quartz content increases up to 5-6% in the centre of the layer but no granophyric intergrowths of quartz and plagioclase have developed. Scattered small to medium sized aggregates of chlorite plus amphibole are taken to be alteration products of orthopyroxene. Cumulus magnetite was not observed in the gabbroic rocks, all opaque minerals appearing as interstitial phases. Toward the base of the layer there is some intermixing of melanogabbro with normal gabbro; melanogabbro appears as small pods or lenses roughly elongate to the contact. They may be rounded blocks of a gradational gabbro phase which was broken by some slight tectonic or magmatic activity in the early stages of gabbro formation.

D. BARTON CREEK SILL

The Barton Creek sill (sometimes called the Munro Mine sill) is an ultramafic-gabbroic body extending from east-central Beatty township to

southwestern Munro township (Fig. 1). This sill is of particular interest because of numerous occurrences of asbestos fibre in the ultramafic portion. Canadian Johns-Manville operated the Munro Mine on a body of asbestos near the southeast end of the sill from 1950-1964. Hendry (1951) describes the sill as follows:

" From an economic standpoint, the most important rock type occuring on the Johns-Manville property is a differentiated basic to ultrabasic sill-like body which has been outlined and traced for a total distance of three and one-half miles ... It has an average strike of N65°-70°W, though deviations from this are caused by cross faults. The sill varies in width from 900 feet on the east end to upwards of 1000 feet in the vicinity of the Beatty-Munro township boundary. Diamond-drilling information indicates that it has a vertical attitude or dips steeply south.

On the north and south the sill is in contact with medium to basic volcanic rocks, classified as dacite and andesite. The volcanic-ultrabasic contact is sharply defined on the south side, as may be seen both in outcrop and in drill cores; no information is available on the north contact. The volcanic rocks at and near the contact show no marked alteration.

In detail, and from north to south, the sill is comprised of a gabbroic phase for a width of approximately 350 feet ... Southward, the gabbro grades quite sharply into coarse grained pyroxenite, a massive green rock, composed almost entirely of pyroxene, with crystals up to half an inch in size. The pyroxenite, in turn, is in contact with the main ultrabasic zone, namely dunite and peridotite, now almost completely serpentinized. The contact is sharply defined ... and there is no evidence to suggest that either type is intrusive into the other. It is concluded that both are differentiates of a common magma. "

E. PERRY LAKE SILL

The Perry Lake sill has been traced for a total length of 8 miles, from the southeast corner of Munro township, along the top end of Perry Lake in Michaud township, to just east of the Michaud-Garrison township boundary (Fig. 1). Average sill width is 900 feet. Exposure is very poor and no contacts crop out. From adjacent outcrops of volcanic rock, tops are indicated to the north for the length of the sill. Composi-

tionally, the sill is wholly gabbroic, and mineralogy and texture closely resemble the upper gabbroic zones of the previously described layered bodies. The central portion of the sill consists of medium grained diabasic orthopyroxene gabbro across a width of 400 feet. Orthopyroxene has completely altered to aggregates of chlorite. Toward both contacts, quartz is slightly more abundant, and general grain size is smaller.

F. ISOLATED INTRUSIONS

Between Centre Hill and Warden-Munro sections of the Munro Lake sill in Munro township are numerous ultramafic and gabbroic rock exposures (Fig. 14). From top determinations on interbanded basaltic and andesitic rock layers, a major southeast trending synclinal axis is indicated to cut approximately through the centre of the area. None of the intrusions which were examined in this area show a complete sequence from peridotite to clinopyroxenite to gabbro as illustrated by the Munro Lake body or the simply differentiated intrusions. Instead, several show a partial sequence from clinopyroxenite or melanogabbro to gabbro, but most are either wholly gabbroic or wholly ultramafic.

Gabbroic sections appear very similar in mineralogy and texture to the upper gabbroic layer of the Munro Lake sill or simply differentiated bodies. Quartz and granophyric intergrowth of plagioclase and quartz are common matrix phases.

Examination of a chill phase on a wholly ultramafic body near the Potterdoal property (Fig. 14; Samples M-104, 105) shows very small, partially resorbed olivine grains in an aphanitic matrix. The matrix has scattered elongate blades of amphibole through it (Fig. 36). Late altera-

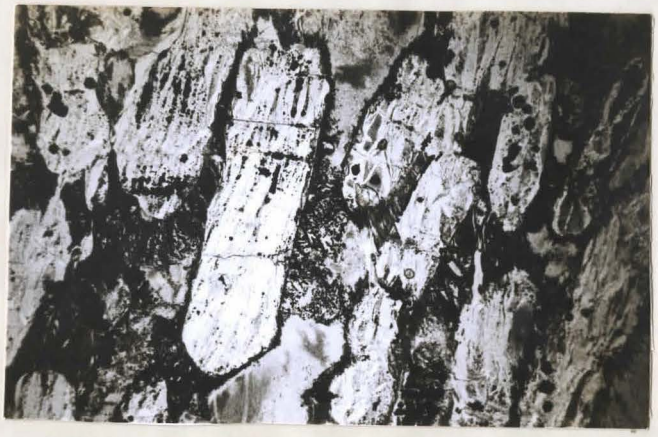

Fig. 35. Photomicrograph: aligned olivine grains in upper peridotite of Garrison sill. X 45

Fig. 36. Photomicrograph: olivine crystals and amphibole needles in altered chill phase of peridotite-dunite body. X 45

Fig. 37. Narrow chromitite band in dunite; Centre Hill

Fig. 38. Partially serpentinized dunite. Reddish-brown areas contain unaltered olivine; Centre Hill

tion of the rock has resulted in the development of much chlorite and serpentine.

North of Centre Hill there are some evidences of multiple intrusion. A 15 to 25 foot wide dyke of peridotite and clinopyroxenite cuts gabbroic rocks at the location of sample M-72, Fig. 15. Peridotite-clinopyroxenite units within the dyke indicate differentiation top to the north. Approximately 600 feet northwest of this location is an outcrop showing dunite inclusions within dunite (samples M-94, 95). The angular inclusions are reddish brown on weathered surface and have numerous asbestos veinlets. The host dunite is grey weathering and rarely contains asbestos. All primary mineralogy and texture have been destroyed in both rocks.

At the western end of Centre Hill is a small body of dunite which apparently is a fault slice of a wholly ultramafic intrusion. A suggestion of internal zoning is evident along the ultramafic-rhyolite contact, where a 5-10 foot wide zone of peridotite is intermediate to the outer contact and the main dunite mass. Brecciation due to late fault movement has destroyed nearly all primary features except a 1½ to 2 inch wide chromitite band which can be followed along strike for only 10 to 15 feet (Fig. 37). Serpentinization has generally followed the fracture pattern such that blocks between fractures commonly contain remnants of fresh olivine, while the material toward the fractures is a mass of secondary minerals (Fig. 38).

In the Ransom Lake area of McCool township (Fig. 25) a large body of peridotite with peripheral gabbro has been outlined by geophysical methods and diamond drilling. Peridotite does not crop out and only two or three gabbroic rocks are exposed. Top determinations on pillow lavas to

the south of the body indicate tops south; no pillow or flow top lavas crop out to the north or east. From the sparse amount of data available, the ultramafic-gabbroic body appears to be situated in the nose of a southwest plunging anticline. Drill cores were not available for study thus little is known of mineralogical or textural features.

Northeast of McCool Hill several zones of ultramafic-gabbroic rocks have been outlined mainly by diamond drilling and geophysical methods. None of the bodies is exposed except toward the eastern boundary of McCool township. Separating the two general areas of intrusion is a 400 to 500 foot belt of andesitic and volcanic rocks. Top determinations on pillows and flows within this belt indicate a major anticlinal axis trending southeast across the middle of the belt. The intrusions on both limbs of the anticline have ultramafic portions relatively toward the fold axis, and gabbroic rocks farthest down the flanks. The intrusions on the southwest limb are sill-like, average approximately 800 feet in width, and may be traced as far as 5 miles in length. On the northeast limb, the only intrusion to crop out is much larger in width than the more southerly ones. Here, an extensive gabbroic layer at least 3000 feet in width has been outlined by geophysical methods. Both sets of intrusions are similar in that the peridotitic basal layers are not continuous.

V. ANALYTICAL METHODS

A. MINERAL DETERMINATIONS

Olivine

Olivine compositions were determined by R. Delabio at the Geological Survey of Canada, Ottawa. The method used was outlined by Jambor and Smith (1964). Unaltered olivine remnants were located in thin sections of the rock, then flaked out with a sharp needle, and the powder mounted in a powder x-ray camera for exposure. Sample compositions were obtained from standard curves correlating 2θ values for particular reflections with per cent forsterite. Results are noted in Table VI.

Clinopyroxene

Clinopyroxene compositions were best obtained from clinopyroxenite samples, since these were less altered than either gabbro or peridotite. The procedure followed is that described by Hess (1960) whereby composition can be determined by obtaining N_y and 2V of a grain.[1] Fragments of approximately 150 to 200 mesh size of crudely separated samples were sprinkled on a glass slide and immersed in oils, determining N_y in sodium light and applying temperature corrections. In addition to N_y, 2V values were obtained by standard universal stage techniques. Optical results were converted to chemical composition by a set of correlation curves (Hess, 1949). The compositions of 31 samples are tabled below (Table VII).

[1] Optical procedure is sufficient for determination of clinopyroxene since contained Al_2O_3 is very low.

Table VI. Olivine Compositions

Rock type and sample location abbreviations as for Fig. 14

Estimated accuracy for determination ± 0.6%

Analyst: R.N. Delabio, G.S.C., Ottawa

Sample	Rock Type	Location	2θ	%Forsterite
M-39	pd	M	142.00	80
M-80	pd	M	142.71	89
M-81	pd	M	142.10	82
M-102	pd	M	142.83	91
M-104	pd	M	142.67	89
M-109	pd	M	142.34	85
M-113	olcpx	W-M	141.59	75
M-162	cpx	W-MH	141.40	73
M-165	pd	Mc	142.08	81
M-175	pd	Mc	141.85	78
M-188	olcpx	GS	141.56	75
M-233	pd	GR	142.13	82
M-234	pd	GR	142.28	84
M-380A	cpx	W-M	141.79	78
M-384	pd	W-M	141.88	79
M-385	pd	W-M	141.85	78

Table VII. Clinopyroxene compositions

Rock type and sample location abbreviations as for Fig. 14
Estimated accuracy for 2V: ±0.5°; for N_y: ±0.005

Sample	Rock Type	Location	2V	N_y	Wo	En	Fs
M-24	fcpx	M	49½	1.683	41	48	11
M-26	gb	M	49	1.689	41	43	16
M-82	fcpx	M	52	1.682	43	48	9
M-84	fcpx	M	50½	1.683	41½	47½	11
M-85	fcpx	M	52	1.685	43	45½	11½
M-86	fcpx	M	49	1.687	41	45	14
M-117	pd	W-M	52	1.684	43	46	11
M-118	ol.cpx	W-M	50½	1.682	41½	48½	10
M-119	pd	W-M	49	1.681	40½	50	9½
M-123	cpx	W-M	53½	1.683	44	46	10
M-125	fcpx	W-M	55½	1.684	45½	44½	10
M-126	fcpx	W-M	52	1.683	43	47	10
M-128	gb	W-M	49½	1.682	41	49	10
M-142	cpx	MH	52	1.685	43	45½	11½
M-143	fcpx	MH	51½	1.685	42½	46	11½
M-162	cpx	W-MH	51	1.685	42½	46	11½
M-167	gb	Mc	54	1.684	44½	45	10½
M-174	cpx	Mc	50	1.686	43	45	12
M-235	fcpx	GR	54	1.683	44	46	10
M-236	ol.cpx	GR	54	1.681	44	48	8
M-330	fcpx	W-M	54	1.683	44½	46	9½
M-340	gb	W-M	53½	1.678	43½	50	6½
M-353	ol.cpx	W-M	52	1.683	43	47	10
M-354	ol.cpx	W-M	50½	1.684	41½	47½	11
M-357	fcpx	W-M	51	1.683	42	47	11
M-358	cpx	W-M	51½	1.678	41½	51½	7
M-359	cpx	W-M	50½	1.680	41	50½	8½
M-361	gb	W-M	50	1.694	41	40	19
M-363	gb	W-M	45	1.696	37½	40½	22
M-369	cpx	W-M	51	1.682	42	48	10
M-382	ol.cpx	W-M	50½	1.682	41	49	10

Plagioclase

With the aid of standard extinction curves a very few reliable plagioclase compositions could be obtained. These were so sparse that they could not be used to outline composition variations, thus are not reported.

Garnet

Whole-rock portions of these samples suspected of containing garnet were mounted and scanned by X-ray diffractometer. The pattern obtained indicated the presence of grossular. Comparison of flakes of garnet with various index oils, however, showed the mineral to be hydrogrossular of approximately 1.72 index rather than grossular of 1.734 index. Hydrogrossular was found in the following samples: M-115, 178, 190, 371, 393.

B. CHEMICAL ANALYSIS

Sample Preparation

Whole rock specimens were crushed in a steel jaw crusher and ground to -150 mesh size in a ceramic disc pulveriser. All sizing was done through steel sieves. Small portions from the crushed samples were split off for spectrochemical analysis and larger portions from several selected samples for major element analysis.

Spectrochemical Analysis

In preparation for determination by emission spectrography, the samples were mixed in a 50-50 ratio with a palladium chloride-indium oxide-cesium carbonate-graphite internal standard and buffer mixture (method prepared by G.E. Pattenden, McMaster University), the mixture mounted in

graphite electrodes, excess moisture dried off, and finally arced in an atmosphere of 80 per cent argon-20 per cent oxygen. Calibration curves for certain elements were made using artificial standards with synthetic matrices. Two sets of matrices were prepared, one with proportions 45:5:13:30:7 of SiO_2, Al_2O_3, Fe_2O_3, MgO, $CaCO_3$ as an "ultramafic" matrix and the second with 50:15:15:7:3:10 of SiO_2, Al_2O_3, Fe_2O_3, MgO, NaCl, $CaCO_3$ as a "mafic" matrix. When the calibration curves were plotted, however, it was discovered that the preparation of two sets of matrices was a needless precaution since cesium carbonate acted as an effective buffer to erase the matrix composition differences. Table VIII gives the wavelengths and precision of determination for each element, and Table IX illustrates the degree of accuracy by comparing (1) the results for rock standard W-1 with the recommended averages, and (2) the results for a series of samples from the Muskox intrusion (Northwest Territories) with the results reported by the Geological Survey of Canada (Private Communication, Irvine, 1964).

The evaluation of ppm (parts per million) of an element has been greatly speeded by the development of machine computation procedures. A programme prepared by D.M. Shaw (1965) and written in Fortran IV for the IBM 7040 computer carries out the more tedious operations by processing the input transmission readings for one analysis in approximately 0.75 second.

Table VIII. Trace element wavelengths and precisions
Precision by analysis of variance for 3 replicates of each sample.

Element	Wavelength	Precision (coeff. of variation in %)
Ba	4554.042	15.1
Co	3453.505	9.5
Cr	4254.346	14.0
	4344.507	9.1
Cu	3273.962	23.3
Li	6707.844	21.5
Mn	4041.361	11.7
Ni	3003.629	10.3
	3413.939	6.5
Rb	7800.227	10.4
Sr	4607.331	16.0
Ti	4305.916	9.6
V	4379.238	10.5
Zr	3391.975	22.9
Cs	6723.279	
	7609.01	
In	4511.323	
Pd	3242.703	
	3609.548	

Table IX. Estimation of Accuracy by Comparison with Rock Standard W-1 and Other Samples

Sample	Ti	Cr	V	Li	Ni	Co	Cu	Mn	Zr	Sr	Ba	Rb
W-1	10,767*	152	323	9	83	38	101	1570	222	238	212	16
	7,400**	124	240	12	82	38	107	1340	100	220	225	22
NO7377***		3000	180		652	92	35			43	60	
		2350	175		565	105	48			69	54	
NO7875		1720	135		550	71	106			94	87	
		1000	150		525	82	140			100	82	
N12720		3800	148		433	76	27			45	60	
		2300	155		370	80	32			70	82	
N15635		7570	tr		1880	114	212			-	18	
		6900	120		1700	115	230			22	27	
NO2113		17	297		44	28	19			283	910	
		30	325		40	47	32			370	1050	
NO2906		91	297		119	37	96			124	195	
		51	280		110	53	88			150	330	
S08823		5820	-		2400	107	2			-	-	
		3650	-		1550	109	4			26	10	
S24847		3800	tr		2103	149	19			tr	-	
		3250	70		2150	155	12			37	35	
NO5622		333	258		128	40	52			202	130	
		160	210		135	37	60			210	125	
S27146		5920	66		2050	167	29			tr	tr	
		5000	85		2100	150				48	37	
S12868		6400	tr		1830	127	3			-	-	
		5900	-		1950	135	88			22	13	

* Upper line of pairs: N.D. MacRae, analyst. Average of triplicate analyses.
** Recommended averages for W-1 (Stevens et al, 1960).
*** Samples from Muskox intrusion, N.W.T. Analysed by Geological Survey of Canada (lower line of pairs).

Major Silicate Analysis

Major elements were determined by rapid silicate analysis[1] by J. Muysson, McMaster University, and are reported as oxide per cent.

---

[1] Modified after procedure outlined by Shapiro and Brannock, 1962.

VI. PETROGENESIS OF THE INTRUSIONS

Two possible origins may be hypothesized for each layered intrusion of the Abitibi belt. The first involves a mechanism of multiple injection of magma of differing composition, and the second requires prolonged differentiation of a magma in situ.

Grubb (1962) suggested that the ultramafic sections of the Matheson area intrusions were emplaced separately from the gabbroic sections. He envisaged a partial fusion of the peridotite substratum which first produced a basaltic or ferriferous liquid, then abruptly gave rise to a highly forsteritic magma. Slight disruption in the overlying crust caused the ferriferous liquid to be tapped, giving rise to a gabbro-pyroxenite sequence, with later emplacement of the ultramafic section.

It would be impossible to explain some of the features observed in the sills if the plutons had been injected in segments, as suggested by Grubb. Flow banding is a common characteristic of plutons emplaced as a partial crystalline mush, but the bands are not nearly as regular and persistent as those formed by crystal settling, and adjoining layers commonly show considerable compositional contrast (Thayer, 1963). At Centre Hill, 1 and 2 inch bands have been followed without deviation for hundreds of feet along strike. At Warden-Munro, cross lamination found in the banded zone can be satisfactorily explained only by the action of currents on settled crystals on a nearly horizontal chamber floor. Further, an evolution in chemical composition, such as

that outlined below for the Munro Lake sill or the Ghost Range intrusion, is one of the main points of evidence against a hypothesis of multiple intrusion of magmas of widely different compositions.

The main points in support of a general differentiation mechanism are outlined below.

A. DIFFERENTIATION BY FRACTIONAL CRYSTALLIZATION

Rock Type Variations

The sequence of phase layers from peridotite to clinopyroxenite to gabbro as exhibited in both the complex Munro Lake sill and the simple Ghost Range type of intrusion is typical of the rock types developed from fractionation of a tholeiitic basalt magma. Partial sequences are repeated several times in the Munro Lake sections, but there is always a consistent order of phase layers. Each cyclic unit or partial sequence of layers may be considered the product of accumulation of a fractionating liquid. Repetitions of cyclic units must be due to chemical alteration of the liquid; this is discussed in a following section.

Mineral Variation

1. Munro Lake Sill

Eight olivine compositions from the Centre Hill section (Fig. 14) show a slight reduction of Fo-content upward in the series from Fo_{78} in the lower marginal zone to Fo_{64} in the uppermost peridotite layer. Only the layers of the Centre Hill section have been sufficiently sampled and analysed to indicate any trend that might exist. Assuming that the indicated trend from Fo_{78} to Fo_{64} is significant, then there is some indication that the liquid from which the upper olivine crystallized was slightly

more Fe-rich than that from which lower olivine formed. Four samples of four consecutive central layers of the ultramafic zone of the Warden-Munro area contain olivine of composition Fo_{79} to Fo_{75}, but there is no regular variation from layer to layer (Table X). Olivine from a peridotite layer outcropping west of McCool Hill is of composition Fo_{73} (Sample M-162, Fig. 25). Since outcrop in that area is sparse, the peridotite layer cannot be assigned to a definite stratigraphic horizon, but it is generally in the upper third of the ultramafic zone.

Clinopyroxene compositions of the ultramafic zone of the Centre Hill section show a fairly regular increase upward in Fs-content from Fs_6 to Fs_{13}. The general trend is indicated in Fig. 39. The melanogabbro layer of the gabbroic zone contains clinopyroxene of Fs_{22}, and two determinations of samples of the upper gabbro both are Fs_{26}. That part of the ultramafic zone which crops out at Warden-Munro contains clinopyroxene ranging in composition from Fs_7 to Fs_{11}, but there is no significant trend. The lower section of the gabbroic zone contains clinopyroxene of composition Fs_{22} and Fs_{19}; no reliable determinations were possible for the upper part of the zone because of extensive alteration of clinopyroxene to amphibole. Two samples of ultramafic rocks at McCool Hill and one west of McCool Hill all contain clinopyroxene of identical composition, $Fs_{11\frac{1}{2}}$. The general trend from low Fs-content in the ultramafic zone to significantly higher in the gabbroic zone is sufficient proof that the liquid from which the stratigraphically higher clinopyroxene formed was more Fe-rich than that from which lower clinopyroxene formed.

Table X. Mineral Composition

Variation in Warden-Munro Section

Layer	Clinopyroxene		Olivine	
	Sample	Composition	Sample	Composition
15				
15'				
14				
13	M-361	$Wo_{41}En_{40}Fs_{19}$		
	M-363	$Wo_{37\frac{1}{2}}En_{40\frac{1}{2}}Fs_{22}$		
12	M-353	$Wo_{43}En_{47}Fs_{10}$		
11				
10	M-354	$Wo_{41\frac{1}{2}}En_{47\frac{1}{2}}Fs_{11}$		
9				
8	M-369	$Wo_{42}En_{48}Fs_{10}$		
	M-357	$Wo_{42}En_{47}Fs_{11}$		
	M-358	$Wo_{41\frac{1}{2}}En_{51\frac{1}{2}}Fs_{7}$		
	M-359	$Wo_{41}En_{50\frac{1}{2}}Fs_{8\frac{1}{2}}$		
7			M-380A	Fo_{78}
6	M-382	$Wo_{41}En_{49}Fs_{10}$	M-384	Fo_{79}
5	M-119	$Wo_{40\frac{1}{2}}En_{50}Fs_{9\frac{1}{2}}$		
4	M-118	$Wo_{41\frac{1}{2}}En_{48\frac{1}{2}}Fs_{10}$	M-118	Fo_{75}
3	M-117	$Wo_{43}En_{46}Fs_{11}$	M-385	Fo_{78}

Fig. 39. Clinopyroxene Composition Trend. CH-Centre Hill (MacRae, 1963). SK-Skaergaard (Brown and Vincent, 1963).

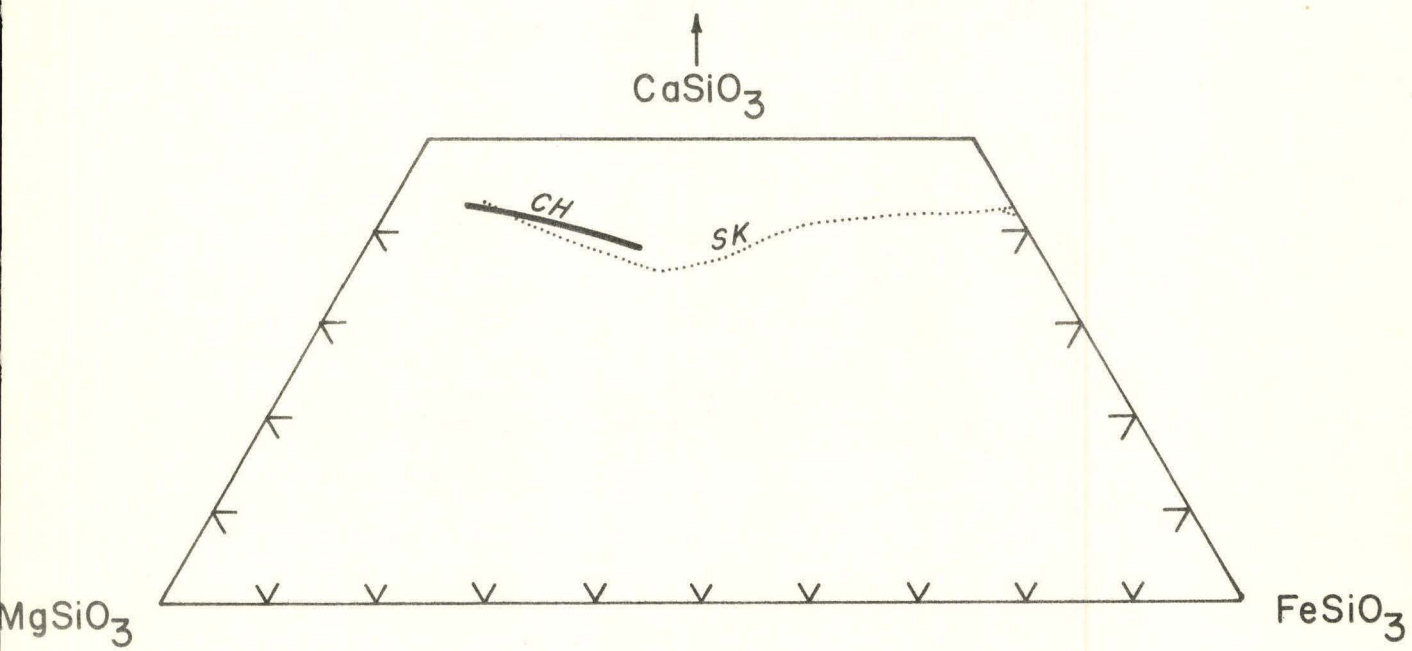

Reliable plagioclase compositions are scarce; at Centre Hill there is a general trend from approximately An_{46} in clinopyroxenite of the ultramafic zone to An_{27} in the upper gabbro, but at Warden-Munro and McCool Hill alteration has been so severe that no determinations are possible. On the basis of such sparse data it is impossible to give significant composition limits, however there is a general indication that the later liquids were less calcic than the earlier.

2. Ghost Range Intrusion

Although the rocks of the Ghost Range are fairly well exposed and thus were easily sampled, alteration of olivine, pyroxene, and plagioclase has been so severe that mineral composition determinations are rare, and the outlining of trends is impossible. Two olivine determinations of Fo_{84} and Fo_{82}, and two clinopyroxene determinations, Fs_8 and Fs_{10}, all from the ultramafic zone, are the only mineral composition determinations from the sill.

3. General

Olivine from two samples from the narrow peridotite-gabbro sill east of McCool Hill are of composition Fo_{78} and Fo_{81}, thus are within the same general range as olivine from the Munro Lake and Ghost Range bodies. Eight clinopyroxene determinations from various scattered gabbroic bodies range from Fs_9 to Fs_{16}.

Order of Crystallization

Textural relationships in peridotite - the lowermost rock type of the simply layered intrusions and cyclic units of the Munro Lake sill -

indicate olivine and chromite to be the only cumulus phases. Clinopyroxene, plagioclase, and, locally, orthopyroxene are the intercumulus minerals. Stratigraphically higher in the series, clinopyroxene appears as the chief cumulus phase and plagioclase the chief intercumulus phase in the clinopyroxenite layers. In gabbroic rocks, clinopyroxene is joined by plagioclase as a primary phase, and quartz, granophyric intergrowth of plagioclase and quartz, and orthopyroxene are interstitial phases. Locally, some gabbroic zones show horizons of accumulation of primary magnetite. The order of crystallization of major minerals is thus established as:

1) olivine + chromite
2) clinopyroxene
3) clinopyroxene + plagioclase
4) clinopyroxene + plagioclase + magnetite

It is significant that orthopyroxene does not occur as a cumulus phase in the sequence, although it is commonly present in small amounts as

---

[1] A few scattered grains of what appear to be altered cumulus orthopyroxene were noted in one sample (M-57) of a gabbro body in the Camp Lake area of Munro township; no similar occurrences were noted elsewhere.

---

an intercumulus phase. In this regard, Coombs (1963) has developed an "indicator ratio" (IR) which is designed to trace the course of any liquid, from which olivine is the chief phase crystallizing, projected on the diopside-olivine-quartz plane of the diopside-olivine-quartz-anorthite tetrahedron. His ratio is expressed as

$$IR = \frac{Hy + 2Qz}{Hy + 2(Qz + Di)}$$

where Hy = hypersthene, Qz = quartz, and Di = diopside expressed in molecular proportions by a standard C.I.P.W. norm calculation. Coombs found that a liquid of IR less than 0.50 should not yield cumulus orthopyroxene during normal crystallization. Molecular norm figures of the Centre Hill primary liquid (see later section) yield an IR of 0.26.

FIGURE 40

Trace element variation diagram for
Centre Hill section (MacRae,1963)

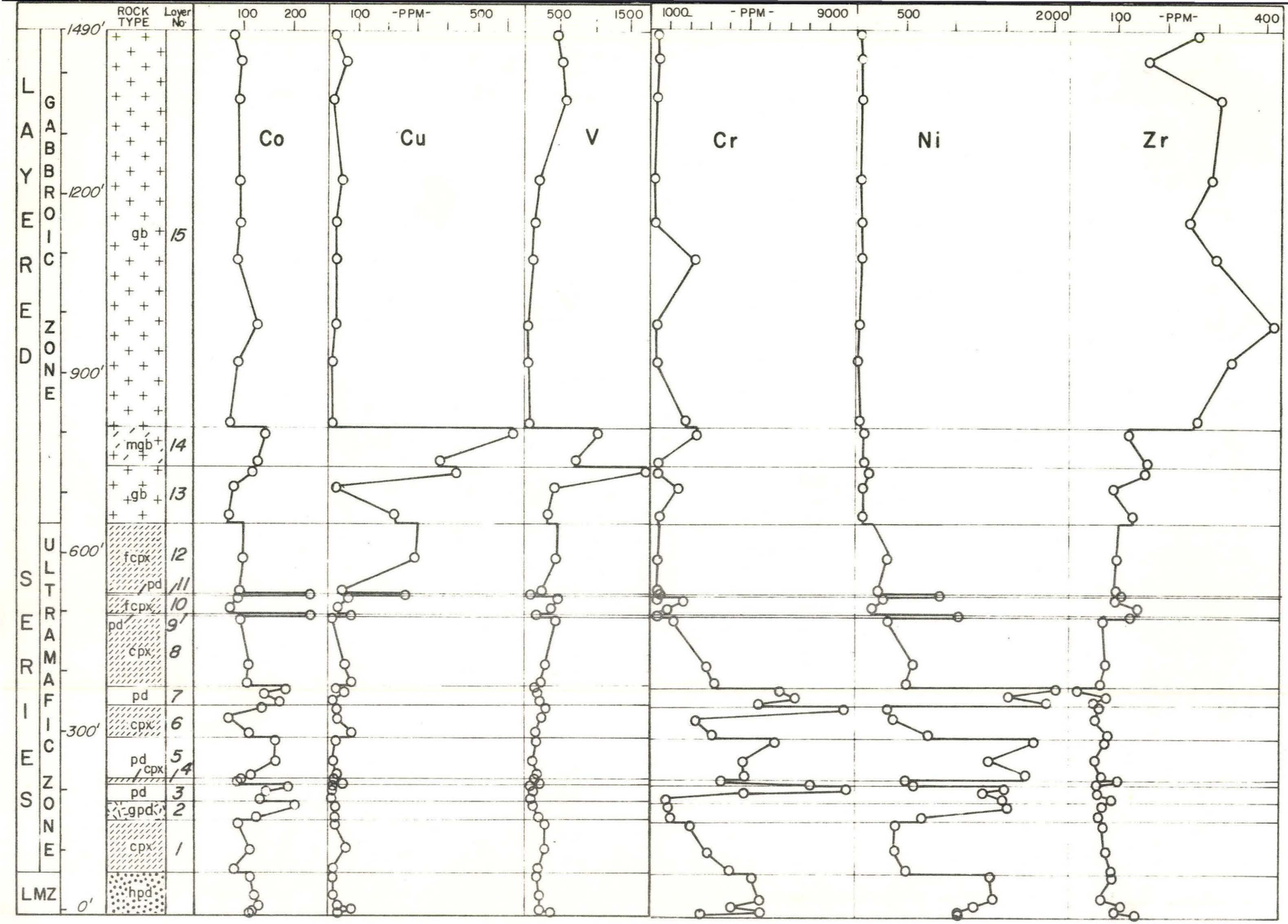
LAYERED SERIES
GABBROIC ZONE
ULTRAMAFIC ZONE
LMZ
ROCK TYPE
Layer No.
1490'
1200'
900'
600'
300'
0'
gb
mgb
fcpx
pd
cpx
gpd
hpd
15
14
13
12
11
10
9'
8
7
6
5
4
3
2
1
100 200
Co
100 -PPM- 500
Cu
500 1500
V
1000 -PPM- 9000
Cr
500 2000
Ni
100 -PPM- 400
Zr

FIGURE 41

Minor element variation diagram for
Warden-Munro section

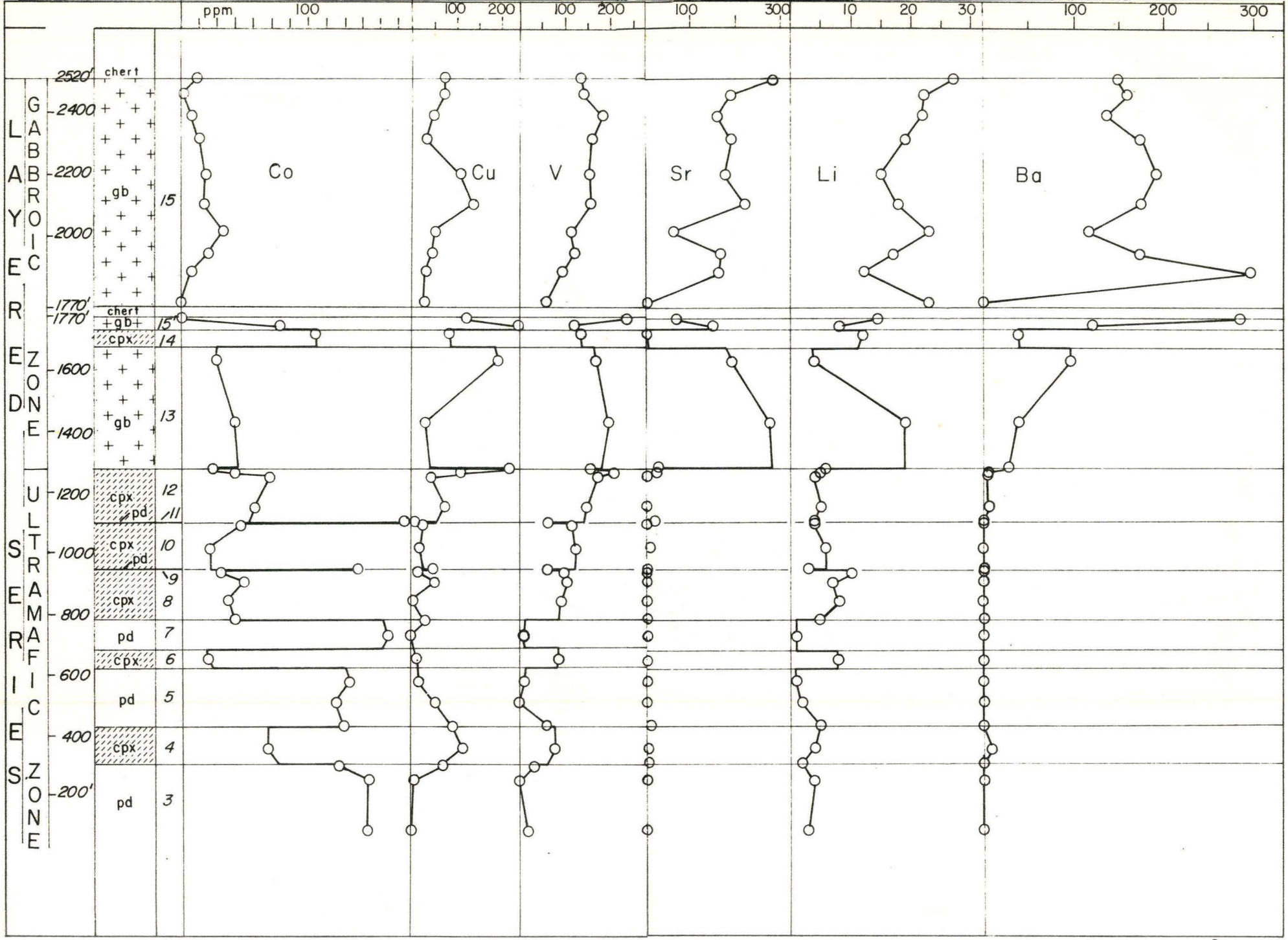
ppm
100
100 200
100 200
100 300
10 20 30
100 200 300
LAYERED SERIES
GABBROIC ZONE
ULTRAMAFIC ZONE
2520'
2400
2200
2000
1770'
1770'
1600
1400
1200
1000
800
600
400
200'
chert
gb
cpx
pd
15
14
13
12
11
10
9
8
7
6
5
4
3
Co
Cu
V
Sr
Li
Ba

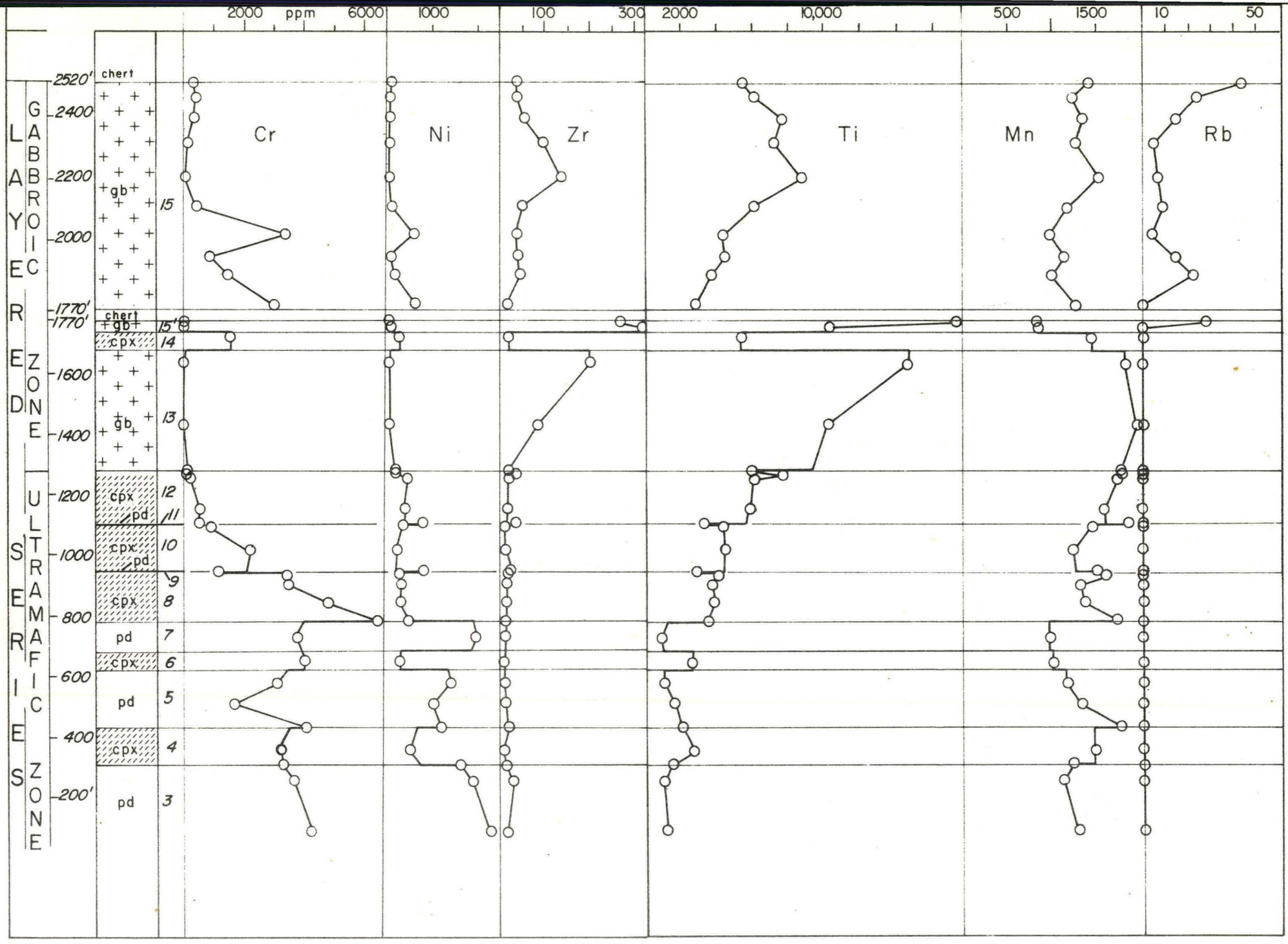
2000 ppm 6000
1000
100 300
2000 10,000
500 1500
10 50
Cr
Ni
Zr
Ti
Mn
Rb
LAYERED SERIES
GABBROIC ZONE
ULTRAMAFIC ZONE
2520'
2400
2200
2000
1770'
1600
1400
1200
1000
800
600
400
200'
chert
gb
cpx
pd
15
15'
14
13
12
11
10
9
8
7
6
5
4
3

FIGURE 42

Minor element variation diagram for
generalized section of Ghost Range

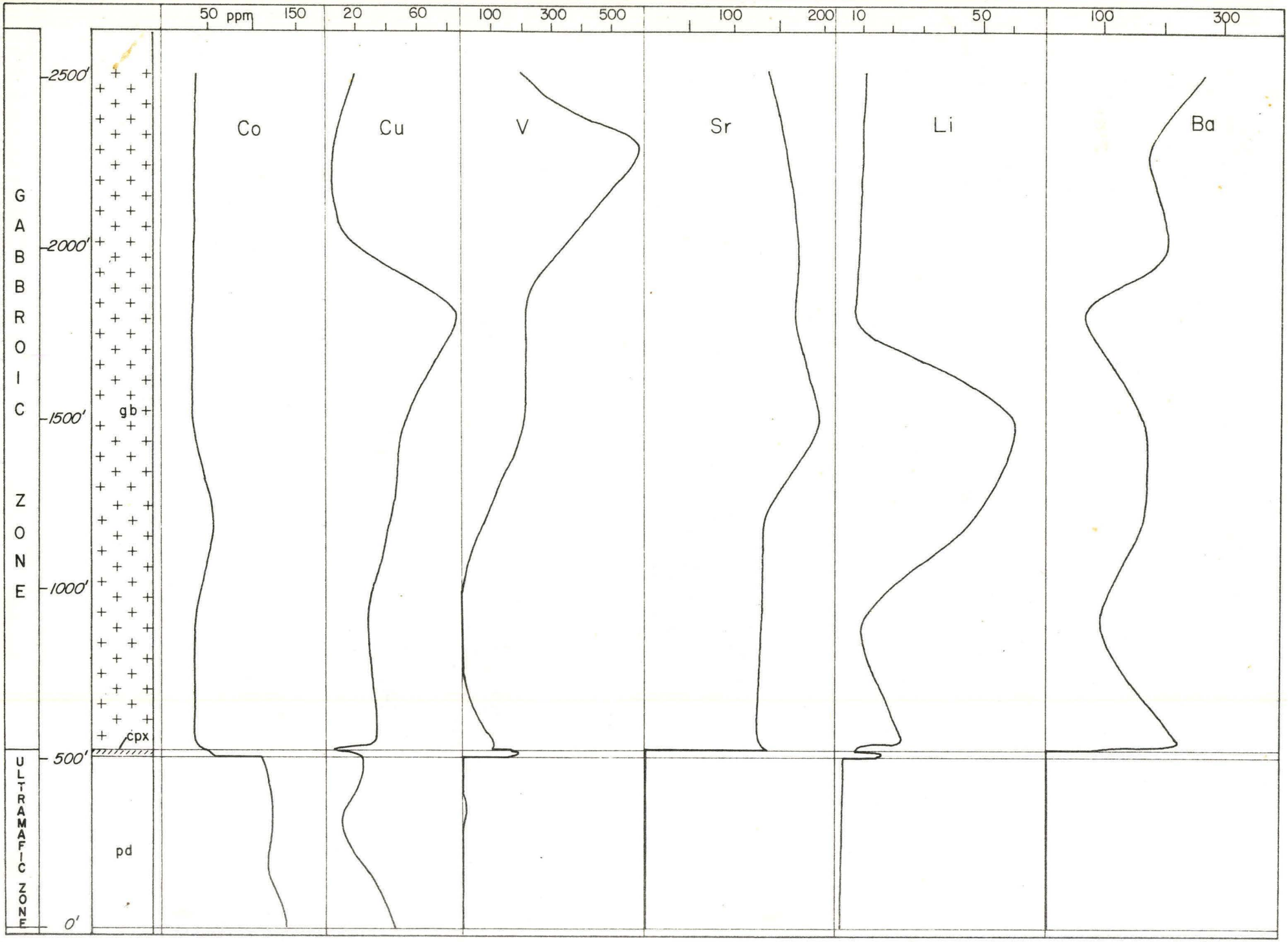
50 ppm 150
20 60
100 300 500
100 200
10 50
100 300
Co
Cu
V
Sr
Li
Ba
GABBROIC ZONE
ULTRAMAFIC ZONE
2500'
2000'
1500'
1000'
500'
0'
gb
cpx
pd

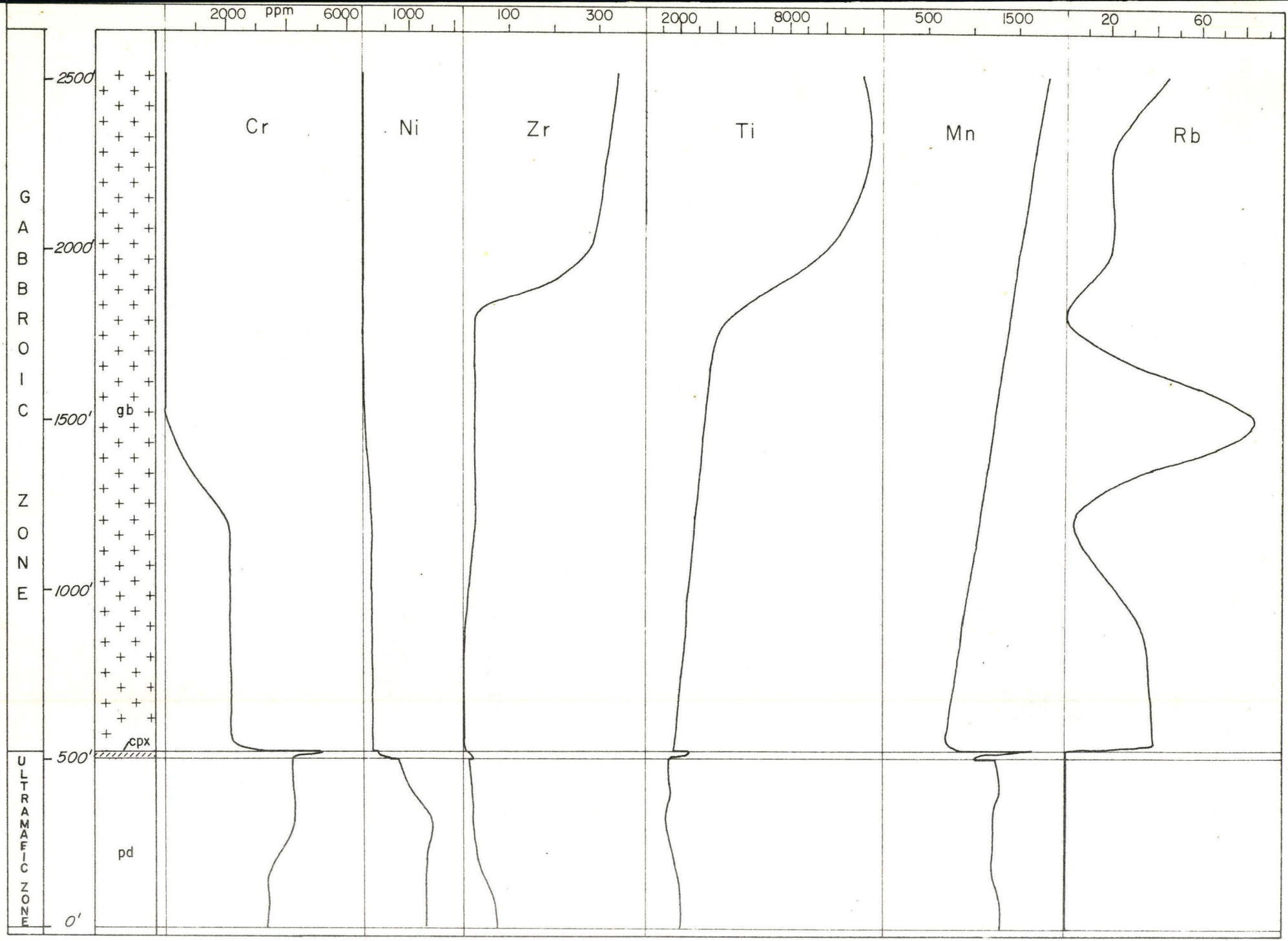
2000 ppm 6000
1000
100 300
2000 8000
500 1500
20 60
Cr
Ni
Zr
Ti
Mn
Rb
2500'
2000'
1500'
1000'
500'
0'
GABBROIC ZONE
ULTRAMAFIC ZONE
gb
cpx
pd

FIGURE 43

Major and minor variation diagrams for Centre Hill section (MacRae,1963). ● rapid silicate analysis, ◒ spectrographic analysis, ○ calculated from mineral mode.

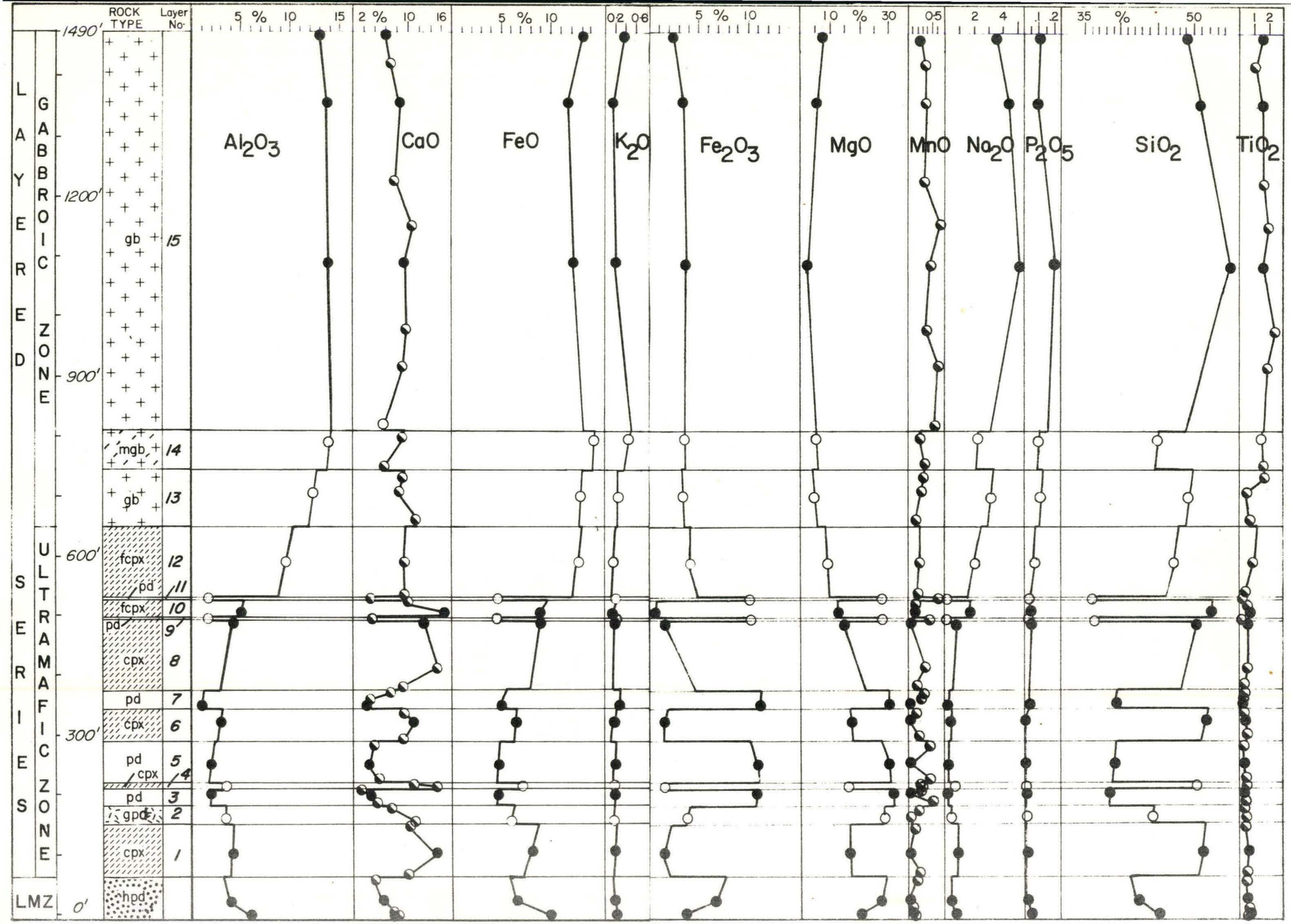
LAYERED SERIES
GABBROIC ZONE
ULTRAMAFIC ZONE
LMZ
ROCK TYPE
Layer No.
1490'
1200'
900'
600'
300'
0'
gb
mgb
fcpx
pd
cpx
gpd
hpd
15
14
13
12
11
10
9
8
7
6
5
4
3
2
1
Al2O3
CaO
FeO
K2O
Fe2O3
MgO
MnO
Na2O
P2O5
SiO2
TiO2

FIGURE 44

Major element variation for Warden-Munro section.
Trend lines generalized between control points.

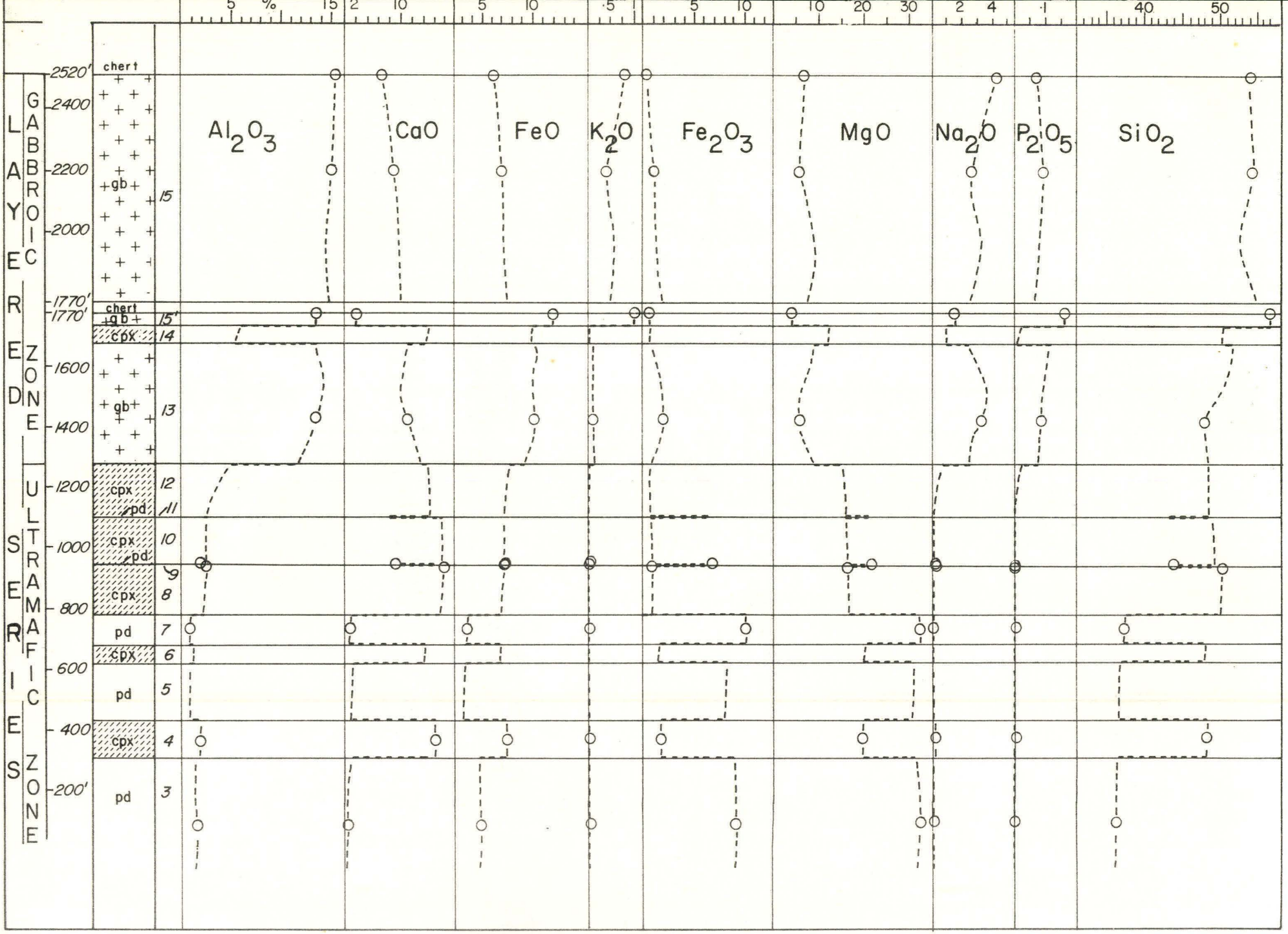
LAYERED SERIES
GABBROIC ZONE
ULTRAMAFIC ZONE
2520'
2400
2200
2000
1770'
1600
1400
1200
1000
800
600
400
200'
chert
gb
cpx
pd
15
15'
14
13
12
11
10
9
8
7
6
5
4
3
Al_2O_3
CaO
FeO
K_2O
Fe_2O_3
MgO
Na_2O
P_2O_5
SiO_2

Chemical Variation

1. Data

Minor and major element analyses are listed in Appendices 2 and 3; for the minor elements, a summary in the form of range of abundance for each rock type is given below (Table XI). Variation diagrams best illustrate the correlation of element abundance with stratigraphic position in the sequence. Trace element variations for the Centre Hill section are illustrated in Fig. 40; minor element variations for the Warden-Munro section in Fig. 41, and for the Ghost Range generalized section in Fig. 42; major and minor elements for the Centre Hill section are in Fig. 43, and major elements for the Warden-Munro section in Fig. 44.

2. Distribution of Minor Elements

i) Hypothetical Model. The distribution of minor elements in the Munro Lake sill and other layered bodies may be largely attributed to fractional crystallization. A simple model of minor element fractionation during fractional crystallization can be readily set up and compared with the actual analytical data[1]. The model, as illustrated in Figures 45 and 46, is based on the mathematical treatment by Neumann, Mead and Vitaliano (1954) of minor element distribution. The relative distribution of each element between solid and liquid phases is represented by a distribution coefficient, denoted K. The notation $K_E^{\alpha\text{-liq}}$ represents, therefore, the concentration of element E in an increment of mineral α divided by its concentration in the liquid from which the solid increment

---

[1] I am indebted to T.N. Irvine for the suggested model.

Table XI. Maximum abundance ranges of trace elements for three major rock types. Values reported in parts per million.

	Dunite-Peridotite	Clinopyroxenite	Gabbro
Ti	580-4373	1715-15,430	1257-32,300
Cr	1133-5130	79-6670	n.d.-3940
V	n.d.*-209	15-415	n.d.-903
Li	tr**-16	4-32	2-64
Ni	370-2900	106-2160	tr-356
Co	46-151	37-143	17-85
Cu	1-145	3-350	1-237
Mn	793-1800	857-2830	607-5173
Zr	n.d.-70	9-135	5-1300
Sr	n.d.-10	n.d.-145	n.d.-283
Ba	n.d.-21	n.d.-210	tr-490
Rb	n.d.-6	n.d.-15	n.d.-85

* n.d.: not detected

** tr: trace

Fig. 45. Diagrammatic Illustration of Fractional Differentiation Model

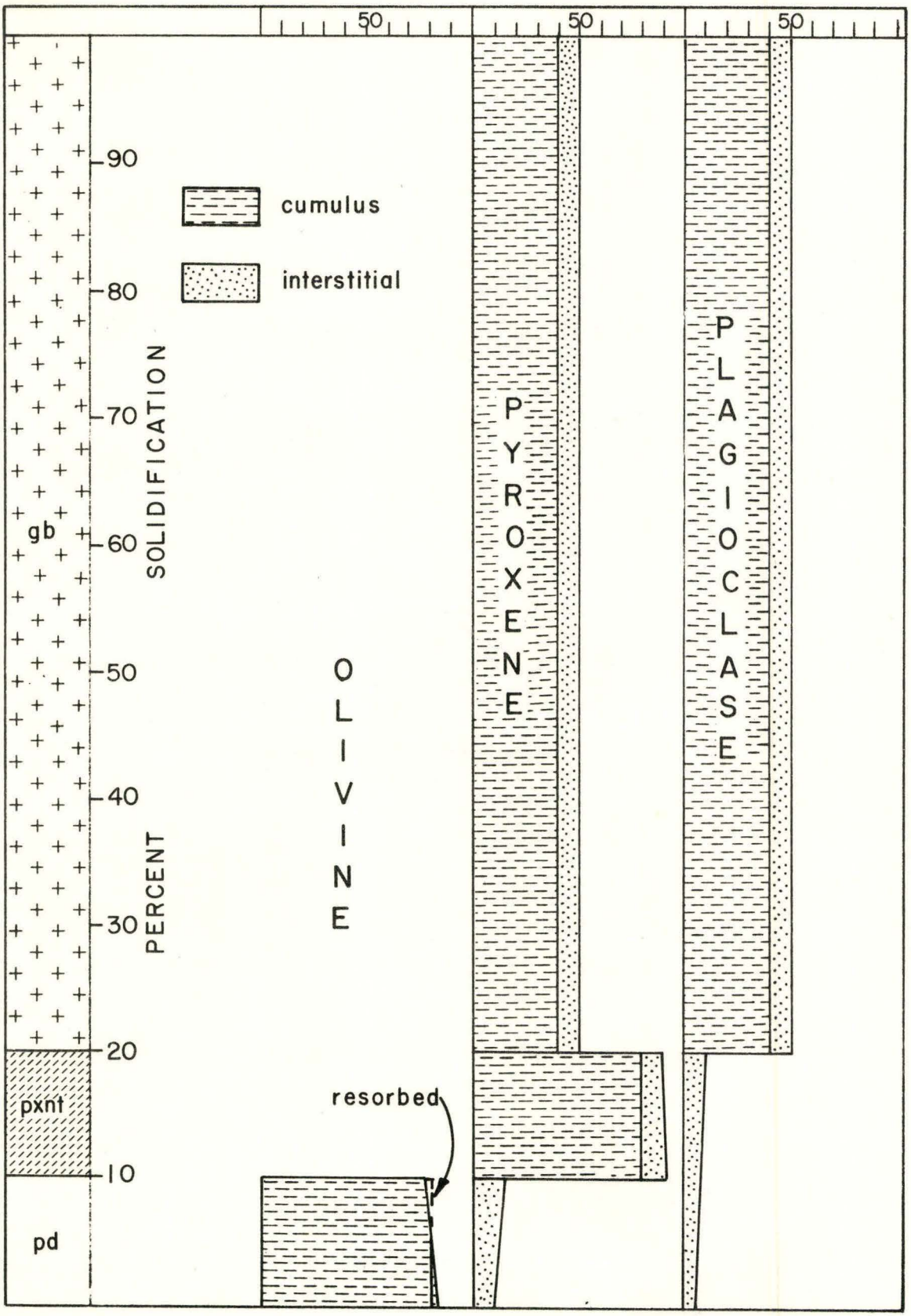

Fig. 46. Trace Element Variation in Hypothetical Model

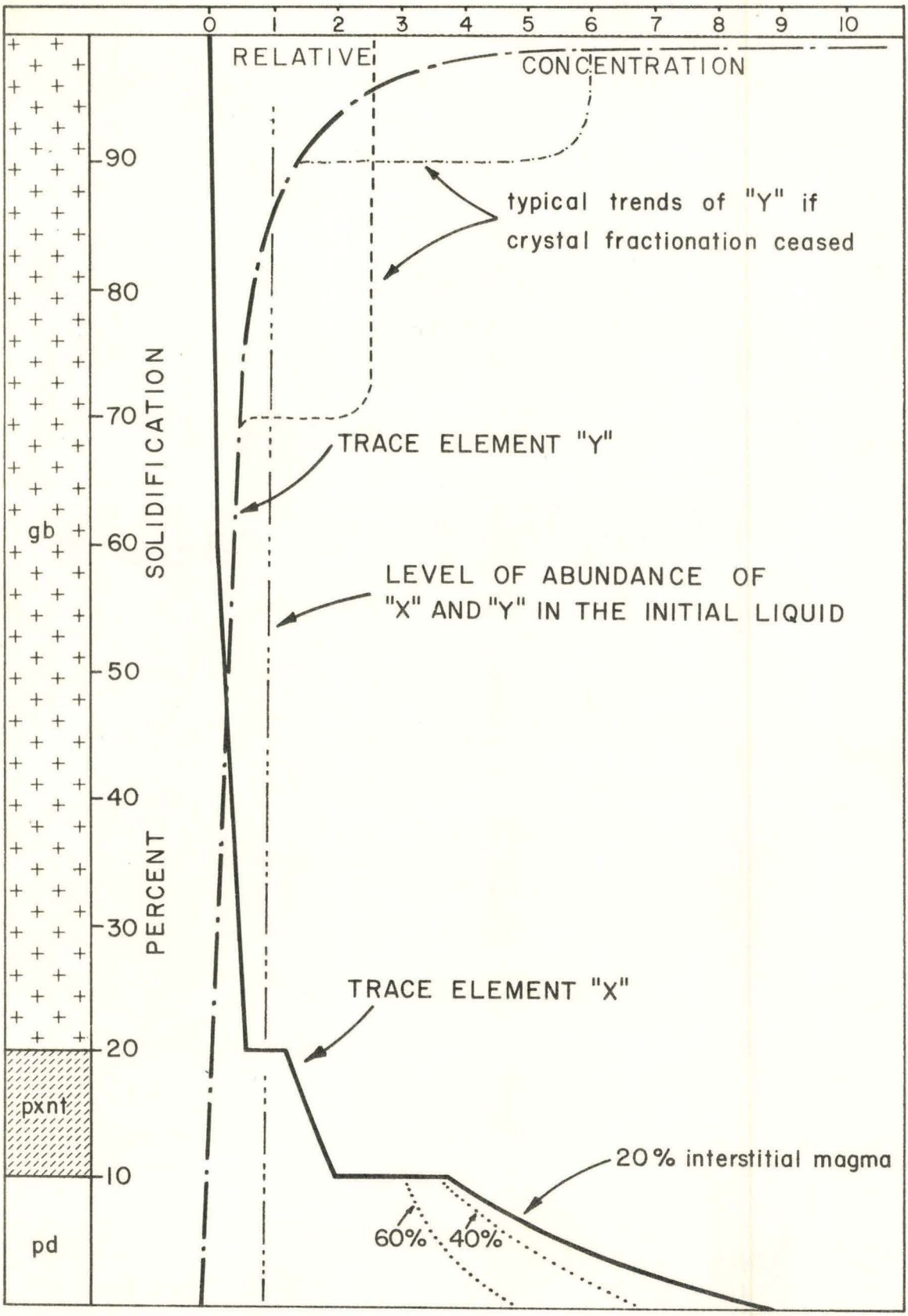

was formed. The various coefficients are assumed to be constants throughout the crystallization, an assumption that is justified as a first approximation by data obtained by Wager and Mitchell (1950) on the Skaergaard intrusion (cf. McIntire, 1963).

The magma of the hypothetical model follows a path of fractional crystallization that yields first olivine, then pyroxene, and then pyroxene plus plagioclase in equal amounts. The minerals are considered to be fractionated by gravity settling to the floor of the magma, and it is assumed that the resulting accumulation within each layer retains 20 per cent of its specific parent liquid trapped interstitially to the settled minerals. The total product - the cumulate - is then assumed to complete solidification without further fractionation. The net result (Fig. 45) is a sequence of layers from peridotite to pyroxenite to gabbro.

Two hypothetical examples of minor element fractionation are considered. In the first, element X is distributed such that: $K_X^{ol\text{-}liq} = 11$; $K_X^{px\text{-}liq} = 6$; and $K_X^{pl\text{-}liq} = 0$. When the 20 per cent intercumulus magma is taken into consideration, the "effective" coefficients for the bulk cumulates become: for "peridotite", $K_X^{pd\text{-}liq} = 9$[1]; for "pyroxenite", $K_X^{pxn\text{-}liq} = 5$; and for "gabbro", $K_X^{gb\text{-}liq} = 2.6$. The significant features of the resulting distribution of X are (a) its gradual decrease in amount with increasing stratigraphic position within each major layer, and (b) the marked discontinuities between layers. The second hypothetical element, Y, does not enter into any of the three major minerals in appreci-

[1] For example, "peridotite" consists of 4 parts olivine and 1 part liquid; thus $K_X^{pd\text{-}liq} = \frac{(4 \times 11)+(1 \times 1)}{5} = 9$.

able quantities. Presumably it would precipitate as a late accessory mineral. In this case, the effective distribution coefficient is determined by the amount of trapped interstitial liquid; if it were a constant 20 per cent, $K_Y^{rock\text{-}liq}$ would be 0.2, and accordingly, the concentration of Y would increase continually as shown in Figure 46. In theory, Y should form 100 per cent of the last increment of solid, but in nature, its marked concentration at late stages would probably be prevented by crystallization of the accessory mineral, or as shown in the diagram, by imperfect crystal fractionation.

ii) Discussion of Specific Elements. The variation of specific elements in nature is obviously more complicated than in the simple model, but there are definite similarities. These are demonstrated by individual cyclic units of the Munro Lake sill and by the simply differentiated bodies.

The distribution of element X is comparable to that of Ni. The latter is well-known to have a strong preference for olivine, and to enter pyroxene in preference to plagioclase. Thus it shows distinctly different levels of abundance in peridotite, clinopyroxenite, and gabbro. Trends within layers are not well developed - due in part to the wide sampling interval - but an upward decrease is present in layers 1, 6, and 8 of the Centre Hill section, in peridotite layer 3 and clinopyroxenite layer 8 of the Warden-Munro section, and peridotite and clinopyroxenite layers of the Ghost Range intrusion. In general, peridotite layers, which in the model show pronounced trends, are relatively uniform. This could mean that the olivine was not formed by crystallization within the intrusion (e.g., it might have been introduced in suspension in magma),

or possibly the model is not applicable in some other aspect. There is, furthermore, a notable correlation between the ratio of olivine/intercumulus material and abundance of Ni in peridotite layers. It is noted that at Centre Hill and the Ghost Range, the only two sections where samples have been taken across the lowermost layers of the intrusions, the abundance of Ni increases successively from the base upward and then falls off. It seems probable that during accumulation of the lower layers, rapid cooling through the floor of the intrusions acted to freeze in larger amounts of interstitial magma.

The distribution of Cr is grossly similar to that of Ni. However, in peridotite layers it is contained in chromite, which is a cumulus mineral despite its small concentration, and thus it is in effect a "major" element, not properly described by the model used above. The model specifically considers association of minor elements with the major elements of only three mineral phases - olivine, pyroxene, and plagioclase. In the clinopyroxenite layers, Cr is almost entirely contained in clinopyroxene, and upward decreases in its concentration in layers 1 and 8 of the Centre Hill section and layers 8, 10, and 12 of the Warden-Munro section is probably a fractional crystallization trend.

Co shows a slight preference for peridotite but is fairly constant through the other layers. Evidently its distribution coefficients are close to unity.

The behaviour of model element Y would seem, at least in part, to describe the trends of Zr, P, Na and to a lesser extent, Ti, V, Ba, and Mn.

The abundances of Zr, P and Na gradually increase from the lower ultramafic rocks to abruptly higher levels in gabbroic rocks. The gradual increase probably reflects their concentration in residual magma during fractional crystallization, and the abrupt increase may result because crystal fractionation was less effective during formation of the gabbro. The latter interpretation is consistent with the textural characteristics of the gabbro; typically, gabbros are diabasic in texture and there is little indication that plagioclase crystals effectively separated from the magma by settling to the chamber floor. The abrupt increase in the abundance of Zr in the granophyric zone of the upper gabbro of the Ghost Range intrusion is correlated with an increase in abundance of apatite. Because Zr is not known to substitute into any position of the apatite structure, presumably the mineral zircon is present although not identified in the rocks, and varies sympathetically with apatite.

Ba, Ti, V and Mn, have roughly the same trends as Zr, P and Na, and can be interpreted in the same way. The fact that they increase in abundance toward the top of the intrusions indicates, as might be expected, that their solid-liquid distribution coefficients were significantly less than unity.

The abundance of V shows a slightirregular increase in the ultramafic zone of the Munro Lake sill. It reaches a peak in the lower part of the gabbroic zone and then drops to a relatively low level in the upper gabbro. The peak can be correlated with the presence of relatively large amounts of cumulus magnetite; formation of the latter may have impoverished the content of V in the residual magma which subsequently solidified

to gabbro. The relatively large abundance of V at the top of the gabbroic zone at Centre Hill suggests that the upper layer solidified by freezing to the roof of the intrusion as well as by accumulating from its base upward.

The trends of Li, Cu, and Sr appear not to follow the trends of either element X or Y, with the exception that all three have a higher abundance in the gabbroic rocks than in clinopyroxenite or peridotite. The behaviour of Cu is strongly governed by the sulphide content in the analysed sample. Small bodies of sulphides, usually containing some chalcopyrite, occur in fault zones and lenses throughout the area; thus it is difficult to justify stating that the small blebs of sulphide noted in the samples of the various intrusions derived solely by separation of immiscible sulphides during crystallization. While it is thought that such is the case for the sulphides of layers 13 and 14 of the Munro Lake sill and the central zone of the Ghost Range gabbroic zone, it is by no means proven.

3. Major Element Variation

In general, major elements vary systematically with changes in mineral phases through the differentiation sequence. Two variation diagrams which roughly outline the differentiation trend are discussed below.[1]

---

[1] In figures 47 and 49 the positions of peridotite samples are on the basis of a contained 1.25% Fe_2O_3, which is an average value for a fresh peridotite containing a few per cent modal chromite.

---

i) Fe-Mg-Ca Diagram. Fe, Mg, and Ca are important elements to a discussion on differentiation trends in a mafic-ultramafic pluton

Fig. 47. FeO-MgO-CaO Variation Diagram for Analysed Rocks

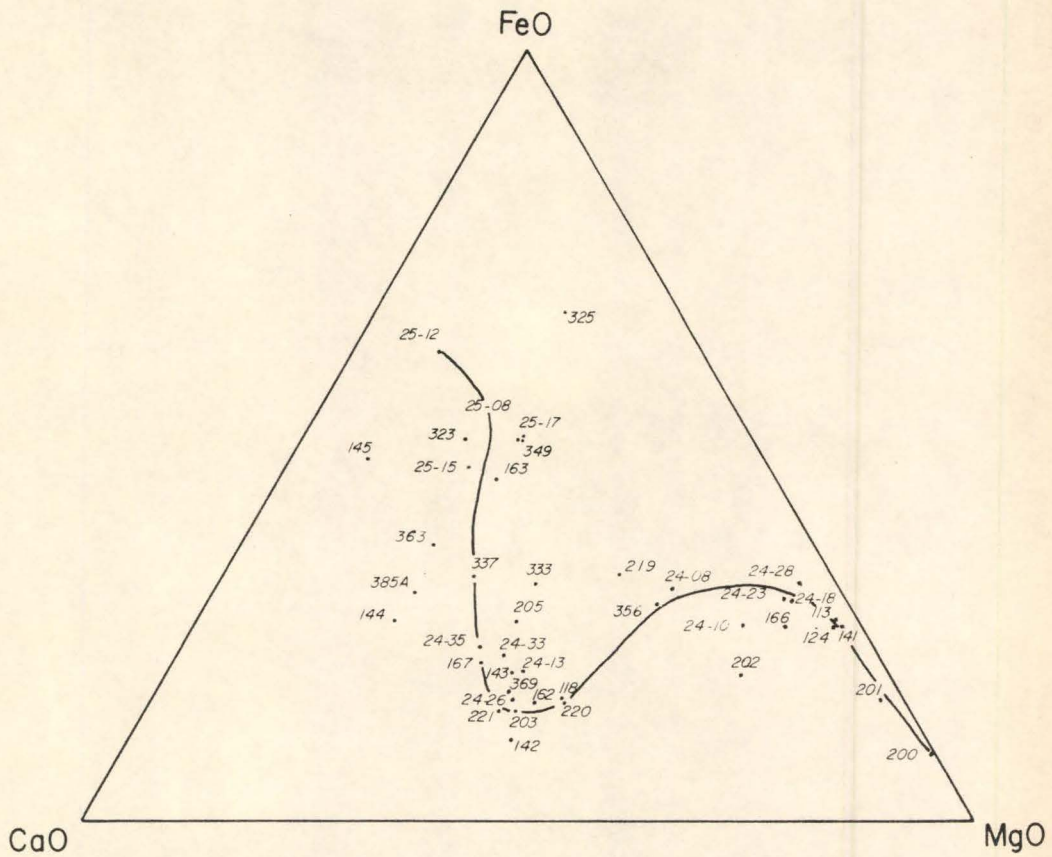

because all three vary considerably as mineralogy changes. The Fe-Mg-Ca variation for the intrusions under study is shown in Fig. 47. Those points closest to the Mg apex represent peridotite, those mid-way between Ca and Mg and furthest from Fe are clinopyroxenite, and those which show iron enrichment but minor change in the Ca/Mg ratio are gabbro. The trend line was established for rocks of the Centre Hill and Warden-Munro sections of the Munro Lake sill, but samples from other localities generally do not contradict the trend. Notable exceptions are M-325, a melanogabbro chill phase from the intermediate chert horizon of the Warden-Munro section; M-219, a garnet-clinopyroxene sample from the Ghost Range intrusion; M-385A, diorite from the dykes at Warden-Munro; M-333, an acidic chill phase from the top of Warden-Munro; M-144 and 145, two apparently normal gabbros from McCool Hill; and 24-08, hornblende peridotite from the lower marginal zone at Centre Hill. It is probable that some of the additional point scatter is due to serpentinization. The general trend of initial Ca enrichment followed by Fe enrichment is common to a number of plutons (Fig. 48), most significantly, the intrusion studied by Naldrett (1964) of Dundonald-Clergue townships, also in the Abitibi area.

ii) Fe-Mg-Total Alkali Diagram. A progressive enrichment of Na and K is clearly shown on an Mg-Fe-alkali variation diagram (Fig. 49). The only points lying far from the trend line are, again, the samples which least fit the Fe-Mg/Ca trend curve. Since neither the Mg/Fe ratio nor the absolute alkali abundance should be radically changed by serpentinization, the points on this diagram probably correspond well with the positions of equivalent unaltered rocks.

Fig.48. FeO-MgO-CaO Variation Diagrams for: A-Tulameen Complex, B-Skaergaard Intrusions, C-Duke Island Complex, D-Dundonald and Clergue Intrusions; c.f. Naldrett, 1964.

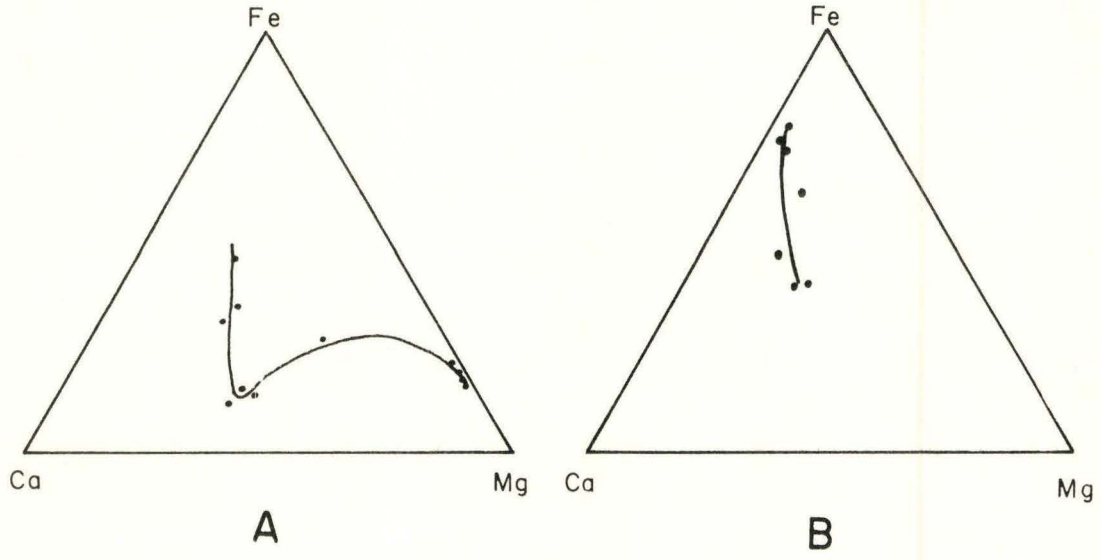

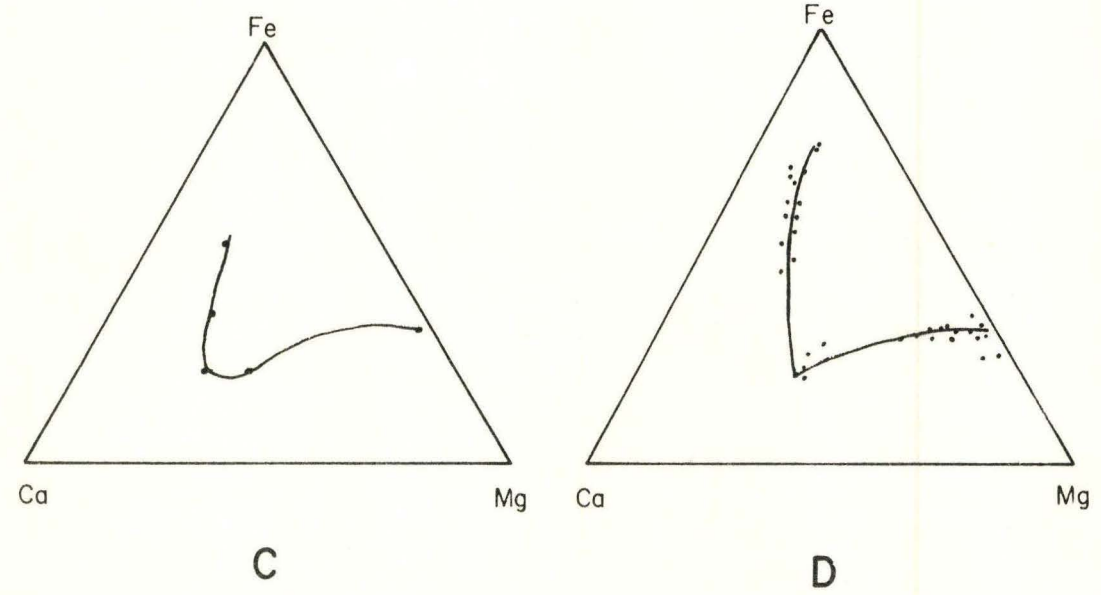

Fig. 49. FeO-MgO-Total Alkali Variation Diagram for Analysed Rocks

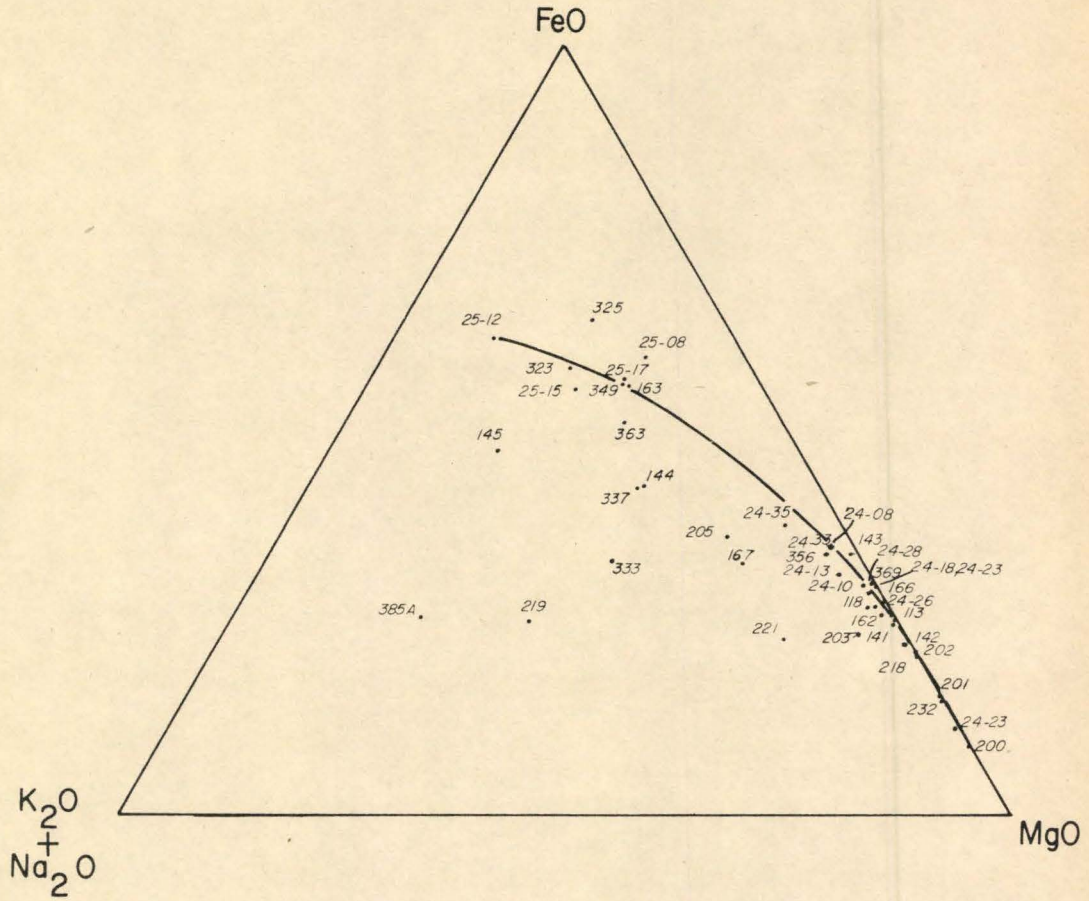

B. PHYSICAL EVOLUTION OF THE INTRUSIONS

Prior to a discussion of the plutons, the following basic assumption is made: all ultramafic and gabbroic intrusions in the area have a common origin. The assumption is based on four major points of evidence: (1) the intrusions are closely associated in space, (2) major rock types are closely similar in composition and texture for all layered intrusions, (3) differentiation trends and ranges of element abundance are similar in all layered intrusions, and (4) the same order of crystallization is repeated in each layered body. It is difficult to associate the non-differentiated bodies with the layered ones except by their close proximity in space. The model proposed for the physical evolution of the ultramafic-gabbroic intrusions must, therefore, include provisions for the cyclic layering exhibited in the strata of the Munro Lake sill, the simple fractional differentiation sequence illustrated by the Ghost Range type of intrusion, and the scattered wholly gabbroic or ultramafic bodies.

The sequence of rock types exhibited in the Munro Lake sill is readily divisible into cycles which contain the mineral phases as they accumulated on the chamber floor. There are no features to contradict the hypothesis that the layers within each cycle are the result of differentiation, not successive injections of different magma. A model may be set up to allow for development of such a sequence if it is proposed that new magma was injected into the chamber from time to time and crystallized in batches. It can further be assumed that each batch of magma had essentially the same composition. Fractional crystallization proceeded between injections, with the cumulate phases piling up on

the chamber floor. Since the chamber was open to the introduction of new magma, then we can similarly suggest that the old magma was largely flushed out of the chamber as the new entered, although it is probable that there would be some contamination of the new liquid by the residual liquid at each stage. An effective mechanism for changing the liquid at intervals within the chamber would exist if the chamber were part of or connected to a major volcanic channelway.[1]

---

[1] A model very similar to that proposed by Brown (1956) to explain the repetitive sequence of the ultramafic rocks of Rhum, Inner Hebrides.

Various bodies showing a single fractional crystallization sequence would develop if magma were injected along certain horizons, forming chambers which remained closed to further magmatic disturbance. Such would be the case if magma from the major volcanic center hypothesized above were to be emplaced outside the main channelway. On the other hand, intrusions of wholly gabbroic composition could be emplaced if, during fractional differentiation of a magma, a major disturbance, say, an earthquake, were to cause residual liquid from one chamber to be expelled and emplaced in a new location. Wholly ultramafic bodies would develop if an olivine crystal mush were emplaced - such an origin is commonly accepted for many peridotite bodies, particularly those of alpine belts. Such an olivine mush was derived from accumulation by differentiation, either from a "lower" chamber or from pockets of magma in the main channelway during periods of quiescence. A schematic structural cross section between Centre Hill and Warden-Munro is shown in Fig. 50.

Evidence that each pulse of magma into the Munro Lake chamber was of essentially the same composition comes from the fact that minerals and trace elements revert to approximately the same level at the start of each cycle, although there is a general trend through the cycles to more acidic composition. Complete conformability of internal contacts to external volcanic contacts indicates that the chamber was horizontal at the time of magma emplacement. Structural evidence of a channelway has not been found, but two factors work strongly against such a discovery: (1) post solidification deformation has been considerable, and (2) exposure in the region is not good.

The Ghost Range intrusion best illustrates the simple sequence of peridotite-clinopyroxenite-gabbro. No cyclic layers are apparent and it can be assumed that intrusions of this type represent solidification in an essentially horizontal chamber of the fractionation products from one pulse of magma.

Wholly ultramafic or gabbroic intrusions are closely associated in space with the Munro Lake sill. Particularly between Centre Hill and Warden-Munro sections in Munro township numerous bodies of very restricted composition crop out. In this respect, the location of the ultramafic bodies with respect to the Munro Lake sill is significant. It has been recorded in a previous section that all the mapped wholly ultramafic bodies lie stratigraphically above the sill. A similar situation has been described by Naldrett (1964) between the "Main Sill" and the "Overlying Lenses" of Dundonald township, some 28 miles to the south west of Centre Hill. This overlying position may be a coincidence of outcrop,

but this is too simple a conclusion and, in fact, it is more likely that their position reflects a fundamental genetic relationship with the Munro Lake sill. The crystal mush probably derived from the Munro Lake chamber and was pushed into roof fractures upon major volcanic disturbance. Although the ultramafic bodies are generally conformable to the surrounding rocks, minor discordance is common. Wholly ultramafic rocks are generally so severely altered that primary texture and mineralogy are destroyed. However, immediately south of the Potterdoal property in Munro township, a chill zone of a dunitic body is exposed which shows relict primary texture. Small, partially resorbed olivine grains are enclosed in a groundmass whose only other apparent primary feature is the development of very elongate amphibole needles. Texture, mineralogy, and chemical composition of rocks in the wholly gabbroic bodies closely resemble those of the upper gabbroic zone of the layered intrusions.

Some circumstantial evidence from a recent detailed study of the activity of Hawaiian volcanoes (Eaton and Murata, 1960) lends some support to the model. Eaton and Murata state that the time for a volcano to grow to maturity is fairly short, and the interval between eruptions of magma pulses is of the order of a few decades. Many magma pulses, particularly late-stage ones, do not reach the surface but flow into fissures which have been opened by earthquakes, these latter phenomena commonly preceding and accompanying volcanicity.

C. CALCULATED LIQUIDS

Both in the previous discussion and in the following calculations and considerations the analytical results have been taken to be repre-

sentative of the original rock, disregarding completely any changes in chemical composition due to serpentinization or associated alteration. This may be a dangerous practice since relatively little is known of element addition or subtraction accompanying serpentinization. As can be seen from the widespread occurrence of magnetite veinlets in highly serpentinized ultramafic rocks, iron is a particularly mobile component, and the size of sample taken in the field may be of considerable importance here. Naldrett (1964) calculated the possible Mg-Fe molecular ratio for fresh peridotite and compared this with the actual value of a serpentinized variety. He came to the conclusion that the ratio did not change significantly although the absolute abundance of both elements could decrease somewhat. Little change is to be expected in Ca content since the bulk of Ca is contained in clinopyroxenite, which is not readily serpentinized. Si, on the other hand, should increase considerably, although exact limits cannot be given.

Accordingly all calculated liquids must be taken as only first approximations of the real thing.

Munro Lake Sill

A rough estimate of the composition of the Munro Lake magma may be made by breaking the total sequence into the respective cycles and obtaining average compositions for the three principal rock types - peridotite, clinopyroxenite, and gabbro.

Across any section of a differentiated body, the true thickness of, say, a peridotite layer is not only a reflection of the composition of the magma, but also some indication of its volume, more specifically,

the height of liquid above the floor. For this reason, the thickness of each cyclic unit in the Munro Lake sill should be condensed according to some reference unit. We will assume (1) that the total thickness of rock in the final unit is the true thickness of chamber that was available to the final pulse of magma, (2) that the thickness is maintained throughout the chamber, and (3) that no magma escaped through fissures. Using this final unit as the reference unit, all other units can be condensed according to the ratio of reference unit thickness to total distance of the base of any particular unit from the chamber roof.[1]

---

[1] For example, to calculate the condensed thickness of layer 13 of the Centre Hill section, we note that its thickness is 95', the total distance from the base of cyclic unit 6 (in which it is contained) to the roof of the chamber is 953', and the thickness of the reference unit (cyclic unit 7) is 735'. Thus, the condensed thickness of layer 13 is $\frac{95 \times 735}{973} = 73.3$ feet.

A detailed calculation may be done for the Centre Hill data, since here a complete section is exposed (Fig. 51). The condensed thickness of each layer is given in Table XII, and compositions of the "average" peridotite, clinopyroxenite, and gabbro are shown in Table XIII. The composition of the central gabbro is assumed to represent the last crystallized liquid, and average compositions and thicknesses are used to obtain the second-last, third-last, and initial liquids (Table XIII).

Fig. 51. Diagrammatic Condensed Section of Centre Hill

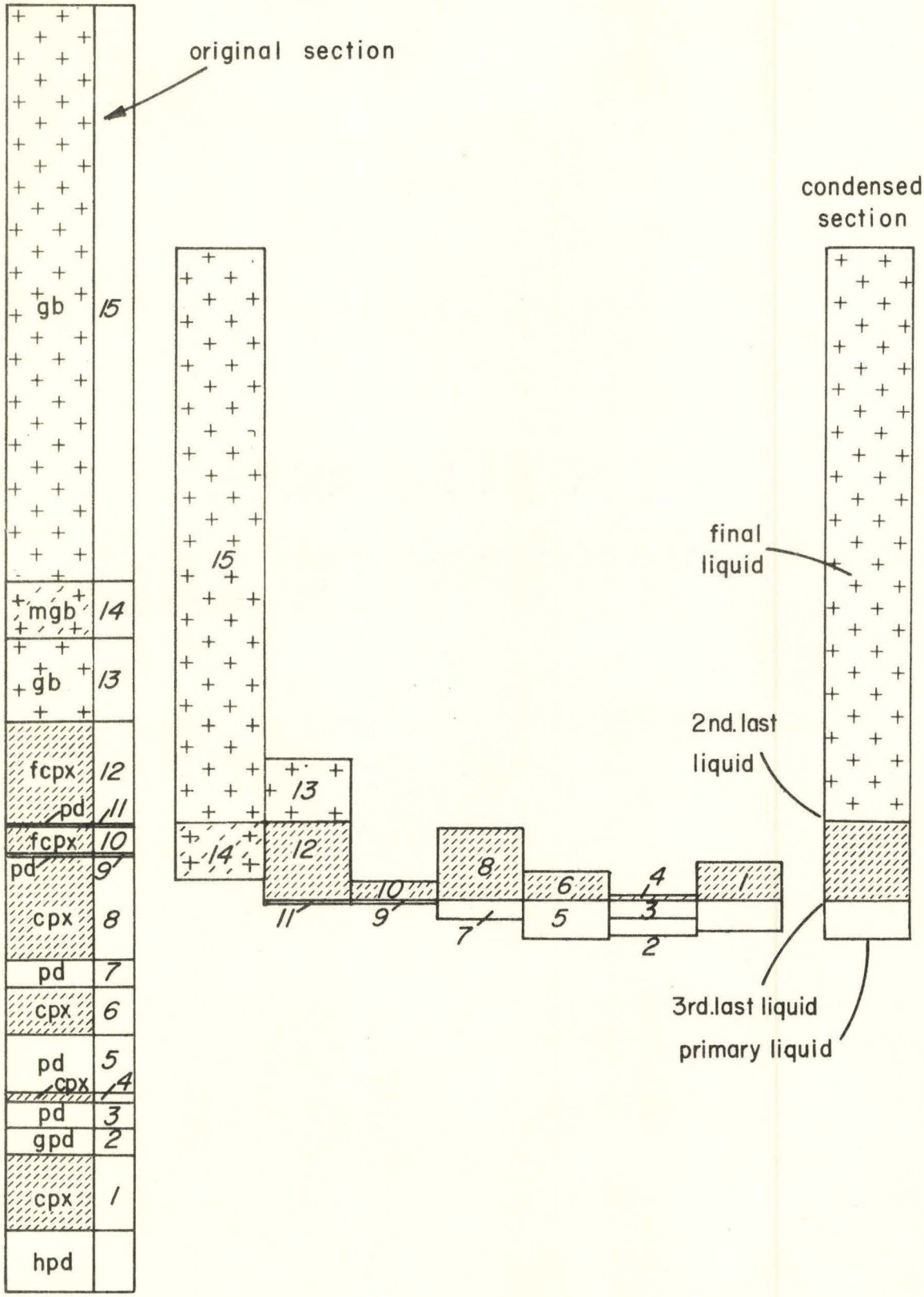

Table XII. Layer thicknesses for condensed section Centre Hill

CYCLIC UNIT	LAYER	ORIGINAL THICKNESS	CONDENSED THICKNESS
7	15	670 (feet)	670 (feet)
	14	65	65
			735
6	13	95	73.3
	12	120	92.5
	11	3	2.3
			168.3
5	10	30	22.4
	9	3	2.2
			24.6
4	8	119	84.5
	7	30	21.3
			105.8
3	6	55	34.8
	5	70	44.3
			79.1
2	4	10	6.0
	3	30	17.9
	2	30	17.9
			31.8
1	1	90	44.4
	LMZ	70	34.5
			78.9

Table XIII. Average composition of three major rock types and composition of liquids for Centre Hill section of Munro Lake sill

	A	B	C	D	E	F	G
SiO_2	51.40	51.71	43.73	55.34	51.40	51.46	51.04
TiO_2	1.46	.63	.35	1.49	1.46	1.36	1.30
Al_2O_3	13.77	4.22	2.93	13.20	13.77	12.61	12.07
Fe_2O_3	3.12	1.24	10.47	3.76	3.12	2.89	3.31
FeO	11.97	8.32	6.19	12.29	11.97	11.52	11.23
MnO	.21	.19	.24	.24	.21	.21	.21
MgO	5.36	15.54	31.79	2.03	5.36	6.59	7.97
CaO	8.19	17.20	4.05	5.99	8.19	9.28	8.99
Na_2O	4.24	.88	.19	5.22	4.24	3.83	3.60
K_2O	.19	.04	.03	.23	.19	.17	.16
P_2O_5	.09	.01	.03	.21	.09	.08	.08
Total	100.00	99.98	100.00	100.00	100.00	100.00	99.96

A: average gabbro; B: average clinopyroxenite; C: average peridotite

D: final liquid = sample 25-12

E: 2nd last liquid = average gabbro comp.

F: 3rd last liquid = (av.gb.)x(cond.thickness gb)+(av.cpx.)x(cond. thickness cpx)

G: initial liquid = (av.gb.)x(cond.thickness gb.)+(av.cpx.)x(cond. thickness cpx.)+(av.pd.)x(cond.thickness pd.)

Liquids cannot be computed for the Warden-Munro section since this section is incompletely exposed. However, rough average compositions of the three major rock types here (Table XIV) compared with the similar average compositions from Centre Hill show close similarity between the two peridotite and clinopyroxenite compositions, but the Warden-Munro gabbro is significantly more silica-rich and iron-poor than its Centre Hill equivalent. Since the Warden-Munro section is much less thoroughly sampled than the Centre Hill section, the apparent discrepancy in composition is not serious.

Ghost Range Intrusion

The upper contact of the Ghost Range sill is not exposed, thus true thickness of the intrusion is not known. Mineral variation diagrams and textural features, however, indicate that the "effective top" is within the granophyric zone of the gabbro layer. For the purpose of estimating composition of the intrusion, the top has been taken at the center of the granophyric zone. The average thickness of the various layers are here estimated as 500 feet of peridotite, 20 feet of clinopyroxenite, and 2000 feet of gabbro, for a total section thickness of 2520 feet. Five rapid silicate chemical analyses of the Ghost Range rocks were completed: 2 peridotite, 1 clinopyroxenite, and 2 gabbro. The pairs of peridotite and gabbro analyses have each been averaged and the resultant composition assumed to apply over the total thickness of each rock type. The various calculated liquid compositions are shown in Table XV.

Table XIV. Average Compositions of Major Rock Types of Warden-Munro Section

	A	B	C
SiO_2	42.99	50.95	54.42
TiO_2	.23	.41	1.07
Al_2O_3	1.77	2.42	14.90
Fe_2O_3	10.54	1.48	1.36
FeO	5.48	7.73	8.77
MnO	.22	.19	.16
MgO	36.13	18.87	6.33
CaO	2.55	17.58	9.11
Na_2O	.04	.33	3.30
K_2O	.04	.02	.47
P_2O_5	.01	.01	.10
Total	100.00	99.99	99.99

A: average peridotite (M-113 x .3 plus M-124 x .2 plus M-356 x .08)

B: average clinopyroxenite (M-369 x .385 plus M-118 x .4)

C: average gabbro (M-337 x .46 plus M-325 x .1 plus M-363 x .4 plus M-333 x .2)

Table XV. Average composition of three major rock types and compositions of successive liquids for Ghost Range intrusion

	A	B	C	D	E	F	G
SiO_2	44.20	51.03	53.12	56.21	53.12	52.78	51.13
TiO_2	.16	.29	.80	1.39	.80	.79	.67
Al_2O_3	5.37	5.32	14.79	13.27	14.79	14.63	12.79
Fe_2O_3	3.20	.62	1.83	2.95	1.83	1.81	2.08
FeO	8.78	6.60	7.71	10.82	7.71	7.67	7.88
MnO	.18	.15	.15	.19	.15	.15	.15
MgO	33.39	19.79	8.20	4.14	8.20	8.28	13.24
CaO	4.45	15.87	10.58	6.96	10.58	10.59	9.37
Na_2O	.11	.32	2.33	3.19	2.33	2.30	1.87
K_2O	.08	.00	.92	.73	.92	.91	.74
P_2O_5	.02	.01	.09	.15	.09	.09	.08
Total	99.94	100.00	100.52	100.00	100.52	100.00	100.00

A: average peridotite: M-232 + M-218/2
B: average clinopyroxenite: M-220
C: average gabbro: M-221 + M-323/2
D: final liquid: M-323
E: 3rd. last liquid: average gabbro
F: 2nd. last liquid: average gabbro + average clinopyroxenite
G: initial liquid: average gabbro + average clinopyroxenite + average peridotite

Chill Zone Characteristics

No true chill phase exists at the Centre Hill section of the Munro Lake intrusion, although the border rocks are significantly different from the inner rocks. At the base of the section is a 70 foot-wide layer of hornblende peridotite, distinguished by red-brown colour, small to medium sized poikilitic plates of hornblende, and very small cumulus olivine grains. It is suggested that this rock phase resulted from the solidification against relatively cold volcanic rocks of basaltic magma carrying partially resorbed olivine grains. Sufficient water was provided by the wall rocks to produce hornblende rather than clinopyroxene in a matrix position. The upper contact, although characterized by fine-grained somewhat mafic gabbro, cannot be termed a chill phase typical of the intruded magma.

At Warden-Munro, a wide chill zone exists against the upper chert wall rocks, and narrower chill zones against the chert slabs found within the intrusion. Presumably the internal chert blocks and slabs resulted from a stoping action during intrusion and solidification of the magma. Development and preservation of a chill phase typical of the intruded magma is improbable under such conditions. As expected, the composition of the chill phases is much more acidic than the bulk magma composition could have been.

A chill phase was sampled and analyses from the north end of the Garrison sill. Although this sill is not of the same type as the Munro Lake intrusion, in that there is no apparent cyclic repetition of phase layers, the magma for both is assumed to have derived from a common source. Assuming the composition of the Garrison chill phase to be representative

of the initial liquid, comparison of its composition and the calculated composition of the Munro Lake sill lends some support to the hypothesis of a common source. Table XVI shows these compositions as compared to those of various other layered intrusions.

D. COURSE OF CRYSTALLIZATION

MgO FeO-Fe_2O_3-SiO_2 System

Osborn (1959) has shown that two fundamentally different courses of crystallization of magma are possible depending upon whether (1) total composition of the magma (liquid plus crystals) remains constant, or (2) partial pressure of oxygen remains constant. The pO_2 (partial pressure of oxygen) is controlled by the water content of the magma. The principal factors operating to decrease pO_2 are (1) decreasing temperature, which reduces the rate of dissociation of water; and (2) continual use of a small amount of oxygen by crystallizing processes, this in turn tending to increase the hydrogen partial pressure. Opposing these effects are two other factors which tend to increase pO_2: (1) continual crystallization of anhydrous minerals results in enrichment of water in the liquid phase, thus an increase in pO_2; and (2) the rate of diffusion of hydrogen is probably high, thus the dissociation of water equilibrium is altered in the direction of increasing pO_2.

Variation in the trend of liquid composition is illustrated in Fig. 52 for conditions of constant total composition, constant pO_2, and increasing pO_2. Fig. 53 shows the actual trends for the Centre Hill liquids as compared with data from Osborn. Points 1, 2, and 3 of the Centre Hill trend, designating the initial and two succeeding

Table XVI. Comparison of Centre Hill and Garrison compositions with other layered intrusions

	A	B	C	D	E	F
SiO_2	51.53	50.99	48.40	51.11	51.28	51.04
TiO_2	.34	.45	1.33	1.07	1.79	1.30
Al_2O_3	18.70	17.75	18.48	13.66	13.19	12.07
Fe_2O_3	.28	.26	1.24	1.18	1.20	3.31
FeO	9.03	9.94	8.66	9.16	13.70	11.23
MnO	.47	.15	.12	.18	.28	.21
MgO	6.85	7.72	8.16	9.78	6.82	7.97
CaO	10.97	10.53	10.87	11.32	7.24	8.99
Na_2O	1.58	1.87	2.44	1.81	4.04	3.60
K_2O	.14	.24	.21	.64	.32	.16
P_2O_5	.09	.09	.08	.10	.14	.08
Total	100.00	99.99	99.99	100.01	100.00	99.96

A-Bushveld, B-Stillwater, C-Skaergaard, D-Muskox, E-Garrison, F-Centre Hill

A, B, C, D: cf. Smith and Kapp, 1963.

Fig. 52. Curves for comparing changes in composition of liquid as mixture of given composition (n) is fractionally crystallized under conditions of (1) constant total composition, (2) constant pO_2, (3) increasing pO_2 (Osborn, 1959).

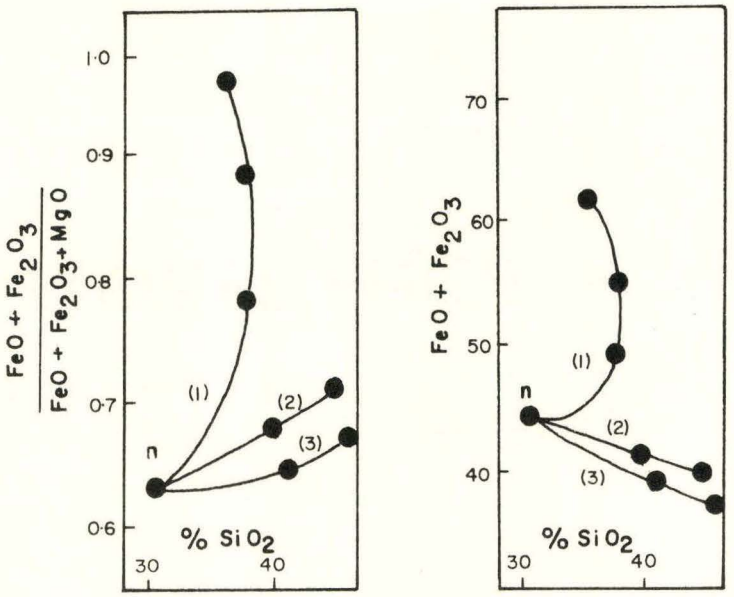

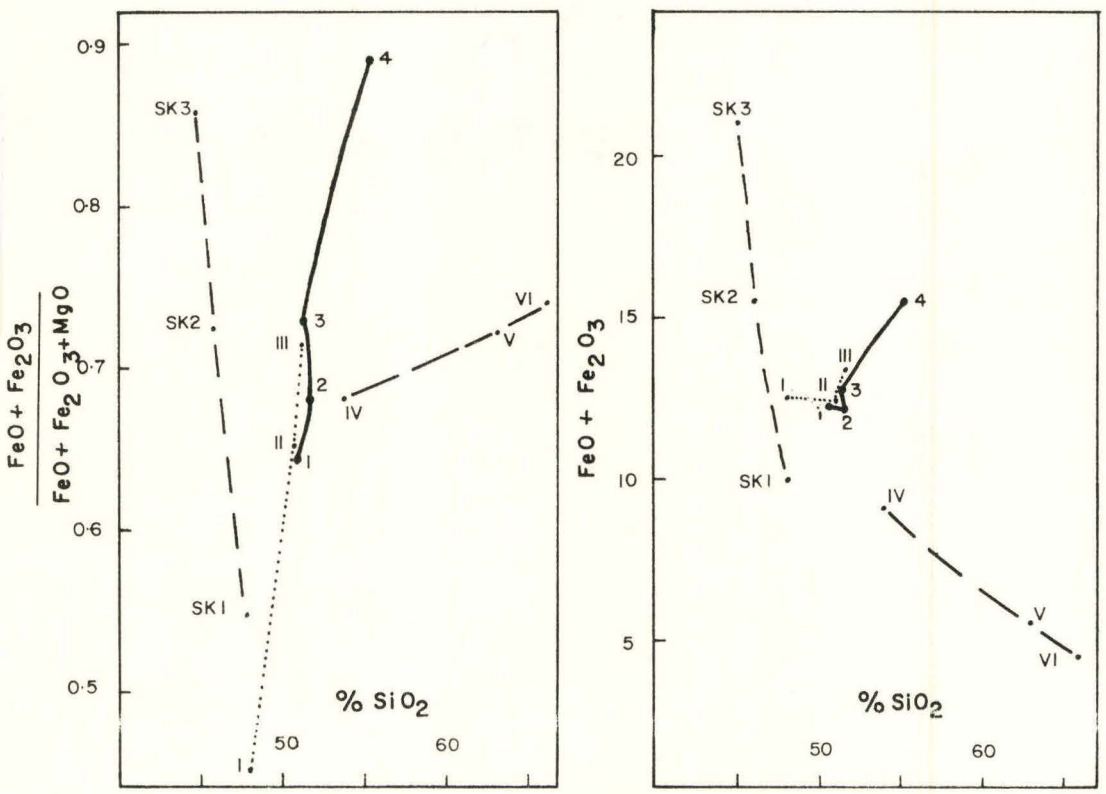

Fig. 53. Curves for liquid trend of Centre Hill magma (1-4) as compared to Skaergaard (Sk), tholeiitic basalt (I-III), andesite-rhyodacite (IV-VI). Data from Osborn, 1959.

liquid compositions, closely approximate the shape of the ideal curve of constant total composition; from point 3 to 4, the trend is slightly toward that of constant pO_2. This course of crystallization is just what should be expected; while the chamber is open to the introduction and expulsion of batches of magma, the pO_2 should decrease somewhat as volatiles escape, but total composition should remain fairly constant.

Diopside-Forsterite-Silica System

The liquidus diagrams of the system diopside-forsterite-silica (weight per cent) is shown in Fig. 54A. Kushiro (1964) found that both the Fo_{ss}-Di_{ss} and the Fo_{ss}-En_{ss} boundaries shift toward forsterite with increasing pressure. At 1 atmosphere, the reaction point A is in the silica-oversaturated part of the system, but at 20 kilobars the equivalent invariant point P (which is either (i) a reaction point where the reaction $En_{ss}+L = Di_{ss}+Fo_{ss}$ takes place or (ii) a ternary eutectic $Fo_{ss}+Di_{ss}+En_{ss}+L$) is within the silica-undersaturated area.

Fig. 54B shows the normative positions of analysed rocks, with the areas of peridotite and clinopyroxenite outlined. The points are projections from the tetrahedron including iron oxide to the Di-Fo-Silica plane. Two points are shown for each peridotite sample; the first was calculated from the original analysis and the second from an adjusted analysis in which Fe^3 has been converted to Fe^2. This step was taken so that the maximum possible effect of oxidation during serpentinization can be illustrated. If the rock had only been hydrated and oxidized during alteration, then its original norm should lie somewhere between the two extremes.

FIGURE 54

A: Synthetic system diopside-forsterite-silica, after Kushiro, 1964

B: Norm plots of all analysed rocks. For peridotite, ○ -unaltered analysis, ● -Fe^3 converted to Fe^2. x -Centre Hill calculated liquids

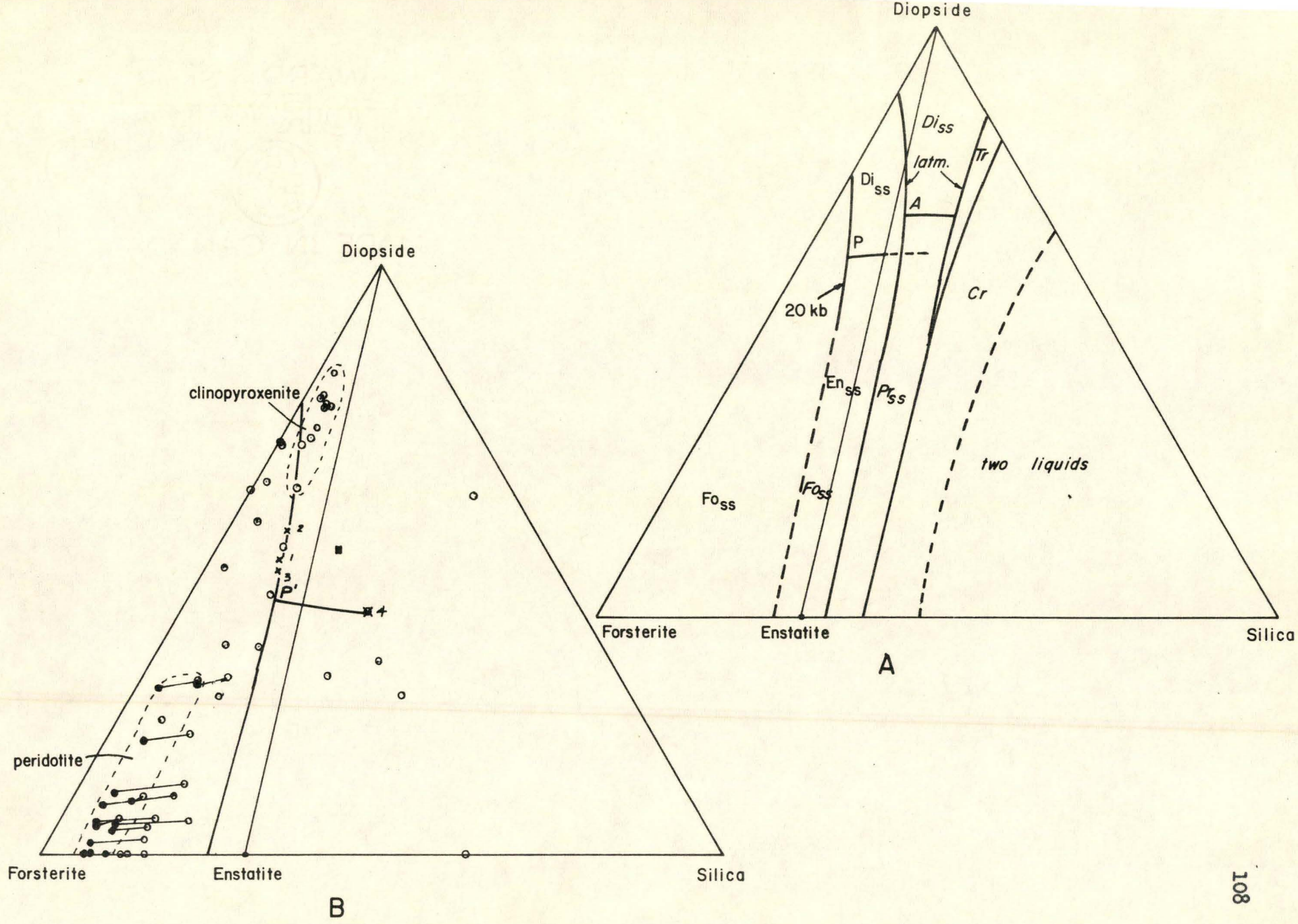
Diopside
Di ss
latm.
Tr
A
P
20 kb
Cr
En ss
Pr ss
two liquids
Fo ss
Fo ss
Forsterite
Enstatite
Silica
A
Diopside
clinopyroxenite
peridotite
Forsterite
Enstatite
Silica
B

The norms of the liquids calculated from the Centre Hill section are also plotted on Fig. 54B. The 'Primary' liquid (L1) and the two succeeding liquids (L2 and L3) lie very close to the Fo_{ss}-En_{ss} boundary outlined by Kushiro for a pressure of 20 kilobars on the synthetic system. The Di_{ss}-En_{ss} boundary, and thus the invariant point P', is defined by the final liquid point (L4). Perhaps due to the addition of iron as a component to the system, this boundary line is lower than in the synthetic system.

The principal conclusions that can be drawn from these diagrams are (1) the primary magma was an olivine tholeiitic liquid, and (2) the invariant point P' is not in the silica-oversaturated part of the system, suggesting fairly high pressure during emplacement and crystallization.

VII. PETROGENESIS OF PLUTONS AND ORIGIN OF MAGMA

A. CRITERIA OF CLASSIFICATION

It has become more or less standard practice to attempt to classify each mafic or ultramafic pluton studied between the limits of alpine type (also called ultramafic type) and stratiform (also called gabbroic type). The criteria of classification have been developed over the past 30 years and deal with three principal areas of investigation: (1) the tectonic condition of the area at time of emplacement, (2) the physical characteristics within the intrusion, and (3) the chemical characteristics of the initial magma (Smith, 1958). While in theory a pluton can be classed in either pure type on the basis of these criteria, in practice the distinction is not so clear. For example, a magma of the same composition can give rise to a stratiform type of body by a process of prolonged differentiation in a quiescent environment, but produce a completely undifferentiated pluton of alpine type in a tectonically active belt. Essential differences as summarized by Smith are listed below (points 1 to 6 inclusive in Table XVI). Thayer (1960) added the characteristics of general form, lineation, and associated chromite (points 7 to 10 in Table XVI).

B. APPLICATION TO ABITIBI INTRUSIONS

In the Abitibi region, geosynclinal sediments - argillite and greywacke - are common to the south of the intrusive belt, while the country rocks within the belt are mainly andesitic and basaltic volcanic

Table XVII. Criteria for comparison of two types of ultramafic plutons. Points 1-6 incl. after Smith (1958); points 7-10 after Thayer (1960)

Feature	Ultrabasic pluton	Gabbroic layered pluton
1. Relation to orogenic belts	Intruded into rocks of eugeosynclinal facies during the early stages of mountain building	Intruded into plateau areas
2. Associated igneous rocks	Gabbroic facies minor	Extensive sill, dykes, and related rocks of gabbroic composition
3. Layering	Rare, except for banding due to various proportions of olivine and pyroxene, without cryplayering	Layered according to specific gravity and mineral composition (cryptic layering)
4. Nature of border zone	Has the same composition as mass of pluton	Has chill zone of intermediate composition representing composition of primary magma
5. Extent of contact metamorphism	Minor effect on adjacent country rock	Greater metamorphic effect on adjacent country rock
6. Chemical composition	Ultrabasic Mg/Fe ratio greater than 7.5 Lime and alumina content low	Basaltic Mg/Fe ratio less than 7.5 Lime and alumina content high
7. Form	Irregular; larger masses may be floored	Lopolithic; floored
8. Lineation	Lineation common, may cross layering	Lineation very rare; associated with convection features
9. Texture	Texture allotriomorphic to cataclastic; poikilitic texture rare	Texture dominated by euhedral settled crystals, modified by reaction with entrapped interstitial magma; poikilitic texture prominent
10. Chromite distribution	Ore bodies in peridotite, scattered at random or near contacts with gabbroic rocks	Chromitites in regular stratigraphic positions in ultramafic rocks

flows. The intrusions are later than the sedimentary sequence and there is no structural evidence to suggest that they were intruded during a major orogenic upheaval.

The gabbroic rocks of the Munro Lake sill and the Ghost Range intrusion are genetically related to the ultramafic rocks that underly them, the principal evidences being: (1) the presence of an intermediate clinopyroxenite, (2) local interbanding of their contacts, (3) no suggestion of chill phases between the two, and (4) gravity stratification carrying over from the upper ultramafic rocks to the lower gabbroic rocks.

With regard to chemical composition, the parameter Mg/Fe molecular ratio was found by Hess (1938) to be a useful means of classification. If the ratio were less than 7.5 in ultramafic rocks, the whole pluton could be classed as stratiform or gabbroic type. All the dunite, peridotite, and clinopyroxenite samples analysed in the present study have Mg/Fe molecular ratios below 7.5 with the exception of samples M-200 and M-201, both serpentinized ultramafic rocks in the Garrison sill (Table XVII). However, while the sill should be classed as alpine on the basis of these two samples, a third peridotite sample, M-202, has an Mg/Fe ratio of 5.3. All three samples were collected at regular intervals along a single section line with M-202 closest to the top of the ultramafic zone (see Fig. 34). There is, therefore, some doubt that the Mg/Fe ratio can be considered an infallible criterion, particularly where serpentinization has been extensive.

Table XVIII. Mg/Fe atomic ratio of ultramafic rocks of all localities

Sample	Wt.%MgO	Wt.%Mg	÷ at.wt.Mg	Wt.%Fe_2O_3 [i]	Wt.%Fe	÷ at.wt.Fe	Mg/Fe
M113	33.25	20.05	.825	14.80	10.36	.185	4.5
M118	20.03	12.08	.497	10.52	7.36	.132	3.8
M124	33.77	20.36	.838	14.51	10.16	.182	4.6
M141	33.93	20.47	.842	14.29	10.00	.179	4.7
M142	18.55	11.19	.460	6.58	4.61	.082	5.6
M143	16.58	10.00	.412	10.08	7.06	.126	3.3
M162	18.80	11.34	.467	8.26	5.78	.103	4.5
M166	27.90	16.82	.692	13.26	9.28	.166	4.2
M200	38.83	23.41	.963	5.69	3.98	.071	13.5
M201	36.20	21.83	.898	9.17	6.42	.115	7.8
M202	29.13	27.57	.723	10.83	7.58	.136	5.3
M218	32.05	19.33	.795	11.56	8.09	.145	5.5
M220	19.01	11.46	.472	7.65	5.36	.096	4.9
M232	28.66	17.28	.711	11.99	8.39	.150	4.7
M356	22.75	13.72	.565	15.34	10.74	.192	2.9
M369	16.80	10.13	.417	9.13	6.39	.114	3.7
24-08	20.6	12.4	.510	14.52	10.19	.182	2.8
24-10	27.0	16.3	.671	13.77	9.65	.173	3.9
24-13	16.0	9.6	.395	10.36	7.25	.130	3.0
24-18	30.8	18.5	.761	16.04	11.20	.200	3.8
24-23	30.1	18.1	.745	16.04	11.20	.200	3.7
24-26	17.1	10.3	.425	8.69	6.09	.109	3.9
24-28	30.2	18.2	.750	16.54	11.60	.208	3.6
24-33	14.9	9.0	.370	11.47	8.03	.144	2.6
24-35	12.9	7.8	.321	10.54	7.38	.132	2.4
25-08	7.1	4.3	.177	20.01	14.00	.250	0.7

[i] Total Fe as Fe_2O_3

Gross chemical and mineralogical variations previously outlined within the layered bodies point to an origin by differentiation, regardless of the composition of the initial magma emplaced.

The isolated wholly ultramafic bodies that crop out sporadically through Munro and McCool townships can tentatively be considered alpine type since there is no apparent differentiation within them other than development of pyroxene-rich borders. Mg/Fe molecular ratios are not at present available for these bodies.

C. ORIGIN OF MAGMA

Hypotheses concerning the origin and nature of primary magma are plentiful and varied. One must look to subcrustal or upper mantle regions to procure magmas of mafic to ultramafic composition, and too little is known about all conditions in these regions to limit wild hypothesizing.

One is tempted to settle for the simplest explanation possible, this being that the primary magma is a basalt which derived from the fusion of eclogite (Yoder and Tilley, 1962). Two principal basalt trends exist; (1) alkalic, and (2) tholeiitic; and both have chemically equivalent eclogites. By varying the pressure either trend can be produced from the same initial bulk composition; alkali basalt magma is derived under greater pressure (greater depth) than tholeiitic basalt. The eclogite itself, assuming the above hypothesis to be correct, may be the partial melting product of a more mafic rock, for example a garnet peridotite.

REFERENCES

Brown, G.M., 1956, The layered ultrabasic rocks of Rhum, Inner Hebrides: Phil. Trans. Royal Soc. London Series B, No. 668, vol. 240.

_____ and Vincent, E.A., 1963, Pyroxenes from the late stages of fractionation of the Skaergaard Intrusion, East Greenland: Jour. Petrol., vol. 4.

Buddington, A.F. and Lindsley, D.H., 1964, Iron-titanium oxide minerals and synthetic equivalents: Jour. Petrol., vol. 5, part 2.

Coombs, D.S., 1963, Trends and affinities of basaltic magmas and pyroxenes as illustrated on the diopside-olivine-silica diagram: Min. Soc. Am. Special Paper 1.

Eaton, J.P. and Murata, K.J., 1960, How volcanoes grow: Science, vol. 132, pp. 925-38.

Fahrig, W.F. and Wanless, R.K., 1963, Age and significance of diabase dyke swarms of the Canadian Shield: Nature, vol. 200.

Grubb, P.L.C., 1962, Serpentinization and chrysotile formation in the Matheson ultrabasic belt, northern Ontario: Econ. Geol., vol. 57.

Hall, A.L., 1932, The Bushveld igneous complex of the central Transvaal: Geol. Survey S. Africa, Mem. 28.

Hendry, N.W., 1951, Chrysotile asbestos in Munro and Beatty townships, Ontario: Trans. Can. Inst. Min. Met., vol. LIV.

Hess, H.H., 1933, The problems of serpentinization: Econ. Geol., vol. 28.

_____ 1938, A primary peridotite magma: Am.Jour.Sci., vol. XXXV, No. 209.

_____ 1949, Chemical composition and optical properties of the common clinopyroxenes, Part I: Am. Min., vol. 34.

Hess, H.H., 1960, Stillwater igneous complex: Mem. 80, Geol. Soc. Am.

Hewitt, D.F. and Satterly, J., 1953, Asbestos in Ontario: Ont. Dept. Mines, Industrial Mineral Circular No. 1.

Irvine, T.N. and Smith, C.H., 1965, Cyclic units in the Muskox intrusion, N.W.T., Canada: Transaction, Am. Geoph. Union, vol. 46, No. 1.

Jackson, E.D., 1963, Stratigraphic and lateral variation of chromite composition in the Stillwater complex: Min. Soc. Am. Special Paper 1.

Jambor, J.L. and Smith, C.H., 1963, Accurate determination of olivine composition with small diameter x-ray powder cameras: Min. Mag., vol. 33, No. 264.

Kushiro, I., 1964, The system diopside-forsterite-enstatite at 20 kilobars: Carnegie Institution of Washington Year Book 63.

MacRae, N.D., 1963, Petrology of the Centre Hill complex: unpublished M.Sc. thesis, McMaster University.

McIntire, W.L., 1963, Trace element partition coefficients: Geochim. et Cosmochim. Acta, vol. 27.

Neumann, H., Mead, J. and Vitaliano, C.J., 1954, Trace element variation during fractional crystallization as calculated from the distribution law: Geochim. et Cosmochim. Acta, vol. 6, pp. 90-99.

Osborn, E.F., 1959, Role of oxygen pressure in the crystallization and differentiation of basaltic magma: Am.Jour.Sci., vol. 257.

Prest, V.K., 1951, Geology of Guibord township: Ont. Dept. Mines, vol. LX, Pt. IX.

Reeves, J.E., 1950, The Ghost Range basic intrusion: unpublished M.Sc. thesis, McMaster University.

Ross, C.S., Foster, M.D. and Myers, T.A., 1954, Origin of dunite and of olivine-rich inclusions in basaltic rocks: Am.Min., vol. 39.

Satterly, J. and Armstrong, H.S., 1947, Geology of Beatty township: Ont. Dept. Mines, vol. LVI, Pt. VII.

_____ 1948, Geology of Michaud township: Ont. Dept. Mines, Vol. LVII, Pt. IV.

_____ 1949, Geology of Garrison township: Ont. Dept. Mines, vol. LVIII, Pt. IV.

_____ 1951, Geology of Harker township: Ont. Dept. Mines, vol. LX, Pt. VII.

_____ 1951, Geology of Munro township: Ont. Dept. Mines, vol. LX, Pt. VIII.

_____ 1952, Geology of McCool township: Ont. Dept. Mines, vol. LXI, Pt. 5.

_____1953, Geology of the north half of Holloway township: Ont. Dept. Mines, vol. LXII, Pt. 7.

Shapiro, L. and Brannock, W.W., 1962, Rapid Analysis of Silicates, Carbonate and Phosphate Rocks: Geol. Survey Bull. 1144-A.

Shaw, D.M., 1964, Principles of machine computation of spectrochemical analysis: Canadian Spectroscopy, vol. 10, No. 1.

Smith, C.H., 1958, Bay of Islands igneous complex, western Nfld.: G.S.C. Memoir 290.

_____ and Kapp, H.E., 1963, The Muskox Intrusion: Min. Soc. of Am. Special Paper 1.

Taylor, F.C., 1955, The petrology of the serpentine bodies in the Matheson district, Ontario: unpublished Ph.D. thesis, McGill University.

Thayer, T.P., 1960, Some critical differences between alpine-type and stratiform peridotite-gabbro complexes: Rep. 21st session, Int. Geol. Cong.

Thayer, T.P., 1963, Flow-layering in alpine peridotite-gabbro complexes: Min. Soc. of Am. Special Paper 1.

Wager, L.R. and Deer, W.A., 1939, Geological investigations in east Greenland, Part III, Petrology of the Skaergaard intrusion, Kangerdluzssuag, east Greenland: Med om Grønland Bd. 105, No. 4.

_____ and Mitchell, R.L., 1951, The distribution of trace elements during strong fractionation of basic magma - a further study of the Skaergaard intrusion, east Greenland: Geochim. et Cosmochim. Acta, vol. 1.

_____, Vincent, E.A. and Smales, A.A., 1957, Sulphides in the Skaergaard intrusion, east Greenland: Econ. Geol., vol. 52.

_____, Brown, G.M. and Wadsworth, W.J., 1960, Types of igneous cumulates: Jour. Petrol., vol. 1.

_____, 1963, The mechanism of adcumulus growth in the layered series of the Skaergaard intrusion: Min. Soc. of Am. Special Paper 1.

Yoder, H.S. and Tilley, C.E., 1962, Origin of basalt magmas: Jour. Petrol., vol. 3, No. 3.

APPENDIX 1

Modal Analyses

Sample	Rock Type	Location	Ol.	Cpx.	Plag.	Opaq.	Opx.	Qtz.	Grano.	Apat.
M-13	fcpx	M	-	46.0	26.8	5.0	(18.8)*	3.4	-	tr
M-14	gb	M	-	20.2	46.4	4.6	(28.8)	-	-	-
M-17	gb	M	-	22.0	60.7	3.2	7.7	5.4	-	tr
M-18	fcpx	M	-	51.3	35.3	10.0	3.4	-	-	-
M-20	cpx	M	-	90	6	4	-	-	-	-**
M-21	fcpx	M	-	70.9	25.0	2.5	1.6	-	-	-
M-23	fcpx	M	-	60.6	28.6	3.4	(7.4)	-	-	-
M-24	fcpx	M	-	60.0	27.6	3.2	(9.2)	-	-	-
M-25	fcpx	M	-	50.6	39.4	5.2	4.8	-	-	tr
M-26	gb	M	-	46.4	38.0	2.6	13.0	-	-	-
M-29	gb	M	-	22.5	49.6	10.4	1.8	5.0	-	0.7
M-30	gb	M	-	28.3	53.7	3.7	14.3	tr	-	tr
M-32	gb	M	-	22.4	47.6	5.0	(22.7)	2.3	-	-
M-36	gb	M	-	33.0	53.6	5.8	7.6	-	-	tr
M-39	pd	M	47.0	29.5	11.0	0.5	12.0	-	-	-
M-42	gb	M	-	30	68	2	-	-	-	-**
M-48	gb	M	-	22.3	60.0	6.5	(11.2)	-	-	-
M-49	gb	M	-	24.6	60.1	4.0	8.2	3.1	-	tr
M-50	gb	M	-	41.6	55.2	3.2	-	-	-	tr
M-53	gb	M	-	31.3	49.8	3.1	-	15.0	-	0.8
M-54	gb	M	-	27.6	59.3	4.9	4.3	3.9	-	tr
M-56	and	M	-	15	84	0.5	0.5	-	-	-**
M-57	gb	M	-	38.0	50.0	0.6	10.8	0.6	-	tr
M-58	gb	M	-	31.4	58.4	0.4	9.8	-	-	-
M-60	fcpx	M	-	76.8	20.8	2.4	-	-	-	tr
M-61	gb	M	-	14.8	56.0	7.6	10.3	10.6	tr	0.7
M-62	gb	M	-	36.5	45.8	7.0	10.7	-	-	-
M-62A	gb	M	-	26.2	52.9	6.4	14.5	-	-	tr

Sample	Rock Type	Location	Ol.	Cpx.	Plag.	Opaq.	Opx.	Qtz.	Grano.	Apat.
M-67	gb	M	-	31.4	48.4	6.3	13.9	-	-	tr
M-68	gb	M	-	28.0	50.3	6.5	15.2	-	-	tr
M-69	gb	M	-	36.5	53.8	5.1	-	4.6	-	tr
M-70	fcpx	M	-	50.8	45.1	4.1	-	-	-	tr
M-71	fcpx	M	-	52.6	(43.6)	3.8	-	-	-	-
M-74	gb	M	-	36.0	56.2	3.0	-	8.8	tr	tr
M-76	gb	M	-	32.3	51.8	4.6	11.3	tr	-	tr
M-79	gb	M	-	19.9	51.5	6.6	(22.1)	-	-	tr
M-80	pd	M	59.0	40.5***		0.5	-	-	-	-
M-81	pd	M	60.8	37.7		1.5	-	-	-	-
M-82	fcpx	M	-	47.5	38.9	2.6	11.0	-	-	-
M-83	gb	M	-	24.3	47.0	5.7	23.0	-	-	tr
M-84	fcpx	M	-	57.2	27.9	3.2	11.7	-	-	-
M-85	fcpx	M	-	56.8	29.4	3.0	10.8	-	-	-
M-86	fcpx	M	-	53.6	36.4	5.6	4.0	0.6	-	-
M-88	grano	M	-	(22.0)	38.8	2.8	-	15.6	20.8	tr
M-90	gb	M	-	33.7	52.0	2.8	5.9	5.6	tr	tr
M-96	gb	M	-	41.6	43.4	1.6	13.4	-	-	-
M-97	gb	M	-	38.5	45.2	2.7	-	8.6	5.0	tr
M-102	pd	M	58.2	41.8		-	-	-	-	-**
M-112	gb	W-M	-	27	60	3	10	-	-	-**
M-113	pd	W-M	70	25	5	-	-	-	-	-**
M-117	pd	W-M	46.4	48.8	L	-	(4.8)	-	-	-
M-118	ol.cpx	W-M	12.0	84.5	2.0	-	1.5	-	-	-
M-119	pd	W-M	56	34	10	tr	-	-	-	-**
M-121	pd	W-M	66.5	17.5	15.0	1.0	-	-	-	-
M-122	pd	W-M	66.5	20.0	13.5	1.0	-	-	-	-
M-123	cpx	W-M	-	86.5	7.8	0.8	(4.9)	-	-	-
M-124	pd	W-M	66.4	28.0	5.6	tr	-	-	-	-
M-125	fcpx	W-M	-	77.4	10.6	1.8	(10.2)	-	-	-
M-126	fcpx	W-M	-	80.3	13.6	1.5	(5.2)	-	-	-

Sample	Rock Type	Location	Ol.	Cpx.	Plag.	Opaq.	Opx.	Qtz.	Grano.	Apat.
M-127A	fcpx	W-M	-	76.0	13.6	2.4	8.0	-	-	-
M-127	fcpx	W-M	-	84.9	12.4	0.8	1.9	-	-	-
M-128	gb	W-M	-	32.6	55.4	2.5	9.5	-	-	-
M-129	gb	W-M	-	34	56	1	-	9	-	-**
M-131	gb	W-M	-	39.0	43.5	2.5	15.5	4.5	-	-
M-137	diabase	M	-	30.0	57.6	6.2	3.7	2.5	-	tr
M-138	diabase	M	-	31.2	59.5	1.4	-	7.9	-	tr
M-140	pd	MH	77.3	12.7	8.0	2.0	-	-	-	-
M-141	pd	MH	70.0	13.5	13.5	3.0	-	-	-	-
M-142	cpx	MH	0.2	84.0	10.5	0.1	5.2	-	-	-
M-143	fcpx	MH	tr	82.3	16.4	1.3	tr	-	-	-
M-144	gb	MH	-	34.0	62.0	2.6	1.4	-	-	-
M-148	fcpx	MH	-	78.8	15.0	1.2	5.4	-	-	-
M-149	cpx	MH	-	78.2	9.9	1.5	10.4	-	-	-
M-150	gb	MH	tr	35.5	56.1	2.1	6.3	-	-	-
M-151	gb	MH	-	35.1	58.6	1.2	5.1	-	-	-
M-152	gb	MH	-	27.2	52.7	6.9	13.1	-	-	-
M-154	gb	MH	-	29.7	46.1	5.3	(18.9)	-	-	tr
M-158	pd	W-MH	68	32		tr	-	-	-	-**
M-160	cpx	W-MH	10.3	84.3	5.0	0.4	-	-	-	-
M-162	cpx	W-MH	9.9	83.8	5.9	0.4	-	-	-	-
M-163	gb	Mc	-	28.4	46.2	4.1	(10.0)	10.1	-	1.1
M-165	pd	Mc	56.5	19.4	23.8	0.3	-	-	-	-
M-166	pd	Mc	51.9	26.9	19.2	2.0	-	-	-	-
M-167	gb	Mc	-	37.4	44.6	0.8	(17.2)	-	-	-
M-168	gb	Mc	-	46.0	48.0	1.4	4.6	tr	-	-
M-169	grano	Mc	-	16.5	39.0	1.6	-	17.9	25.0	tr
M-171	gb	Mc	-	46.7	52.1	1.2	-	-	-	-
M-172	pd	Mc	50.3	17.5	22.5	0.5	-	-	-	-
M-173	pd	Mc	70.6	9.6	19.3	0.5	-	-	-	-
M-174	cpx	Mc	tr	61.1	(38.7)	0.2	-	-	-	-

Sample	Rock Type	Location	Ol.	Cpx.	Plag.	Opaq.	Opx.	Qtz.	Grano.	Apat.
M-175	pd	Mc	74.3	14.5	-	1.0	(10.2)	-	-	-
M-187	gb	GS	-	33.0	64.3	2.7	-	-	-	-
M-195	pd	GS	78.0	14.0	4.5	3.5	-	-	-	-
M-196	pd	GS	51.0	39.5	9.5	tr	-	-	-	-
M-198	gb	GS	-	50.0	43.0	2.0	-	5.0	-	-
M-200	pd	GS	81.7	11.8	5.0	1.5	-	-	-	-
M-201	pd	GS	73.5	15.0	2.0	0.5	9.0	-	-	-
M-202	pd	GS	73.0	12.0	6.0	3.0	6.0	-	-	-
M-203	gb	GS	-	45	40	tr	15	-	-	-**
M-204	gb	GS	-	47.0	46.4	tr	4.5	2.1	-	tr
M-205	gb	GS	-	56.8	42.4	0.8	-	-	-	tr
M-208	gb	GS	-	51	44	tr	5	-	-	-**
M-211	pd	GS	79.5	5.0	9.0	1.5	5.0	-	-	-
M-212	gb	GS	-	37	58	tr	5	-	-	-**
M-217	gb	GR	-	39.7	51.6	1.7	7.0	-	-	tr
M-218	pd	GR	66.5	11.0	19.0	3.5	-	-	-	-
M-220	fcpx	GR	-	59.8	39.8	0.4	-	-	-	-
M-221	gb	GR	0.5	46.2	46.9	tr	6.4	-	-	-
M-222	gb	GR	-	37.9	49.9	2.9	-	6.1	3.2	tr
M-223	gb	GR	-	34.0	42.9	9.1	-	5.0	9.1	tr
M-224	gb	GR	-	28.8	60.1	0.8	(10.3)	-	-	-
M-225	gb	GR	-	39.9	47.9	2.3	9.9	-	-	-
M-226	pd	GR	53.7	18.7	26.6	1.0	-	-	-	-
M-227	gb	GR	-	49	42	-	9	-	-	-**
M-229	gb	GR	-	35.0	51.0	1.5	(12.5)	-	-	-
M-230	gb	GR	-	40.7	51.7	0.3	7.3	-	-	-
M-231	pd	GR	54.3	22.0	20.7	3.0	-	-	-	-
M-232	pd	GR	56.1	21.4	21.0	1.5	-	-	-	-
M-233	pd	GR	62.9	20.7	13.4	3.0	-	-	-	-
M-234	pd	GR	60.1	19.2	19.2	1.5	-	-	-	-
M-235	fcpx	GR	6.2	75.2	14.9	tr	3.7	-	-	-
M-236	ol.cpx	GR	22.9	64.7	12.0	tr	0.4	-	-	-
M-237	gb	GR	-	42.6	44.3	tr	(13.1)	-	-	-

Sample	Rock Type	Location	Ol.	Cpx.	Plag.	Opaq.	Opx.	Qtz.	Grano.	Apat.
M-300	gb	GR	-	34.0	48.0	1.4	11.2	5.4	tr	tr
M-302	gb	GR	-	24.6	60.4	2.0	-	13.0	tr	-
M-307	grano	GR	-	19.6	40.2	3.8	-	9.2	27.2	tr
M-308	gb	GR	-	26.0	55.6	3.4	-	9.4	11.6	tr
M-311	gb	GR	0.5	39.8	45.6	tr	14.1	-	-	-
M-312	pd	GR	57	15	25	3	-	-	-	-**
M-316	gb	GR	-	52.4	38.6	tr	(9.0)	-	-	-
M-317A	gb	PL-Md	-	32.0	53.2	5.0	8.6	1.2	-	-
M-317B	gb	PL-Md	-	37.0	88.5	4.0	2.0	8.5	-	tr
M-317C	gb	PL-Md	-	45	54	1	-	-	-	-**
M-317D	diabase	PL-Md	-	35.8	44.0	2.5	(16.2)	1.5	-	-
M-317E	gb	PL-Md	-	35	58	1	2	4	-	-**
M-318	gb	PL-Mc	-	30.6	56.0	4.2	1.0	8.2	-	tr
M-319	gb	GR	-	45.0	50.6	2.0	-	2.4	-	tr
M-320	gb	GR	-	45.5	48.5	6.0	-	-	-	-
M-321A	grano	GR	-	(34.8)	40.6	3.4	-	7.0	14.2	tr
M-322	grano	GR	-	(32.6)	35.6	-	4.6	11.0	16.0	0.2
M-323	gb	GR	-	32.2	41.8	-	4.4	9.0	11.8	0.8
M-324	gb	GR	-	30.0	64.2	1.2	-	4.6	-	-
M-329	grano	W-M	-	29.0	41.8	4.8	2.0	8.8	13.4	tr
M-330	fcpx	W-M	-	75.5	23.3	1.2	-	-	-	-
M-331	fcpx	W-M	-	77.6	21.7	0.7	-	-	-	-
M-335	gb	W-M	-	38	52	2	-	8	-	-**
M-337	gb	W-M	-	38.0	51.5	tr	1.0	8.0	1.5	tr
M-338	gb	W-M	-	29.6	50.0	1.4	(14.2)	4.8	-	tr
M-339	gb	W-M	-	(53.0)	46.3	0.7	-	-	-	-
M-340	gb	W-M	-	33.2	45.4	2.0	(14.2)	5.0	-	-
M-341	gb	W-M	-	36	57	tr	1	-	-	-**
M-343	pd	GS	80	18		2	-	-	-	-**
M-349A	gb	GS	-	41	48	7	-	4	-	-**
M-351	fcpx	W-M	-	78.8	13.8	1.0	6.4	-	-	-
M-352A	cpx	W-M	-	85.6	(13.6)	0.8	-	-	-	-
M-353	ol.cpx	W-M	12.0	61.2	18.8	0.4	7.6	-	-	-

Sample	Rock Type	Location	Ol.	Cpx.	Plag.	Opaq.	Opx.	Qtz.	Grano.	Apat.
M-354	ol.cpx	W-M	12.0	78.0	7.4	tr	2.6	-	-	-
M-356	pd	W-M	43.0	50.0	7.0	tr	-	-	-	-
M-357	fcpx	W-M	-	82.5	14.0	1.0	2.5	-	-	-
M-358	cpx	W-M	-	86.0	8.0	-	6.0	-	-	-
M-359	cpx	W-M	-	83.0	8.6	-	8.4	-	-	-
M-360	gb	W-M	-	34.2	44.6	3.4	(17.8)	-	-	-
M-361	gb	W-M	-	39.8	42.6	7.6	10.0	-	-	-
M-363	gb	W-M	-	38.0	41.8	8.8	11.4	-	-	-
M-364	gb	W-M	-	24.6	59.4	6.0	10.0	-	-	-
M-366	fcpx	W-M	-	15.2	68.2	1.4	13.2	-	-	-
M-368	gpd	W-M	41.5	41.5	8.0	tr	9.0	-	-	-
M-369	cpx	W-M	-	74.3	12.7	tr	(13.0)	-	-	-
M-376	fcpx	W-M	-	60	34	1	5	-	-	-**
M-380	cpx	W-M	-	96.7	3.3	tr	-	-	-	-
M-380A	cpx	W-M	tr	84.2	10.2	0.2	5.4	-	-	-
M-382	ol.cpx	W-M	17.8	79.2	2.6	0.6	-	-	-	-
M-384	pd	W-M	49	40	11	tr	-	-	-	-**
M-385	pd	W-M	45	36	17	2	-	-	-	-**
M-385A	diorite	W-M	-	26.2	70.4	2.4	-	-	-	1.0
M-387	gb	CH	-	29	68	3	-	-	-	-**
M-388	gb	CH	-	(33.7)	64.5	0.4	-	1.4	-	-
M-390	fcpx	CH	-	78.5	15.2	tr	6.3	-	-	-
M-391	gb	CH	-	31.4	58.6	0.7	9.3	-	-	-
M-392	fcpx	CH	-	88	12	-	-	-	-	-**

* Brackets have been placed about those figures for which positive identification of the mineral is doubtful.

** Rough approximation only.

*** Cpx and plag have been grouped where alteration has been too severe to allow separate identification.

APPENDIX 2

Spectrochemical Analyses; averages of triplicates. Location of Samples noted GSC is Muskox intrusion (N.W.T.)

Sample	Rock Type	Location	Ti	Cr	V	Li	Ni	Co	Cu	Mn	Zr	Sr	Ba	Rb
M-3	gb	CH	8150	-	273	5	69	52	20	2070	282	195	123	8
M-4	gb	CH	11830		305	7	39	49	34	1770	299	240	253	23
M-5	rhyolite	CH	5550	1970	235	7	248	64	151	1630	68	113	97	-
M-6-1	"	CH	9570	1095	279	8	213	63	195	1900	158	128	113	-
M-6-2	"	CH	8900	720	247	5	167	49	133	1380	123	151	135	-
M-6-3	"	CH	8800	700	255	9	209	48	155	1150	116	113	101	-
M-6-4	"	CH	8050	685	229	5	228	57	272	1650	144	138	161	-
M-6-5	"	CH	8000	800	223	5	185	51	109	1253	105	185	156	-
M-7	"	CH	5883	1990	182	7	470	69	151	1460	64	62	16	-
M-9	cpx	CH	1060	6670	15	6	2160	102	3	857	9	-	-	-
M-16	gb	M	14700	10	305	20	52	60	33	2063	117	119	55	-
M-19	cpx	M	7267	1030	271	14	265	49	57	1670	27	36	14	-
M-22	gb	M	6767	470	205	19	221	50	66	1643	69	30	11	-
M-24	fcpx	M	7300	230	230	7	223	60	215	1483	67	22	39	-
M-25	fcpx	M	11700	90	263	7	106	37	64	1325	135	66	47	-
M-26	gb	M	7633	19	308	5	153	57	166	1537	84	99	45	-
M-27	gb	M	7900	-	267	9	43	41	22	1703	111	75	43	tr
M-29	gb	M	13600	1	310	7	33	57	127	1950	170	68	60	-
M-30	gb	M	10167	tr	278	13	99	77	11	1850	115	166	214	6
M-31	gb	M	12667	-	282	5	52	59	27	1867	210	255	30	-
M-32	gb	M	12000	-	243	3	33	46	79	1723	196	115	90	10
M-45	gb	M	4800	83	236	19	77	39	50	1530	41	138	165	20
M-49	gb	M	10130	-	256	5	191	49	91	1503	555	138	83	tr
M-50	gb	M	10833	-	277	4	51	35	6	1043	139	139	33	-
M-51	gb	M	11770	tr	297	8	41	39	49	1643	180	98	56	-
M-61	gb	M	15430	-	257	9	33	37	38	1610	428	143	35	-
M-82	fcpx	M	10000	567	325		180	46	47	1500	73	60	24	-
M-83	gb	M	10970	-	273	6	43	44	54	1707	115	130	63	tr

Sample	Rock Type	Location	Ti	Cr	V	Li	Ni	Co	Cu	Mn	Zr	Sr	Ba	Rb
M-84	fcpx	M	13100	2220	318	6	205	54	228	2760	105	76	101	-
M-85	fcpx	M	7200	2030	273	5	234	52	155	2830	106	14	32	-
M-86	fcpx	M	7300	55	268	8	153	49	172	1670	132	88	64	-
M-87	pd	M	3310	2330	97	16	1140	107	57	1330	58	-	-	-
M-88	grano	M	9470	-	228	25	21	17	1	1130	640	145	109	-
M-91	gb	M	9470	-	357	11	15	43	60	1743	129	39	101	24
M-92	gb	M	2817	743	121	18	91	23	2	823	12	142	122	-
M-94	du	M	3430	3660	155	1	880	80	38	1317	22	tr	21	-
M-95	du	M	1090	2300	100	1	825	86	7	1053	8	-	tr	-
M-100	du	M	1560	4280	78	6	1680	111	6	1083	15	-	-	-
M-102	pd	M	1780	3430	133	2	1530	88	145	1447	16	tr	5	-
M-103	du	M	1660	2830	92	4	1330	78	45	1450	14	tr	-	-
M-107	pd	M	1913	2650	99	4	520	119	44	1587	19	-	tr	-
M-112	gb	W-M	4950	85	193	22	81	38	53	1383	93	126	127	38
M-113	pd	W-M	1150	4200	35	3	2380	132	2	1290	18	-	-	-
M-114	cpx	W-M	2480	4160	122	9	576	65	178	1290	11	64	11	-
M-115	gb	W-M	3400	143	69	8	115	9	1	1180	11	tr	-	-
M-116	pd	W-M	993	3670	-	4	1970	133	7	1120	31	-	-	-
M-117	pd	W-M	1450	3280	65	2	1700	116	72	1230	15	-	-	-
M-118	ol.cpx	W-M	2670	3220	155	4	558	77	140	1460	13	-	9	-
M-119	pd	W-M	2130	4070	112	5	1270	129	93	1760	22	-	-	-
M-121	pd	W-M	1640	1650	tr	2	1095	114	56	1320	13	-	-	-
M-122	pd	W-M	1027	3100	20	1	1480	150	18	1180	12	-	-	-
M-123	cpx	W-M	2620	4010	172	8	378	45	14	1020	10	-	-	-
M-124	pd	W-M	930	3780	20	1	2030	144	1	983	13	-	-	-
M-125	fcpx	W-M	2900	4900	141	7	430	51	60	1560	13	-	-	-
M-126	fcpx	W-M	4600	1960	210	7	292	48	48	1370	13	5	-	-
M-127	fcpx	W-M	6200	54	308	4	237	68	350	1890	68	5	tr	-
M-128	gb	W-M	6470	9	273	11	116	40	13	1030	21	262	95	15
M-129	gb	W-M	7000	98	269	18	42	28	38	1150	69	240	337	52
M-130	cpx/pd	W-M	2590	2300	109	9	683	93	27	100	31	-	tr	-
M-131	gb	W-M	4730	457	236	30	115	34	69	1033	20	188	205	22
M-134	cpx	W-M	3770	1935	100	32	1230	143	136	1350	58	tr	tr	-
M-137	diab	M	10330	30	301	7	40	29	63	1450	132	133	245	45
M-138	diab	M	10270	78	350	14	63	40	147	2230	68	155	69	tr
M-139	basalt	M	2197	3030	153	3	1163	96	31	1567	20	tr	tr	-

Sample	Rock Type	Location	Ti	Cr	V	Li	Ni	Co	Cu	Mn	Zr	Sr	Ba	Rb
M-140	pd	MH	1047	4230	tr	0.5	1360	151	8	993	30	-	-	-
M-141	pd	MH	1183	4830	tr	0.5	1507	146	1	1407	20	-	-	-
M-142	cpx	MH	3325	3570	164	13	408	46	23	1250	9	-	-	-
M-143	fcpx	MH	4000	747	222	4	299	55	25	1623	20	tr	tr	-
M-144	gb	MH	4140	14	237	14	103	39	219	1040	21	275	160	50
M-145	gb	MH	12900	-	-	2	5	23	19	2607	1300	87	60	-
M-147A	fcpx	MH	6400	67	402	2	214	60		1883	39	24	9	-
M-153	sul.+fcpx	MH	15370	-	tr	7	3	20	4	2580	627	221	68	-
M-154	gb	MH	16000	1	620	7	19	51	67	2213	228	250	121	9
M-156	gb	W-MH	18750	tr	tr	5	7	12	33	5173	358	64	20	-
M-162	cpx	W-MH	3733	4350	273	8	367	57	29	1907	10	tr	tr	-
M-163	gb	Mc	9600	12	328	13	34	36	53	2327	168	137	78	tr
M-164	gb	Mc	8180	26	277	13	35	28	43	1477	122	167	197	20
M-165	pd	Mc	2017	3700	83	5	1067	112	11	1800	25	10	17	6
M-166	pd	Mc	1950	5120	89	8	970	122	1	1350	20	tr	tr	-
M-167	gb	Mc	3230	3940	186	16	164	35	32	1407	23	238	262	16
M-168	gb	Mc	3700	780	200	13	89	26	62	1253	21	78	42	-
M-169	grano	Mc	6930	-	45	9	4	19	27	1380	723	99	144	-
M-170	gb	Mc	14600	-	903	18	7	56	35	1810	149	78	133	29
M-172	pd	Mc	1043	2320	tr	2	980	106	27	1283	13	tr	-	-
M-174	cpx	Mc	6337	99	295	21	208	65	267	1700	67	145	210	15
M-175	pd	Mc	2717	3750	60	7	1600	133	16	1103	39	tr	-	-
M-176	xenolith	GS	24170	45	353	7	161	10	3	983	727	tr	15	-
M-187	gb	GS	32300	-	203	13	179	12	10	923	207	103	69	-
M-188	ol.cpx	GS	3830	2100	186	30	468	65	63	1600	32	62	64	17
M-189	pd	GS	1647	3500	tr	2	1850	92	4	1498	10	-	-	-
M-192	pd	GS	4373	4280	209	12	743	97	47	1407	36	tr	tr	tr
M-196	pd	GS	2360	2880	116	16	370	88	82	1507	17	-	-	-
M-197	andesite	GS	16330	107	396	15	65	39	96	1377	560	63	93	19
M-198	gb	GS	20000	162	503	10	65	47	62	2070	228	193	252	34
M-199	gb	GS	16070	107	516	9	69	37	40	1880	285	245	141	-
M-200	pd	GS		4800		0.5	2900	128	5	865	14			-
M-201	pd	GS	1007	5130	tr	1	1280	104	1	1300	6	-	-	-
M-202	pd	GS	2057	3300	100	1	617	88	171	1207	15	-	-	-
M-203	gb	GS	1530	2370	121	24	356	37	74	607	8	54	53	tr

Sample	Rock Type	Location	Ti	Cr	V	Li	Ni	Co	Cu	Mn	Zr	Sr	Ba	Rb
M-204	gb	GS	2040	1347	141	36	170	38	82	780	8	100	43	-
M-205	gb	GS	7123	720	338	23	179	34	84	1410	63	118	125	35
M-210	pd	GS	1377	2970	tr	1	1880	93	45	900	13	-	-	-
M-211	pd	GS	580	3605	tr	1	643	88	88	1190	9	-	-	-
M-212	gb	GS	1257	1670	87	57	232	37	71	930	7	-	tr	-
M-216	gb	GR	3937	15	220	60	54	30	48	1217	29	195	320	85
M-218	pd	GR	1110	4260	tr	3	1560	130	6	1260	19	-	-	-
M-219	xenolith	GR	4800	98	153	14	56	30	17	693	722	145	54	-
M-220	fcpx	GR	2673	4130	197	16	375	54	32	1060	16	-	tr	-
M-221	gb	GR	1657	2157	113	23	225	36	35	743	5	123	220	39
M-222	gb	GR	12870	-	405	16	33	46	24	2077	154	113	158	48
M-225	gb	GR	3010	2650	163	53	163	31	61	1217	20	132	122	-
M-226	pd	GR	1637	4000	tr	5	985	139	28	1423	21	-	-	-
M-227	gb	GR	2887	2100	80	45	198	59	43	1010	25	129	163	2
M-228	gb	GR	11300	tr	-	6	tr	33	83	2110	334	147	197	tr
M-229	gb	GR	1963	2100	tr	8	192	36	27	843	5	132	90	32
M-230	gb	GR	1703	2530	tr	64	175	26	13	677	tr	249	490	41
M-231	pd	GR	1210	4080	tr	2	833	113	23	1253	10	-	-	-
M-232	pd	GR	1803	3130	tr	2	1093	114	29	1143	40	tr	tr	-
M-234	pd	GR	1917	3400	tr	2	1395	132	39	1303	70	tr	tr	-
M-235	fcpx	GR	2467	6000	171	7	308	50	8	1767	10	-	-	-
M-236	ol.cpx	GR	2033	3780	149	12	398	57	16	1010	17	-	tr	-
M-237	gb	GR	1290	2780	60	29	263	46	20	735	tr	152	123	10
M-300	gb	GR	3517	56	202	7	83	35	87	1340	26	166	63	-
M-304	gb	GR	7400	tr	290	6	30	35	55	1697	140	144	89	-
M-307	grano	GR	9233	-	-	4	tr	22	13	1553	553	161	370	-
M-309	gb	GR	10366	-	328	5	29	40	6	1610	178	132	92	-
M-312	pd	GR	873	4330	20	1	1360	120	9	1183	11	-	-	-
M-314	fcpx	GR	1715	4430	128	8	963	69	9	1037	12	-	tr	-
M-315	gb	GR	1453	3400	101	7	288	43	5	860	6	137	63	10
M-316	gb	GR	1993	2820	153	8	229	37	6	1077	7	125	96	10
M-319	gb	GR	5330	-	253	5	39	34	2	1277	45	203	192	36
M-320	gb	GR	12730	-	797	6	18	49	2	1277	132	173	220	22
M-322	grano	GR	12730	-	385	9	10	35	7	1887	473	139	108	15
M-323	gb	GR	10100	-	348	8	11	36	9	1680	307	170	205	22
M-324	gb	GR	3700	80	183	12	74	25	69	980	14	227	151	37

Sample	Rock Type	Location	Ti	Cr	V	Li	Ni	Co	Cu	Mn	Zr	Sr	Ba	Rb
M-325	gb	W-M	17300	16	470	17	75	27	123	823	270	69	285	28
M-329	grano	W-M	10300	10	237	8	116	85	237	863	320	152	120	tr
M-330	fcpx	W-M	5417	1153	270	12	312	104	87	1430	18	-	39	-
M-333	gb	W-M	5500	630	270	27	107	39	75	1383	37	283	149	44
M-334	gb	W-M	6133	432	285	22	83	31	75	1203	40	188	160	24
M-335	gb	W-M	7633	340	367	22	88	44	50	1330	56	160	137	15
M-336	gb	W-M	7270	132	320	19	67	40	34	1260	99	190	173	5
M-337	gb	W-M	8730	60	312	15	66	44	110	1510	138	178	191	7
M-338	gb	W-M	6100	472	313	18	125	43	139	1177	51	223	176	9
M-339	gb	W-M	4400	3350	229	23	622	65	53	963	43	67	117	5
M-340	gb	W-M	4500	897	245	17	120	33	45	1123	41	168	172	15
M-341	gb	W-M	3820	1480	191	12	206	55	36	1010	47	163	295	22
M-342		W-M	2853	3040	118	23	647	65	30	1267	20	-	-	-
M-343	pd	GS	907	4670	-	-	2450	46	2	793	-	-	-	-
M-344	du	GS	1950	2057	-	-	2450	102	12	1163	10	-	-	-
M-345	du	GS	790	3930	-	1	2460	96	1	1277	8	-	-	-
M-346	du	GS	765	4820	-	tr	2630	120	12	837	8	-	-	-
M-347	du	GS	1173	5080	tr	1	2210	104	2	1020	6	-	-	-
M-349	chilled gb	GS	15267	36	547	18	32	35	19	1947	137	97	56	tr
M-350	cpx	W-M	5930	127	311	6	226	47	220	1763	21	31	29	-
M-351	fcpx	W-M	7667	79	415	5	250	60	109	1780	39	23	5	-
M-352	cpx	W-M	6033	225	343	4	510	79	43	1710	21	tr	5	-
M-353	ol.cpx	W-M	5877	540	290	5	453	85	79	1580	20	tr	6	-
M-354	ol.cpx	W-M	4330	963	230	4	403	63	24	1407	12	tr	-	-
M-355	cpx	W-M	4430	2190	245	6	273	45	19	1227	13	5	tr	-
M-356	pd	W-M	2817	1133	118	3	880	127	49	1500	25	tr	tr	-
M-357	fcpx	W-M	3700	3530	216	7	373	65	53	1300	18	tr	-	-
M-358	cpx	W-M	3867	4780	184	8	367	56	4	1373	16	tr	tr	-
M-359	cpx	W-M	3567	6430	181	5	570	60	32	1710	13	tr	-	-
M-360	gb	W-M	14500	16	337	4	84	49	193	1810	208	192	97	-
M-363	gb	W-M	10170	-	392	19	85	60	31	1950	85	277	40	-
M-368	gpd	W-M	3117	520	120	4	837	153	10	1860	35	20	-	-

Sample	Rock Type	Location	Ti	Cr	V	Li	Ni	Co	Cu	Mn	Zr	Sr	Ba	Rb
M-369	cpx	W-M	4033	3400	193	10	317	52	13	1590	18	tr	tr	-
M-385A	xenolith	GR	11150	-	-	1	16	6	3	830	777	217	74	-
M-393	xenolith	GR	10017	18	274	1	63	13	6	1733	91	27	15	-
M-397	pd	GR	1780	4570	60	5	1450	119	20	1730	17	-	-	-
N07377	ol.cpx	GSC	3817	3000	180	10	653	92	35	1337	53	43	60	-
N07875	gb	GSC	2897	1720	135	29	550	71	106	1583	21	94	87	-
N12720	cpx	GSC	3767	3800	148	19	433	76	27	1960	42	45	60	-
N15635	ol.cpx	GSC	2257	7570	tr	9	1880	114	212	973	21	-	18	-
N02113	mafic grano	GSC	16500	17	297	39	44	28	19	880	637	283	910	144
N02906	grano gb	GSC	10700	91	297	235	119	37	96	400	110	124	195	85
S08823	serp. du	GSC	1265	5820	-	0.5	2400	107	2	619	3	-	-	
S24847	fresh du	GSC	750	3800	tr		2103	149	19	1210	27	tr	-	
N05622	gb	GSC	5400	333	258	19	128	40	52	1220	23	202	130	25
S27146	fresh du	GSC	1450	5920	66	5	2050	167	29	1463	31	tr	tr	-
S12868	serp. du	GSC	530	6400	tr	-	1830	127	3	1380	15	-	-	-
W-1 (standard)			10767	152	323	9	83	38	101	1570	222	238	212	16
PCC-1				3480	-	tr	713	103	10	930	9	-	-	-
DTS-1			280	5730	-	1	877	139	5	1027	9	-	-	-
BCR-1			17870	3	480	15	12	32	13	1617	1320	505	695	83
24-08		CH	4900	3430	158	1	970	88	15	1327	79	21	16	-
24-13		CH	5100	3400	237	7	390	81	31	1740	29	21	15	-
24-23		CH	1550	4220	70	-	1610	130	6	1433	29	-	-	-
24-26		CH	3917	2250	245	6	353	48	32	1543	23	tr	tr	-
24-28		CH	1773	4160	tr	1	2470	155	11	2000	31	-	-	-
24-33		CH	4940	122	337	12	352	79	6	2320	81	18	-	-
24-34		CH	2633	22	50	1	940	205	56	2597	82	-	-	-
25-08		CH	10330	-	367	8	65	92	270	1903	393	232	48	24
25-12		CH	10400	-	-	1	3	39	9	2850	2550	267	73	-
25-15		CH	13000	-	373	2	73	59	10	2120	263	167	56	-
25-17		CH	12100	-	200	9	63	73	21	4340	273	128	124	-

APPENDIX 3

Silicate Analyses

Sample No.	M-113	M-118	M-124	M-325	M-333	M-337	M-356	M-363	M-369	M-385A	M-141	M-142	M-143
Rock Type	pd.	cpx	pd.	gb	gb	gb	pd.	gb	cpx	diorite	pd	cpx	cpx
Location	W-M	W-M	W-M	W-M	W-M	W-M	W-M	W-M	W-M	W-M	MH	MH	MH
SiO_2	36.84	48.71	37.81	57.51	54.52	54.63	44.38	48.62	50.96	60.64	37.29	50.57	50.13
TiO_2	.21	.36	.15	2.14	.74	.88	.32	1.08	.45	1.25	.18	.34	.53
Al_2O_3	1.82	2.06	1.00	13.61	15.61	14.91	2.10	13.56	2.69	15.27	1.48	1.94	2.96
Fe_2O_3	9.34	1.94	10.28	.88	.55	1.11	6.98	2.06	.93	.45	9.98	.96	.79
FeO	4.91	7.72	3.81	12.09	6.31	7.16	7.52	10.25	7.38	4.00	3.88	5.06	8.36
MnO	.20	.20	.17	.10	.16	.15	.22	.19	.19	.09	.17	.15	.20
MgO	33.25	20.03	33.77	4.02	7.31	6.02	22.75	6.25	16.80	3.08	33.93	18.55	16.58
CaO	.82	16.22	1.67	2.25	6.98	8.79	9.64	11.50	18.20	6.29	1.15	19.69	18.19
Na_2O	.00	.31	.03	1.70	4.48	2.87	.23	3.33	.33	7.82	.02	.23	.22
K_2O	.06	.03	.01	1.11	.83	.49	.04	.07	.00	.04	.00	.00	.00
P_2O_5	.01	.01	.01	.17	.07	.10	.01	.09	.01	.30	.00	.01	.02
$H_2O+110°$	10.39	1.41	9.67	3.87	2.13	2.61	4.59	2.51	.94	.82	10.45	1.34	1.48
$H_2O-110°$	.49	.11	.41	.22	.12	.15	.29	.13	.07	.04	.43	.10	.13
CO_2	.39	.04	.08	.03	.19	.11	.03	.24	.02	.28	.08	.03	.03
Cr_2O_3	.64		.65								.73		
Total	99.37	99.15	99.52	99.70	100.00	99.98	99.10	99.88	98.97	100.37	99.77	98.97	99.62

Sample No.	M-144	M-145	M-162	M-163	M-166	M-167	M-200	M-201	M-202	M-203	M-205	M-349
Rock Type	gb	gb	cpx	gb	pd	gb	pd	pd	pd	gb	gb	gb
Location	MH	MH	W-MH	McC	McC	McC	GS	GS	GS	GS	GS	GS
SiO_2	47.33	59.83	50.33	52.67	39.44	49.16	38.45	37.76	40.96	46.71	50.18	49.93
TiO_2	.56	1.10	.32	1.08	.28	.41	.15	.13	.17	.18	.77	1.74
Al_2O_3	18.32	13.81	1.73	13.57	5.45	14.88	2.34	2.64	3.18	14.38	14.81	12.84
Fe_2O_3	.81	2.76	.81	1.22	5.08	.90	4.25	6.92	5.98	.59	.84	1.17
FeO	7.14	6.96	6.70	10.86	7.36	6.14	1.30	2.02	4.36	4.74	7.28	13.34
MnO	.13	.16	.16	.18	.18	.13	.11	.16	.17	.08	.15	.27
MgO	6.01	1.31	18.80	5.91	27.90	10.11	38.83	36.20	29.13	14.13	10.02	6.64
CaO	13.59	6.43	18.07	7.59	3.65	12.92	.14	1.11	7.29	14.94	10.70	7.05
Na_2O	2.01	6.23	.22	3.16	.19	2.15	.00	.02	.05	.66	2.22	3.93
K_2O	1.19	.08	.00	.37	.04	.60	.00	.00	.00	.25	.56	.31
P_2O_5	.04	.18	.01	.11	.02	.04	.02	.01	.01	.02	.08	.14
$H_2O+110°$	2.72	.98	1.19	2.82	8.59	2.08	12.33	11.26	6.43	3.04	2.30	2.64
$H_2O-110°$	.14	.14	.09	.20	.49	.08	.58	.54	.23	.09	.08	.09
CO_2	.02	.01	.02	.03	.05	.04	.15	.11	.05	.04	.05	.02
Cr_2O_3					.77		.73	.57				
Total	100.01	99.98	98.45	99.77	99.49	99.64	99.38	99.45	98.01	99.85	100.04	100.11

Sample No.	M-218	M-219	M-220	M-221	M-232	M-323
Rock Type	pd	cpx-gn	cpx	gb	pd	gb
Location	GR	GR	GR	GR	GR	GR
SiO_2	38.95	56.69	49.02	47.59	41.43	54.87
TiO_2	.11	.67	.28	.19	.29	1.36
Al_2O_3	4.57	17.55	5.11	15.58	5.20	12.95
Fe_2O_3	4.18	.67	.60	.65	1.63	2.88
FeO	6.64	4.50	6.34	4.32	9.32	10.56
MnO	.16	.07	.14	.09	.17	.19
MgO	32.05	6.01	19.01	11.77	28.66	4.04
CaO	3.56	2.98	15.24	13.62	4.54	6.79
Na_2O	.06	7.32	.31	1.39	.14	3.11
K_2O	.00	.00	.00	1.07	.15	.71
P_2O_5	.01	.43	.01	.02	.02	.15
$H_2O+110°$	8.84	2.55	2.66	3.37	7.75	2.35
$H_2O-110°$	.39	.10	.08	.17	.31	.11
CO_2	.06	.02	.03	.05	.05	.03
Cr_2O_3	.50				.41	
Total	100.08	99.56	98.83	99.88	100.07	100.10

Sample No.	24-08	24-10	24-13	24-18	24-23	24-26	24-28	24-33	24-35	25-08	25-12	25-15	25-17
Rock Type	hpd	hpd	cpx	pd	pd	cpx	pd	cpx	fcpx	mgb	gb	gb	gb
Location	CH	CH	CH	CH	CH	CH	CH	CH	CH	CH	CH	CH	CH
SiO_2	44.6	41.8	50.4	38.0	38.6	51.2	38.8	49.5	51.5	44.9	54.5	50.3	48.7
TiO_2	.70	.49	.52	.21	.27	.45	.22	.66	.82	1.52	1.47	1.41	1.52
Al_2O_3	6.04	3.97	4.21	2.00	2.02	3.03	1.68	4.23	5.06	13.6	13.0	13.5	13.0
Fe_2O_3	3.71	6.78	1.49	10.7	10.8	1.34	11.0	1.52	.53	3.8	3.7	3.2	2.2
FeO	9.73	6.29	7.99	4.81	4.73	6.62	5.01	8.96	9.02	14.6	12.1	11.4	13.0
MnO	.18	.18	.19	.21	.22	.17	.27	.20	.19	.25	.24	.21	.22
MgO	20.6	27.0	16.0	30.8	30.1	17.1	30.2	14.9	12.9	7.1	2.0	5.0	6.5
CaO	7.92	5.50	16.3	2.87	3.27	18.2	1.97	16.6	16.3	7.7	5.9	8.2	6.8
Na_2O	.72	.52	.79	.05	.04	.39	.04	.63	1.65	2.29	5.14	4.28	3.32
K_2O	.10	.02	.03	.01	.01	.00	.03	.03	.10	.52	.23	.15	.37
P_2O_5	.05	.02	.01	.01	.01	.01	.02	.00	.04	.07	.21	.09	.11
$H_2O+110°$	4.89	6.68	1.45	9.32	8.79	1.30	9.40	1.69	.95	3.00	1.38	2.26	3.51
$H_2O-110°$	.13	.25	.17	.51	.51	.17	.56	.18	.16	.20	.20	.16	.26
CO_2	.05	.09	.15	.06	.06	.01	.04	.75	.34	.07	.13	.12	.62
	5.09	6.99	1.9	10.0		1.8							
Total	99.4	99.6	99.7	99.6	99.4	100.0	99.2	99.9	99.6	99.6	100.2	100.3	100.1

APPENDIX 4-A

WARDEN-MUNRO SECTION

Layer	Rock Type	Thickness	Footage	Sample	Footage
15	Gabbro	750	1770-2520	M-333	2520
				M-334	2470
				M-335	2400
				M-336	2320
				M-337	2210
				M-338	2110
				M-339	2020
				M-340	1950
				M-341	1890
				M-342	1790
	(Chert)	(35)			
15	Gabbro	40	1730-1770	M-325	1765
				M-329	1748
14	Clinopyroxenite	65	1665-1730	M-330	1710
13	Gabbro	390	1275-1665	M-360	1617
				M-361	1607
				M-364	1442
				M-363	1412
				M-366	1287
				M-350	1257
12	Clinopyroxenite	170	1100-1275	M-351	1237
				M-352	1237
				M-353	1145
11	Peridotite	2"		M-368	1105
10	Clinopyroxenite	160	940-1100	M-354	1095
				M-355	1015
9	Peridotite	6"		M-356	945
8	Clinopyroxenite	175	775-940	M-369	925
				M-357	905
				M-358	845
				M-359	777
7	Peridotite	90	685-775	M-124	725

Layer	Rock Type	Thickness	Footage	Sample	Footage
6	Clinopyroxenite	65	620-685	M-123	650
				M-382	622
5	Peridotite	190	430-620	M-122	580
				M-121	510
				M-119	431
4	Clinopyroxenite	130	300-430	M-118	360
3	Peridotite	300+	0-300	M-117	300
				M-116	260
				M-113	90

APPENDIX 4-B

CENTRE HILL SECTION

Layer	Rock Type	Thickness	Contact Footage	Sample	Sample Footage
15	Gabbro	670(ft)	820-1490	25-17	1485
				25-16	1440
				25-15	1375
				25-14	1240
				25-13	1165
				25-12	1105
				25-11	995
				25-10	930
				25-09	830
14	Melanogabbro	65	755-820	25-08	810
				25-07	760
13	Feldspathic Clinopyroxenite	95	660-755	25-05	745
				25-04	720
				25-03	670
12	Feldspathic Clinopyroxenite	120	540-660	25-02	600
				25-01	541
11	Peridotite	3	537-540	24-37	539
10	Feldspathic Clinopyroxenite	30	507-537	24-36	535
				24-35	515
9	Peridotite	3	504-507	24-34	505
8	Clinopyroxenite	119	385-504	24-33	500
				24-32	425
				24-31	388
7	Peridotite	30	355-385	24-30	384
				24-29	370
				24-28	357
6	Clinopyroxenite	55	300-355	24-27	351
				24-26	330
				24-25	303

Layer	Rock Type	Thickness	Contact Footage	Sample	Sample Footage
5	Peridotite	70	230-300	24-24	295
				24-23	260
				24-22	231
4	Clinopyroxenite	10	220-230	24-21	229
				24-20	222
3	Peridotite	30	190-220	24-19	218
				24-18	210
				24-17	191
2	Granular Peridotite	30	160-190	24-16	185
				24-15	161
1	Clinopyroxenite	90	70-160	24-14	157
				24-13	110
				24-12	72
LMZ	Hornblende Peridotite	70	0-70	24-11	69
				24-10	30
				24-09	15
				24-08	6
				24-07	2

APPENDIX 5

Diamond Drill Program

As an aid to field research, the department of geology, McMaster University, purchased a portable diamond drill and accessory supplies. The drill, the GW-10 "Winkie", is manufactured and distributed by J.K. Smit and Sons, a Toronto firm. When mounted on a unipress - a mechanical pressure feed device - the machine is capable of drilling to depths of approximately 250 to 300 feet with EX 97/8" core steel rods in medium hard rock, or to 450 feet with magnesium-zirconium light-weight rods. The drill, unipress, and motor can readily be dismantled, transported in 2 or 3 pack loads to the drill site and quickly reassembled. It is not necessary that an experienced driller operate this machine, although much time could be saved if an amateur operator were to set up the drill and complete a practice hole before going into the field. The drill crew should consist of operator and assistant.

During the 1964 field season I drilled two short holes in the ultramafic-gabbroic intrusions of the Abitibi region. The first, on the south limb of the Ghost Range intrusion, was designed to test the peridotite-gabbro contact where outcrop was not available. The second, drilled north of Monahan Lake in McCool township to test the southern contact of the Munro Lake sill at this point, was abandoned at 44 feet when the piston on the engine was scored. I decided to sacrifice completing the hole rather than additional field mapping, since little time remained in the field season. Logs of the drill holes are summarized below.

Hole: NM-1

Attitude: N14°E;-43°

Location: Claim L40537, Hoffman Property, northern Harker township.

From	To	Rock Type
0'	47'	Peridotite: high serpentinized; poikilitic clinopyroxene plates up to 3/4" diameter; scattered shear zones.
47'	53½'	Pyroxene Felsite Porphyry: phenocrysts (1/16 to 1/8" diameter) now amphibole but have form of pyroxene; approximately 85 per cent fine grained groundmass.
53½'	58'	Clinopyroxenite: very severely altered, primary mineralogy and texture destroyed.
58'	61'	Pyroxene Felsite Porphyry
61'	63'	Melanogabbro: fine grained; cumulus plagioclase and clinopyroxene.
	63'	End of Hole.

Hole: NM-2

Attitude: S30°W;-40°

Location: north end of Monahan Lake; Lot 9, Concession II, McCool township

From	To	Rock Type
0'	44'	Peridotite: generally badly sheared; some relict poikilitic clinopyroxene grains.
	44'	End of Hole.

APPENDIX 6

Norm Calculations

```
11300 WEIGHT AND MOLE PERCENTAGES
11300  Q      0.000     0.000  C      .328     .334  OR     .404     .377
11300  AB     0.000     0.000  AN    4.558    4.259  LC    0.000    0.000
11300  NE     0.000     0.000  KP    0.000    0.000  AC    0.000    0.000
11300  DI     0.000     0.000  HE    0.000    0.000  EN   38.221   39.582
11300  FS      .089      .070  FO   39.300   43.559  FA     .101     .078
11300  WO     0.000     0.000  LA    0.000    0.000  MT   15.422   10.369
11300  IL      .454      .311  CR   1.092     .760  HM    0.000    0.000
11300  AP      .026      .022  PY    0.000    0.000  NS    0.000    0.000
11300  KS     0.000     0.000  RU    0.000    0.000

11300 MAGNESIUM/IRON RATIO        99.821

11300   *****  COMPUTE FE3 WITH FE2  *****

11300 WEIGHT AND MOLE PERCENTAGES
11300  Q      0.000     0.000  C      .331     .334  OR     .408     .377
11300  AB     0.000     0.000  AN    4.607    4.259  LC    0.000    0.000
11300  NE     0.000     0.000  KP    0.000    0.000  AC    0.000    0.000
11300  DI     0.000     0.000  HE    0.000    0.000  EN   15.167   15.540
11300  FS     4.276     3.334  FO   56.167   61.590  FA   17.450   13.214
11300  WO     0.000     0.000  LA    0.000    0.000  MT    0.000    0.000
11300  IL      .459      .311  CR   1.103     .760  HM    0.000    0.000
11300  AP      .026      .022  PY    0.000    0.000  NS    0.000    0.000
11300  KS     0.000     0.000  RU    0.000    0.000

11300 MAGNESIUM/IRON RATIO        82.334

11800 WEIGHT AND MOLE PERCENTAGES
11800  Q      0.000     0.000  C      0.000    0.000  OR     .181     .178
11800  AB    2.687     2.798  AN    4.243    4.164  LC    0.000    0.000
11800  NE     0.000     0.000  KP    0.000    0.000  AC    0.000    0.000
11800  DI   51.185    51.631  HE   11.050    9.729  EN   7.371    8.018
11800  FS    1.825     1.511  FO   14.022   16.326  FA   3.826    3.076
11800  WO     0.000     0.000  LA    0.000    0.000  MT   2.882    2.039
11800  IL      .700      .504  CR    0.000    0.000  HM    0.000    0.000
11800  AP      .023      .021  PY    0.000    0.000  NS    0.000    0.000
11800  KS     0.000     0.000  RU    0.000    0.000

11800 MAGNESIUM/IRON RATIO        84.143
```

```
11800   *****  COMPUTE FE3 WITH FE2  *****

11800 WEIGHT AND MOLE PERCENTAGES
11800   Q      0.000      0.000  C      0.000      0.000  OR      .182       .178
11800   AB     2.692      2.798  AN     4.251      4.164  LC     0.000      0.000
11800   NE     0.000      0.000  KP     0.000      0.000  AC     0.000      0.000
11800   DI    48.305     48.629  HE    14.489     12.731  EN     3.978      4.319
11800   FS     1.368      1.130  FO    17.406     20.225  FA     6.598      5.295
11800   WO     0.000      0.000  LA     0.000      0.000  MT     0.000      0.000
11800   IL      .701       .504  CR     0.000      0.000  HM     0.000      0.000
11800   AP      .023       .021  PY     0.000      0.000  NS     0.000      0.000
11800   KS     0.000      0.000  RU     0.000      0.000

11800 MAGNESIUM/IRON RATIO          79.251

12400 WEIGHT AND MOLE PERCENTAGES
12400   Q      0.000      0.000  C      0.000      0.000  OR      .066       .062
12400   AB      .284       .282  AN     2.879      2.691  LC     0.000      0.000
12400   NE     0.000      0.000  KP     0.000      0.000  AC     0.000      0.000
12400   DI     4.942      4.748  HE     0.000      0.000  EN    35.622     36.906
12400   FS     0.000      0.000  FO    39.603     43.912  FA     0.000      0.000
12400   WO     0.000      0.000  LA     0.000      0.000  MT    11.659      7.857
12400   IL      .319       .219  CR     1.093       .762  HM     3.501      2.280
12400   AP      .026       .021  PY     0.000      0.000  NS     0.000      0.000
12400   KS     0.000      0.000  RU     0.000      0.000

12400 MAGNESIUM/IRON RATIO          100.000

12400   *****  COMPUTE FE3 WITH FE2  *****

12400 WEIGHT AND MOLE PERCENTAGES
12400   Q      0.000      0.000  C      0.000      0.000  OR      .067       .062
12400   AB      .288       .282  AN     2.913      2.691  LC     0.000      0.000
12400   NE     0.000      0.000  KP     0.000      0.000  AC     0.000      0.000
12400   DI     4.142      3.933  HE      .983       .815  EN    13.451     13.775
12400   FS     3.663      2.855  FO    56.174     61.566  FA    16.859     12.760
12400   WO     0.000      0.000  LA     0.000      0.000  MT     0.000      0.000
12400   IL      .323       .219  CR     1.106       .762  HM     0.000      0.000
12400   AP      .026       .021  PY     0.000      0.000  NS     0.000      0.000
12400   KS     0.000      0.000  RU     0.000      0.000

12400 MAGNESIUM/IRON RATIO          82.832

14100 WEIGHT AND MOLE PERCENTAGES
14100   Q      0.000      0.000  C      0.000      0.000  OR     0.000      0.000
14100   AB      .191       .189  AN     4.463      4.160  LC     0.000      0.000
14100   NE     0.000      0.000  KP     0.000      0.000  AC     0.000      0.000
14100   DI     1.545      1.480  HE     0.000      0.000  EN    36.321     37.525
14100   FS     0.000      0.000  FO    40.972     45.304  FA     0.000      0.000
14100   WO     0.000      0.000  LA     0.000      0.000  MT    11.613      7.804
14100   IL      .386       .264  CR     1.236       .859  HM     3.270      2.124
14100   AP     0.000      0.000  PY     0.000      0.000  NS     0.000      0.000
14100   KS     0.000      0.000  RU     0.000      0.000

14100 MAGNESIUM/IRON RATIO          100.000
```

14100 ***** COMPUTE FE3 WITH FE2 *****

14100 WEIGHT AND MOLE PERCENTAGES

14100	Q	0.000	0.000	C	0.000	0.000	OR	0.000	0.000
14100	AB	.193	.189	AN	4.514	4.160	LC	0.000	0.000
14100	NE	0.000	0.000	KP	0.000	0.000	AC	0.000	0.000
14100	DI	1.301	1.232	HE	.300	.248	EN	14.398	14.707
14100	FS	3.807	2.960	FO	57.179	62.511	FA	16.664	12.580
14100	WO	0.000	0.000	LA	0.000	0.000	MT	0.000	0.000
14100	IL	.390	.264	CR	1.250	.859	HM	0.000	0.000
14100	AP	0.000	0.000	PY	0.000	0.000	NS	0.000	0.000
14100	KS	0.000	0.000	RU	0.000	0.000			

14100 MAGNESIUM/IRON RATIO 83.246

14200 WEIGHT AND MOLE PERCENTAGES

14200	Q	0.000	0.000	C	0.000	0.000	OR	0.000	0.000
14200	AB	1.995	2.076	AN	4.370	4.285	LC	0.000	0.000
14200	NE	0.000	0.000	KP	0.000	0.000	AC	0.000	0.000
14200	DI	65.649	66.148	HE	10.180	8.953	EN	4.385	4.765
14200	FS	.779	.645	FO	8.799	10.234	FA	1.724	1.385
14200	WO	0.000	0.000	LA	0.000	0.000	MT	1.427	1.009
14200	IL	.662	.476	CR	0.000	0.000	HM	0.000	0.000
14200	AP	.023	.021	PY	0.000	0.000	NS	0.000	0.000
14200	KS	0.000	0.000	RU	0.000	0.000			

14200 MAGNESIUM/IRON RATIO 88.078

14200 ***** COMPUTE FE3 WITH FE2 *****

14200 WEIGHT AND MOLE PERCENTAGES

14200	Q	0.000	0.000	C	0.000	0.000	OR	0.000	0.000
14200	AB	1.997	2.076	AN	4.374	4.285	LC	0.000	0.000
14200	NE	0.000	0.000	KP	0.000	0.000	AC	0.000	0.000
14200	DI	63.520	63.941	HE	12.703	11.161	EN	2.660	2.808
14200	FS	.610	.504	FO	10.732	12.469	FA	2.712	2.176
14200	WO	0.000	0.000	LA	0.000	0.000	MT	0.000	0.000
14200	IL	.662	.476	CR	0.000	0.000	HM	0.000	0.000
14200	AP	.023	.021	PY	0.000	0.000	NS	0.000	0.000
14200	KS	0.000	0.000	RU	0.000	0.000			

14200 MAGNESIUM/IRON RATIO 85.138

14300 WEIGHT AND MOLE PERCENTAGES

14300	Q	0.000	0.000	C	0.000	0.000	OR	0.000	0.000
14300	AB	1.899	2.003	AN	7.235	7.194	LC	0.000	0.000
14300	NE	0.000	0.000	KP	0.000	0.000	AC	0.000	0.000
14300	DI	52.279	53.421	HE	15.672	13.977	EN	8.931	9.842
14300	FS	3.070	2.575	FO	6.285	7.414	FA	2.381	1.939
14300	WO	0.000	0.000	LA	0.000	0.000	MT	1.168	.857
14300	IL	1.027	.749	CR	0.000	0.000	HM	0.000	0.000
14300	AP	.047	.042	PY	0.000	0.000	NS	0.000	0.000
14300	KS	0.000	0.000	RU	0.000	0.000			

14300 MAGNESIUM/IRON RATIO 79.261

14300 ***** COMPUTE FE3 WITH FE2 *****

14300 WEIGHT AND MOLE PERCENTAGES

14300	Q	0.000	0.000	C	0.000	0.000	OR	0.000	0.000
14300	AB	1.901	2.003	AN	7.241	7.194	LC	0.000	0.000
14300	NE	0.000	0.000	KP	0.000	0.000	AC	0.000	0.000
14300	DI	50.866	51.936	HE	17.351	15.463	EN	7.517	8.277
14300	FS	2.941	2.464	FO	7.759	9.145	FA	3.345	2.722
14300	WO	0.000	0.000	LA	0.000	0.000	MT	0.000	0.000
14300	IL	1.028	.749	CR	0.000	0.000	HM	0.000	0.000
14300	AP	.047	.042	PY	0.000	0.000	NS	0.000	0.000
14300	KS	0.000	0.000	RU	0.000	0.000			

14300 MAGNESIUM/IRON RATIO 77.057

14400 WEIGHT AND MOLE PERCENTAGES

14400	Q	0.000	0.000	C	0.000	0.000	OR	7.246	7.236
14400	AB	13.288	14.083	AN	38.556	38.515	LC	0.000	0.000
14400	NE	2.285	2.682	KP	0.000	0.000	AC	0.000	0.000
14400	DI	14.900	15.296	HE	10.207	9.146	EN	0.000	0.000
14400	FS	0.000	0.000	FO	5.957	7.056	FA	5.157	4.220
14400	WO	0.000	0.000	LA	0.000	0.000	MT	1.209	.870
14400	IL	1.094	.802	CR	0.000	0.000	HM	0.000	0.000
14400	AP	.095	.086	PY	0.000	0.000	NS	0.000	0.000
14400	KS	0.000	0.000	RU	0.000	0.000			

14400 MAGNESIUM/IRON RATIO 62.581

14400 ***** COMPUTE FE3 WITH FE2 *****

14400 WEIGHT AND MOLE PERCENTAGES

14400	Q	0.000	0.000	C	0.000	0.000	OR	7.252	7.236
14400	AB	12.272	12.995	AN	38.568	38.515	LC	0.000	0.000
14400	NE	2.844	3.335	KP	0.000	0.000	AC	0.000	0.000
14400	DI	14.017	14.378	HE	11.242	10.064	EN	0.000	0.000
14400	FS	0.000	0.000	FO	6.252	7.403	FA	6.338	5.182
14400	WO	0.000	0.000	LA	0.000	0.000	MT	0.000	0.000
14400	IL	1.095	.802	CR	0.000	0.000	HM	0.000	0.000
14400	AP	.095	.086	PY	0.000	0.000	NS	0.000	0.000
14400	KS	0.000	0.000	RU	0.000	0.000			

14400 MAGNESIUM/IRON RATIO 58.823

14500 WEIGHT AND MOLE PERCENTAGES

14500	Q	8.661	8.066	C	0.000	0.000	OR	.478	.481
14500	AB	53.322	56.895	AN	9.596	9.650	LC	0.000	0.000
14500	NE	0.000	0.000	KP	0.000	0.000	AC	0.000	0.000
14500	DI	5.402	5.584	HE	12.969	11.700	EN	.795	.886
14500	FS	2.189	1.857	FO	0.000	0.000	FA	0.000	0.000
14500	WO	0.000	0.000	LA	0.000	0.000	MT	4.048	2.935
14500	IL	2.113	1.558	CR	0.000	0.000	HM	0.000	0.000
14500	AP	.422	.383	PY	0.000	0.000	NS	0.000	0.000
14500	KS	0.000	0.000	RU	0.000	0.000			

14500 MAGNESIUM/IRON RATIO 32.307

14500 ***** COMPUTE FE3 WITH FE2 *****

14500 WEIGHT AND MOLE PERCENTAGES

14500	Q	5.525	5.131	C	0.000	0.000	OR	.480	.481
14500	AB	53.471	56.895	AN	9.622	9.650	LC	0.000	0.000
14500	NE	0.000	0.000	KP	0.000	0.000	AC	0.000	0.000
14500	DI	3.574	3.684	HE	15.117	13.599	EN	1.652	1.836
14500	FS	8.012	6.778	FO	0.000	0.000	FA	0.000	0.000
14500	WO	0.000	0.000	LA	0.000	0.000	MT	0.000	0.000
14500	IL	2.119	1.558	CR	0.000	0.000	HM	0.000	0.000
14500	AP	.423	.383	PY	0.000	0.000	NS	0.000	0.000
14500	KS	0.000	0.000	RU	0.000	0.000			

14500 MAGNESIUM/IRON RATIO 21.317

16200 WEIGHT AND MOLE PERCENTAGES

16200	Q	0.000	0.000	C	0.000	0.000	OR	0.000	0.000
16200	AB	1.915	1.997	AN	3.842	3.775	LC	0.000	0.000
16200	NE	0.000	0.000	KP	0.000	0.000	AC	0.000	0.000
16200	DI	58.030	58.599	HE	12.324	10.862	EN	8.762	9.543
16200	FS	2.134	1.768	FO	8.776	10.229	FA	2.355	1.896
16200	WO	0.000	0.000	LA	0.000	0.000	MT	1.208	.856
16200	IL	.625	.450	CR	0.000	0.000	HM	0.000	0.000
16200	AP	.023	.021	PY	0.000	0.000	NS	0.000	0.000
16200	KS	0.000	0.000	RU	0.000	0.000			

16200 MAGNESIUM/IRON RATIO 84.362

16200 ***** COMPUTE FE3 WITH FE2 *****

16200 WEIGHT AND MOLE PERCENTAGES

16200	Q	0.000	0.000	C	0.000	0.000	OR	0.000	0.000
16200	AB	1.917	1.997	AN	3.845	3.775	LC	0.000	0.000
16200	NE	0.000	0.000	KP	0.000	0.000	AC	0.000	0.000
16200	DI	56.522	57.029	HE	14.117	12.432	EN	7.242	7.881
16200	FS	2.074	1.718	FO	10.359	12.064	FA	3.270	2.629
16200	WO	0.000	0.000	LA	0.000	0.000	MT	0.000	0.000
16200	IL	.626	.450	CR	0.000	0.000	HM	0.000	0.000
16200	AP	.023	.021	PY	0.000	0.000	NS	0.000	0.000
16200	KS	0.000	0.000	RU	0.000	0.000			

16200 MAGNESIUM/IRON RATIO 82.102

16300 WEIGHT AND MOLE PERCENTAGES

16300	Q	3.542	3.318	C	0.000	0.000	OR	2.262	2.288
16300	AB	27.641	29.663	AN	22.489	22.748	LC	0.000	0.000
16300	NE	0.000	0.000	KP	0.000	0.000	AC	0.000	0.000
16300	DI	6.417	6.670	HE	6.647	6.031	EN	12.241	13.723
16300	FS	14.543	12.408	FO	0.000	0.000	FA	0.000	0.000
16300	WO	0.000	0.000	LA	0.000	0.000	MT	1.828	1.353
16300	IL	2.120	1.573	CR	0.000	0.000	HM	0.000	0.000
16300	AP	.263	.240	PY	0.000	0.000	NS	0.000	0.000
16300	KS	0.000	0.000	RU	0.000	0.000			

16300 MAGNESIUM/IRON RATIO 52.516

16300 ***** COMPUTE FE3 WITH FE2 *****

16300 WEIGHT AND MOLE PERCENTAGES

16300	Q	2.121	1.984	C	0.000	0.000	OR	2.265	2.288
16300	AB	27.676	29.663	AN	22.517	22.748	LC	0.000	0.000
16300	NE	0.000	0.000	KP	0.000	0.000	AC	0.000	0.000
16300	DI	5.937	6.164	HE	7.214	6.537	EN	12.482	13.976
16300	FS	17.395	14.822	FO	0.000	0.000	FA	0.000	0.000
16300	WO	0.000	0.000	LA	0.000	0.000	MT	0.000	0.000
16300	IL	2.123	1.573	CR	0.000	0.000	HM	0.000	0.000
16300	AP	.264	.240	PY	0.000	0.000	NS	0.000	0.000
16300	KS	0.000	0.000	RU	0.000	0.000			

16300 MAGNESIUM/IRON RATIO 48.531

16600 WEIGHT AND MOLE PERCENTAGES

16600	Q	0.000	0.000	C	0.000	0.000	OR	.262	.248
16600	AB	1.786	1.792	AN	15.444	14.609	LC	0.000	0.000
16600	NE	0.000	0.000	KP	0.000	0.000	AC	0.000	0.000
16600	DI	3.247	3.156	HE	.319	.270	EN	28.326	29.697
16600	FS	3.192	2.547	FO	33.191	37.242	FA	4.122	3.194
16600	WO	0.000	0.000	LA	0.000	0.000	MT	8.183	5.580
16600	IL	.590	.409	CR	1.281	.904	HM	0.000	0.000
16600	AP	.051	.043	PY	0.000	0.000	NS	0.000	0.000
16600	KS	0.000	0.000	RU	0.000	0.000			

16600 MAGNESIUM/IRON RATIO 92.100

16600 ***** COMPUTE FE3 WITH FE2 *****

16600 WEIGHT AND MOLE PERCENTAGES

16600	Q	0.000	0.000	C	0.000	0.000	OR	.264	.248
16600	AB	1.796	1.792	AN	15.531	14.609	LC	0.000	0.000
16600	NE	0.000	0.000	KP	0.000	0.000	AC	0.000	0.000
16600	DI	2.897	2.801	HE	.742	.626	EN	16.527	17.229
16600	FS	4.857	3.854	FO	41.880	46.727	FA	13.565	10.452
16600	WO	0.000	0.000	LA	0.000	0.000	MT	0.000	0.000
16600	IL	.594	.409	CR	1.289	.904	HM	0.000	0.000
16600	AP	.051	.043	PY	0.000	0.000	NS	0.000	0.000
16600	KS	0.000	0.000	RU	0.000	0.000			

16600 MAGNESIUM/IRON RATIO 81.720

16700 WEIGHT AND MOLE PERCENTAGES

16700	Q	0.000	0.000	C	0.000	0.000	OR	3.642	3.587
16700	AB	18.668	19.512	AN	29.945	29.502	LC	0.000	0.000
16700	NE	0.000	0.000	KP	0.000	0.000	AC	0.000	0.000
16700	DI	21.212	21.477	HE	7.416	6.554	EN	1.817	1.964
16700	FS	.728	.605	FO	9.941	11.617	FA	4.393	3.545
16700	WO	0.000	0.000	LA	0.000	0.000	MT	1.339	.951
16700	IL	.799	.577	CR	0.000	0.000	HM	0.000	0.000
16700	AP	.095	.084	PY	0.000	0.000	NS	0.000	0.000
16700	KS	0.000	0.000	RU	0.000	0.000			

16700 MAGNESIUM/IRON RATIO 76.617

16700 ***** COMPUTE FE3 WITH FE2 *****

16700 WEIGHT AND MOLE PERCENTAGES

16700	Q	0.000	0.000	C	0.000	0.000	OR	3.645	3.587
16700	AB	18.685	19.512	AN	29.973	29.502	LC	0.000	0.000
16700	NE	0.000	0.000	KP	0.000	0.000	AC	0.000	0.000
16700	DI	20.189	20.422	HE	8.618	7.609	EN	.459	.501
16700	FS	.225	.186	FO	11.242	13.125	FA	6.065	4.890
16700	WO	0.000	0.000	LA	0.000	0.000	MT	0.000	0.000
16700	IL	.799	.577	CR	0.000	0.000	HM	0.000	0.000
16700	AP	.095	.084	PY	0.000	0.000	NS	0.000	0.000
16700	KS	0.000	0.000	RU	0.000	0.000			

16700 MAGNESIUM/IRON RATIO 72.854

20000 WEIGHT AND MOLE PERCENTAGES

20000	Q	0.000	0.000	C	2.481	2.410	OR	0.000	0.000
20000	AB	0.000	0.000	AN	.655	.583	LC	0.000	0.000
20000	NE	0.000	0.000	KP	0.000	0.000	AC	0.000	0.000
20000	DI	0.000	0.000	HE	0.000	0.000	EN	36.037	35.350
20000	FS	0.000	0.000	FO	53.557	56.544	FA	0.000	0.000
20000	WO	0.000	0.000	LA	0.000	0.000	MT	2.153	1.361
20000	IL	.331	.216	CR	1.272	.844	HM	3.457	2.144
20000	AP	.053	.043	PY	0.000	0.000	NS	0.000	0.000
20000	KS	0.000	0.000	RU	0.000	0.000			

20000 MAGNESIUM/IRON RATIO 100.000

20000 ***** COMPUTE FE3 WITH FE2 *****

20000 WEIGHT AND MOLE PERCENTAGES

20000	Q	0.000	0.000	C	2.493	2.410	OR	0.000	0.000
20000	AB	0.000	0.000	AN	.658	.563	LC	0.000	0.000
20000	NE	0.000	0.000	KP	0.000	0.000	AC	0.000	0.000
20000	DI	0.000	0.000	HE	0.000	0.000	EN	27.296	26.794
20000	FS	2.280	1.703	FO	60.074	63.111	FA	5.530	4.011
20000	WO	0.000	0.000	LA	0.000	0.000	MT	0.000	0.000
20000	IL	.332	.216	CR	1.278	.844	HM	0.000	0.000
20000	AP	.054	.043	PY	0.000	0.000	NS	0.000	0.000
20000	KS	0.000	0.000	RU	0.000	0.000			

20000 MAGNESIUM/IRON RATIO 94.022

20100 WEIGHT AND MOLE PERCENTAGES

20100	Q	0.000	0.000	C	.702	.697	OR	0.000	0.000
20100	AB	.193	.187	AN	6.234	5.669	LC	0.000	0.000
20100	NE	0.000	0.000	KP	0.000	0.000	AC	0.000	0.000
20100	DI	0.000	0.000	HE	0.000	0.000	EN	31.851	32.102
20100	FS	0.000	0.000	FO	50.062	54.000	FA	0.000	0.000
20100	WO	0.000	0.000	LA	0.000	0.000	MT	5.601	3.672
20100	IL	.282	.188	CR	.978	.663	HM	4.065	2.576
20100	AP	.026	.021	PY	0.000	0.000	NS	0.000	0.000
20100	KS	0.000	0.000	RU	0.000	0.000			

20100 MAGNESIUM/IRON RATIO 100.000

```
 20100   *****  COMPUTE FE3 WITH FE2  *****

 20100 WEIGHT AND MOLE PERCENTAGES
 20100  Q      0.000      0.000  C      .707      .697  OR     0.000      0.000
 20100  AB      .195       .187  AN    6.284     5.669  LC     0.000      0.000
 20100  NE     0.000      0.000  KP    0.000     0.000  AC     0.000      0.000
 20100  DI     0.000      0.000  HE    0.000     0.000  EN    17.506     17.504
 20100  FS     2.761      2.101  FO   60.694    64.949  FA    10.550      7.796
 20100  WO     0.000      0.000  LA    0.000     0.000  MT     0.000      0.000
 20100  IL      .285       .188  CR     .986      .663  HM     0.000      0.000
 20100  AP      .026       .021  PY    0.000     0.000  NS     0.000      0.000
 20100  KS     0.000      0.000  RU    0.000     0.000

 20100 MAGNESIUM/IRON RATIO         89.282

 20200 WEIGHT AND MOLE PERCENTAGES
 20200  Q      0.000      0.000  C     0.000     0.000  OR     0.000      0.000
 20200  AB      .463       .463  AN    9.258     8.738  LC     0.000      0.000
 20200  NE     0.000      0.000  KP    0.000     0.000  AC     0.000      0.000
 20200  DI    22.830     22.146  HE     .851      .720  EN    20.021     20.945
 20200  FS      .855       .681  FO   34.231    38.327  FA     1.612      1.246
 20200  WO     0.000      0.000  LA    0.000     0.000  MT     9.496      6.462
 20200  IL      .353       .244  CR    0.000     0.000  HM     0.000      0.000
 20200  AP      .025       .021  PY    0.000     0.000  NS     0.000      0.000
 20200  KS     0.000      0.000  RU    0.000     0.000

 20200 MAGNESIUM/IRON RATIO         96.848

20200   *****  COMPUTE FE3 WITH FE2  *****

20200 WEIGHT AND MOLE PERCENTAGES
20200  Q      0.000      0.000  C     0.000     0.000  OR     0.000      0.000
20200  AB      .466       .463  AN    9.319     8.738  LC     0.000      0.000
20200  NE     0.000      0.000  KP    0.000     0.000  AC     0.000      0.000
20200  DI    19.973     19.247  HE    4.302     3.619  EN     7.048      7.325
20200  FS     1.741      1.377  FO   44.618    49.629  FA    12.148      9.331
20200  WO     0.000      0.000  LA    0.000     0.000  MT     0.000      0.000
20200  IL      .355       .244  CR    0.000     0.000  HM     0.000      0.000
20200  AP      .025       .021  PY    0.000     0.000  NS     0.000      0.000
20200  KS     0.000      0.000  RU    0.000     0.000

20200 MAGNESIUM/IRON RATIO         84.173

20300 WEIGHT AND MOLE PERCENTAGES
20300  Q      0.000      0.000  C     0.000     0.000  OR     1.529      1.492
20300  AB     5.775      5.981  AN   36.757    35.882  LC     0.000      0.000
20300  NE     0.000      0.000  KP    0.000     0.000  AC     0.000      0.000
20300  DI    26.359     26.444  HE    5.269     4.614  EN     5.119      5.538
20300  FS     1.173       .966  FO   13.354    15.463  FA     3.374      2.698
20300  WO     0.000      0.000  LA    0.000     0.000  MT      .884       .622
20300  IL      .353       .253  CR    0.000     0.000  HM     0.000      0.000
20300  AP      .047       .042  PY    0.000     0.000  NS     0.000      0.000
20300  KS     0.000      0.000  RU    0.000     0.000

20300 MAGNESIUM/IRON RATIO         85.142
```

20300 ***** COMPUTE FE3 WITH FE2 *****

20300 WEIGHT AND MOLE PERCENTAGES

20300	Q	0.000	0.000	C	0.000	0.000	OR	1.530	1.492
20300	AB	5.779	5.981	AN	36.779	35.882	LC	0.000	0.000
20300	NE	0.000	0.000	KP	0.000	0.000	AC	0.000	0.000
20300	DI	25.684	25.750	HE	6.065	5.307	EN	4.032	4.360
20300	FS	1.092	.898	FO	14.350	16.606	FA	4.283	3.423
20300	WO	0.000	0.000	LA	0.000	0.000	MT	0.000	0.000
20300	IL	.353	.253	CR	0.000	0.000	HM	0.000	0.000
20300	AP	.048	.042	PY	0.000	0.000	NS	0.000	0.000
20300	KS	0.000	0.000	RU	0.000	0.000			

20300 MAGNESIUM/IRON RATIO 82.910

20500 WEIGHT AND MOLE PERCENTAGES

20500	Q	0.000	0.000	C	0.000	0.000	OR	3.393	3.356
20500	AB	19.242	20.197	AN	29.497	29.182	LC	0.000	0.000
20500	NE	0.000	0.000	KP	0.000	0.000	AC	0.000	0.000
20500	DI	13.975	14.208	HE	5.704	5.062	EN	12.264	13.448
20500	FS	5.741	4.791	FO	4.778	5.608	FA	2.465	1.998
20500	WO	0.000	0.000	LA	0.000	0.000	MT	1.247	.889
20500	IL	1.498	1.087	CR	0.000	0.000	HM	0.000	0.000
20500	AP	.190	.169	PY	0.000	0.000	NS	0.000	0.000
20500	KS	0.000	0.000	RU	0.000	0.000			

20500 MAGNESIUM/IRON RATIO 73.731

20500 ***** COMPUTE FE3 WITH FE2 *****

20500 WEIGHT AND MOLE PERCENTAGES

20500	Q	0.000	0.000	C	0.000	0.000	OR	3.396	3.356
20500	AB	19.258	20.197	AN	29.522	29.182	LC	0.000	0.000
20500	NE	0.000	0.000	KP	0.000	0.000	AC	0.000	0.000
20500	DI	13.361	13.573	HE	6.426	5.697	EN	10.582	11.593
20500	FS	5.837	4.866	FO	6.172	7.237	FA	3.752	3.038
20500	WO	0.000	0.000	LA	0.000	0.000	MT	0.000	0.000
20500	IL	1.499	1.087	CR	0.000	0.000	HM	0.000	0.000
20500	AP	.190	.169	PY	0.000	0.000	NS	0.000	0.000
20500	KS	0.000	0.000	RU	0.000	0.000			

20500 MAGNESIUM/IRON RATIO 70.433

21800 WEIGHT AND MOLE PERCENTAGES

21800	Q	0.000	0.000	C	0.000	0.000	OR	0.000	0.000
21800	AB	.560	.552	AN	13.472	12.505	LC	0.000	0.000
21800	NE	0.000	0.000	KP	0.000	0.000	AC	0.000	0.000
21800	DI	4.310	4.111	HE	.375	.312	EN	20.182	20.763
21800	FS	2.016	1.578	FO	46.218	50.888	FA	5.087	3.868
21800	WO	0.000	0.000	LA	0.000	0.000	MT	6.692	4.478
21800	IL	.230	.157	CR	.827	.572	HM	0.000	0.000
21800	AP	.025	.021	PY	0.000	0.000	NS	0.000	0.000
21800	KS	0.000	0.000	RU	0.000	0.000			

21800 MAGNESIUM/IRON RATIO 92.935

21800 ***** COMPUTE FE3 WITH FE2 *****

21800 WEIGHT AND MOLE PERCENTAGES

21800	Q	0.000	0.000	C	0.000	0.000	OR	0.000	0.000
21800	AB	.563	.552	AN	13.535	12.505	LC	0.000	0.000
21800	NE	0.000	0.000	KP	0.000	0.000	AC	0.000	0.000
21800	DI	3.965	3.765	HE	.794	.658	EN	11.126	11.393
21800	FS	2.555	1.991	FO	52.964	58.045	FA	13.406	10.146
21800	WO	0.000	0.000	LA	0.000	0.000	MT	0.000	0.000
21800	IL	.231	.157	CR	.831	.572	HM	0.000	0.000
21800	AP	.025	.021	PY	0.000	0.000	NS	0.000	0.000
21800	KS	0.000	0.000	RU	0.000	0.000			

21800 MAGNESIUM/IRON RATIO 85.120

21900 WEIGHT AND MOLE PERCENTAGES

21900	Q	0.000	0.000	C	1.159	1.216	OR	0.000	0.000
21900	AB	63.920	65.150	AN	12.353	11.867	LC	0.000	0.000
21900	NE	0.000	0.000	KP	0.000	0.000	AC	0.000	0.000
21900	DI	0.000	0.000	HE	0.000	0.000	EN	7.539	8.027
21900	FS	3.391	2.748	FO	5.541	6.315	FA	2.747	2.162
21900	WO	0.000	0.000	LA	0.000	0.000	MT	1.002	.694
21900	IL	1.313	.925	CR	0.000	0.000	HM	0.000	0.000
21900	AP	1.029	.892	PY	0.000	0.000	NS	0.000	0.000
21900	KS	0.000	0.000	RU	0.000	0.000			

21900 MAGNESIUM/IRON RATIO 74.493

21900 ***** COMPUTE FE3 WITH FE2 *****

21900 WEIGHT AND MOLE PERCENTAGES

21900	Q	0.000	0.000	C	1.160	1.216	OR	0.000	0.000
21900	AB	63.964	65.150	AN	12.362	11.867	LC	0.000	0.000
21900	NE	0.000	0.000	KP	0.000	0.000	AC	0.000	0.000
21900	DI	0.000	0.000	HE	0.000	0.000	EN	6.183	6.579
21900	FS	3.467	2.808	FO	6.499	7.401	FA	4.017	3.159
21900	WO	0.000	0.000	LA	0.000	0.000	MT	0.000	0.000
21900	IL	1.314	.925	CR	0.000	0.000	HM	0.000	0.000
21900	AP	1.030	.892	PY	0.000	0.000	NS	0.000	0.000
21900	KS	0.000	0.000	RU	0.000	0.000			

21900 MAGNESIUM/IRON RATIO 70.085

22000 WEIGHT AND MOLE PERCENTAGES

22000	Q	0.000	0.000	C	0.000	0.000	OR	0.000	0.000
22000	AB	2.730	2.824	AN	13.066	12.740	LC	0.000	0.000
22000	NE	0.000	0.000	KP	0.000	0.000	AC	0.000	0.000
22000	DI	43.406	43.494	HE	8.749	7.652	EN	13.994	15.122
22000	FS	3.235	2.660	FO	10.625	12.289	FA	2.707	2.162
22000	WO	0.000	0.000	LA	0.000	0.000	MT	.905	.636
22000	IL	.553	.395	CR	0.000	0.000	HM	0.000	0.000
22000	AP	.024	.021	PY	0.000	0.000	NS	0.000	0.000
22000	KS	0.000	0.000	RU	0.000	0.000			

22000 MAGNESIUM/IRON RATIO 85.038

22000 ***** COMPUTE FE3 WITH FE2 *****

22000 WEIGHT AND MOLE PERCENTAGES

22000	Q	0.000	0.000	C	0.000	0.000	OR	0.000	0.000
22000	AB	2.732	2.824	AN	13.075	12.740	LC	0.000	0.000
22000	NE	0.000	0.000	KP	0.000	0.000	AC	0.000	0.000
22000	DI	42.568	42.627	HE	9.746	8.518	EN	12.741	13.760
22000	FS	3.345	2.749	FO	11.797	13.636	FA	3.414	2.725
22000	WO	0.000	0.000	LA	0.000	0.000	MT	0.000	0.000
22000	IL	.553	.395	CR	0.000	0.000	HM	0.000	0.000
22000	AP	.024	.021	PY	0.000	0.000	NS	0.000	0.000
22000	KS	0.000	0.000	RU	0.000	0.000			

22000 MAGNESIUM/IRON RATIO 83.344

22100 WEIGHT AND MOLE PERCENTAGES

22100	Q	0.000	0.000	C	0.000	0.000	OR	6.572	6.416
22100	AB	11.217	11.620	AN	34.386	33.578	LC	0.000	0.000
22100	NE	.539	.619	KP	0.000	0.000	AC	0.000	0.000
22100	DI	23.355	23.438	HE	5.036	4.411	EN	0.000	0.000
22100	FS	0.000	0.000	FO	13.743	15.919	FA	3.746	2.996
22100	WO	0.000	0.000	LA	0.000	0.000	MT	.978	.689
22100	IL	.374	.268	CR	0.000	0.000	HM	0.000	0.000
22100	AP	.048	.042	PY	0.000	0.000	NS	0.000	0.000
22100	KS	0.000	0.000	RU	0.000	0.000			

22100 MAGNESIUM/IRON RATIO 84.159

22100 ***** COMPUTE FE3 WITH FE2 *****

22100 WEIGHT AND MOLE PERCENTAGES

22100	Q	0.000	0.000	C	0.000	0.000	OR	6.577	6.416
22100	AB	10.392	10.759	AN	34.409	33.578	LC	0.000	0.000
22100	NE	.990	1.135	KP	0.000	0.000	AC	0.000	0.000
22100	DI	22.576	22.641	HE	5.950	5.208	EN	0.000	0.000
22100	FS	0.000	0.000	FO	14.011	16.218	FA	4.667	3.731
22100	WO	0.000	0.000	LA	0.000	0.000	MT	0.000	0.000
22100	IL	.375	.268	CR	0.000	0.000	HM	0.000	0.000
22100	AP	.048	.042	PY	0.000	0.000	NS	0.000	0.000
22100	KS	0.000	0.000	RU	0.000	0.000			

22100 MAGNESIUM/IRON RATIO 81.297

23200 WEIGHT AND MOLE PERCENTAGES

23200	Q	0.000	0.000	C	0.000	0.000	OR	.966	.909
23200	AB	1.290	1.288	AN	14.293	13.448	LC	0.000	0.000
23200	NE	0.000	0.000	KP	0.000	0.000	AC	0.000	0.000
23200	DI	6.790	6.565	HE	1.234	1.041	EN	20.821	21.713
23200	FS	4.341	3.445	FO	37.703	42.080	FA	8.663	6.677
23200	WO	0.000	0.000	LA	0.000	0.000	MT	2.575	1.746
23200	IL	.600	.414	CR	.669	.469	HM	0.000	0.000
23200	AP	.050	.042	PY	0.000	0.000	NS	0.000	0.000
23200	KS	0.000	0.000	RU	0.000	0.000			

23200 MAGNESIUM/IRON RATIO 86.305

23200 ***** COMPUTE FE3 WITH FE2 *****

23200 WEIGHT AND MOLE PERCENTAGES

23200	Q	0.000	0.000	C	0.000	0.000	OR	.968	.909
23200	AB	1.292	1.288	AN	14.318	13.448	LC	0.000	0.000
23200	NE	0.000	0.000	KP	0.000	0.000	AC	0.000	0.000
23200	DI	6.558	6.330	HE	1.515	1.277	EN	17.318	18.027
23200	FS	4.591	3.637	FO	40.330	44.932	FA	11.782	9.065
23200	WO	0.000	0.000	LA	0.000	0.000	MT	0.000	0.000
23200	IL	.601	.414	CR	.670	.469	HM	0.000	0.000
23200	AP	.050	.042	PY	0.000	0.000	NS	0.000	0.000
23200	KS	0.000	0.000	RU	0.000	0.000			

23200 MAGNESIUM/IRON RATIO 83.211

32300 WEIGHT AND MOLE PERCENTAGES

32300	Q	10.169	9.668	C	0.000	0.000	OR	4.302	4.415
32300	AB	26.956	29.360	AN	19.751	20.277	LC	0.000	0.000
32300	NE	0.000	0.000	KP	0.000	0.000	AC	0.000	0.000
32300	DI	4.994	5.269	HE	6.544	6.026	EN	7.991	9.093
32300	FS	12.010	10.400	FO	0.000	0.000	FA	0.000	0.000
32300	WO	0.000	0.000	LA	0.000	0.000	MT	4.277	3.166
32300	IL	2.646	1.992	CR	0.000	0.000	HM	0.000	0.000
32300	AP	.356	.330	PY	0.000	0.000	NS	0.000	0.000
32300	KS	0.000	0.000	RU	0.000	0.000			

32300 MAGNESIUM/IRON RATIO 46.648

32300 ***** COMPUTE FE3 WITH FE2 *****

32300 WEIGHT AND MOLE PERCENTAGES

32300	Q	6.859	6.502	C	0.000	0.000	OR	4.315	4.415
32300	AB	27.036	29.360	AN	19.809	20.277	LC	0.000	0.000
32300	NE	0.000	0.000	KP	0.000	0.000	AC	0.000	0.000
32300	DI	4.001	4.209	HE	7.718	7.086	EN	8.482	9.623
32300	FS	18.766	16.202	FO	0.000	0.000	FA	0.000	0.000
32300	WO	0.000	0.000	LA	0.000	0.000	MT	0.000	0.000
32300	IL	2.653	1.992	CR	0.000	0.000	HM	0.000	0.000
32300	AP	.357	.330	PY	0.000	0.000	NS	0.000	0.000
32300	KS	0.000	0.000	RU	0.000	0.000			

32300 MAGNESIUM/IRON RATIO 37.262

32500 WEIGHT AND MOLE PERCENTAGES

32500	Q	25.927	24.962	C	6.202	7.038	OR	6.869	7.139
32500	AB	15.048	16.598	AN	10.514	10.931	LC	0.000	0.000
32500	NE	0.000	0.000	KP	0.000	0.000	AC	0.000	0.000
32500	DI	0.000	0.000	HE	0.000	0.000	EN	10.473	12.069
32500	FS	18.964	16.630	FO	0.000	0.000	FA	0.000	0.000
32500	WO	0.000	0.000	LA	0.000	0.000	MT	1.334	1.000
32500	IL	4.252	3.242	CR	0.000	0.000	HM	0.000	0.000
32500	AP	.412	.387	PY	0.000	0.000	NS	0.000	0.000
32500	KS	0.000	0.000	RU	0.000	0.000			

32500 MAGNESIUM/IRON RATIO 42.053

23200 ***** COMPUTE FE3 WITH FE2 *****

23200 WEIGHT AND MOLE PERCENTAGES

23200	Q	0.000	0.000	C	0.000	0.000	OR	.968	.909
23200	AB	1.292	1.288	AN	14.318	13.448	LC	0.000	0.000
23200	NE	0.000	0.000	KP	0.000	0.000	AC	0.000	0.000
23200	DI	6.558	6.330	HE	1.515	1.277	EN	17.318	18.027
23200	FS	4.591	3.637	FO	40.330	44.932	FA	11.782	9.065
23200	WO	0.000	0.000	LA	0.000	0.000	MT	0.000	0.000
23200	IL	.601	.414	CR	.670	.469	HM	0.000	0.000
23200	AP	.050	.042	PY	0.000	0.000	NS	0.000	0.000
23200	KS	0.000	0.000	RU	0.000	0.000			

23200 MAGNESIUM/IRON RATIO 83.211

32300 WEIGHT AND MOLE PERCENTAGES

32300	Q	10.169	9.668	C	0.000	0.000	OR	4.302	4.415
32300	AB	26.956	29.360	AN	19.751	20.277	LC	0.000	0.000
32300	NE	0.000	0.000	KP	0.000	0.000	AC	0.000	0.000
32300	DI	4.994	5.269	HE	6.544	6.026	EN	7.991	9.093
32300	FS	12.010	10.400	FO	0.000	0.000	FA	0.000	0.000
32300	WO	0.000	0.000	LA	0.000	0.000	MT	4.277	3.166
32300	IL	2.646	1.992	CR	0.000	0.000	HM	0.000	0.000
32300	AP	.356	.330	PY	0.000	0.000	NS	0.000	0.000
32300	KS	0.000	0.000	RU	0.000	0.000			

32300 MAGNESIUM/IRON RATIO 46.648

32300 ***** COMPUTE FE3 WITH FE2 *****

32300 WEIGHT AND MOLE PERCENTAGES

32300	Q	6.859	6.502	C	0.000	0.000	OR	4.315	4.415
32300	AB	27.036	29.360	AN	19.809	20.277	LC	0.000	0.000
32300	NE	0.000	0.000	KP	0.000	0.000	AC	0.000	0.000
32300	DI	4.001	4.209	HE	7.718	7.086	EN	8.482	9.623
32300	FS	18.766	16.202	FO	0.000	0.000	FA	0.000	0.000
32300	WO	0.000	0.000	LA	0.000	0.000	MT	0.000	0.000
32300	IL	2.653	1.992	CR	0.000	0.000	HM	0.000	0.000
32300	AP	.357	.330	PY	0.000	0.000	NS	0.000	0.000
32300	KS	0.000	0.000	RU	0.000	0.000			

32300 MAGNESIUM/IRON RATIO 37.262

32500 WEIGHT AND MOLE PERCENTAGES

32500	Q	25.927	24.962	C	6.202	7.038	OR	6.869	7.139
32500	AB	15.048	16.598	AN	10.514	10.931	LC	0.000	0.000
32500	NE	0.000	0.000	KP	0.000	0.000	AC	0.000	0.000
32500	DI	0.000	0.000	HE	0.000	0.000	EN	10.473	12.069
32500	FS	18.964	16.630	FO	0.000	0.000	FA	0.000	0.000
32500	WO	0.000	0.000	LA	0.000	0.000	MT	1.334	1.000
32500	IL	4.252	3.242	CR	0.000	0.000	HM	0.000	0.000
32500	AP	.412	.387	PY	0.000	0.000	NS	0.000	0.000
32500	KS	0.000	0.000	RU	0.000	0.000			

32500 MAGNESIUM/IRON RATIO 42.053

33700 ***** COMPUTE FE3 WITH FE2 *****

33700 WEIGHT AND MOLE PERCENTAGES

33700	Q	6.010	5.580	C	0.000	0.000	OR	2.987	2.994
33700	AB	25.032	26.627	AN	27.170	27.240	LC	0.000	0.000
33700	NE	0.000	0.000	KP	0.000	0.000	AC	0.000	0.000
33700	DI	7.831	8.068	HE	6.289	5.655	EN	11.824	13.139
33700	FS	10.890	9.209	FO	0.000	0.000	FA	0.000	0.000
33700	WO	0.000	0.000	LA	0.000	0.000	MT	0.000	0.000
33700	IL	1.723	1.266	CR	0.000	0.000	HM	0.000	0.000
33700	AP	.239	.216	PY	0.000	0.000	NS	0.000	0.000
33700	KS	0.000	0.000	RU	0.000	0.000			

33700 MAGNESIUM/IRON RATIO 58.791

34900 WEIGHT AND MOLE PERCENTAGES

34900	Q	0.000	0.000	C	0.000	0.000	OR	1.883	1.899
34900	AB	34.154	36.554	AN	16.929	17.078	LC	0.000	0.000
34900	NE	0.000	0.000	KP	0.000	0.000	AC	0.000	0.000
34900	DI	7.118	7.379	HE	7.947	7.191	EN	5.738	6.416
34900	FS	7.349	6.253	FO	5.568	6.663	FA	7.858	6.494
34900	WO	0.000	0.000	LA	0.000	0.000	MT	1.742	1.267
34900	IL	3.375	2.496	CR	0.000	0.000	HM	0.000	0.000
34900	AP	.333	.303	PY	0.000	0.000	NS	0.000	0.000
34900	KS	0.000	0.000	RU	0.000	0.000			

34900 MAGNESIUM/IRON RATIO 50.644

34900 ***** COMPUTE FE3 WITH FE2 *****

34900 WEIGHT AND MOLE PERCENTAGES

34900	Q	0.000	0.000	C	0.000	0.000	OR	1.885	1.899
34900	AB	34.195	36.554	AN	16.950	17.078	LC	0.000	0.000
34900	NE	0.000	0.000	KP	0.000	0.000	AC	0.000	0.000
34900	DI	6.675	6.912	HE	8.474	7.659	EN	4.305	4.807
34900	FS	6.268	5.327	FO	6.731	8.045	FA	10.800	8.914
34900	WO	0.000	0.000	LA	0.000	0.000	MT	0.000	0.000
34900	IL	3.379	2.496	CR	0.000	0.000	HM	0.000	0.000
34900	AP	.333	.303	PY	0.000	0.000	NS	0.000	0.000
34900	KS	0.000	0.000	RU	0.000	0.000			

34900 MAGNESIUM/IRON RATIO 47.437

35600 WEIGHT AND MOLE PERCENTAGES

35600	Q	0.000	0.000	C	0.000	0.000	OR	.251	.246
35600	AB	2.065	2.152	AN	4.862	4.775	LC	0.000	0.000
35600	NE	0.000	0.000	KP	0.000	0.000	AC	0.000	0.000
35600	DI	32.252	32.555	HE	3.932	3.464	EN	26.182	28.502
35600	FS	3.661	3.033	FO	13.323	15.522	FA	2.053	1.652
35600	WO	0.000	0.000	LA	0.000	0.000	MT	10.744	7.607
35600	IL	.645	.464	CR	0.000	0.000	HM	0.000	0.000
35600	AP	.024	.021	PY	0.000	0.000	NS	0.000	0.000
35600	KS	0.000	0.000	RU	0.000	0.000			

35600 MAGNESIUM/IRON RATIO 90.380

35600 ***** COMPUTE FE3 WITH FE2 *****

35600 WEIGHT AND MOLE PERCENTAGES

35600	Q	0.000	0.000	C	0.000	0.000	OR	.253	.246
35600	AB	2.061	2.152	AN	4.898	4.775	LC	0.000	0.000
35600	NE	0.000	0.000	KP	0.000	0.000	AC	0.000	0.000
35600	DI	26.853	26.904	HE	10.424	9.115	EN	11.281	12.169
35600	FS	5.022	4.130	FO	25.834	29.875	FA	12.675	10.122
35600	WO	0.000	0.000	LA	0.000	0.000	MT	0.000	0.000
35600	IL	.650	.464	CR	0.000	0.000	HM	0.000	0.000
35600	AP	.024	.021	PY	0.000	0.000	NS	0.000	0.000
35600	KS	0.000	0.000	RU	0.000	0.000			

35600 MAGNESIUM/IRON RATIO 74.692

36300 WEIGHT AND MOLE PERCENTAGES

36300	Q	0.000	0.000	C	0.000	0.000	OR	.426	.429
36300	AB	29.044	31.050	AN	22.523	22.696	LC	0.000	0.000
36300	NE	0.000	0.000	KP	0.000	0.000	AC	0.000	0.000
36300	DI	15.718	16.277	HE	13.816	12.488	EN	.198	.221
36300	FS	.200	.170	FO	5.998	7.169	FA	6.663	5.500
36300	WO	0.000	0.000	LA	0.000	0.000	MT	3.079	2.236
36300	IL	2.114	1.562	CR	0.000	0.000	HM	0.000	0.000
36300	AP	.215	.195	PY	0.000	0.000	NS	0.000	0.000
36300	KS	0.000	0.000	RU	0.000	0.000			

36300 MAGNESIUM/IRON RATIO 56.587

36300 ***** COMPUTE FE3 WITH FE2 *****

36300 WEIGHT AND MOLE PERCENTAGES

36300	Q	0.000	0.000	C	0.000	0.000	OR	.427	.429
36300	AB	26.715	28.499	AN	22.571	22.696	LC	0.000	0.000
36300	NE	1.295	1.530	KP	0.000	0.000	AC	0.000	0.000
36300	DI	13.802	14.263	HE	16.079	14.503	EN	0.000	0.000
36300	FS	0.000	0.000	FO	6.783	8.091	FA	9.988	8.227
36300	WO	0.000	0.000	LA	0.000	0.000	MT	0.000	0.000
36300	IL	2.119	1.562	CR	0.000	0.000	HM	0.000	0.000
36300	AP	.215	.195	PY	0.000	0.000	NS	0.000	0.000
36300	KS	0.000	0.000	RU	0.000	0.000			

36300 MAGNESIUM/IRON RATIO 49.582

36900 WEIGHT AND MOLE PERCENTAGES

36900	Q	0.000	0.000	C	0.000	0.000	OR	0.000	0.000
36900	AB	2.850	2.998	AN	5.962	5.930	LC	0.000	0.000
36900	NE	0.000	0.000	KP	0.000	0.000	AC	0.000	0.000
36900	DI	54.718	55.748	HE	14.133	12.568	EN	10.680	11.736
36900	FS	3.164	2.645	FO	4.671	5.493	FA	1.525	1.238
36900	WO	0.000	0.000	LA	0.000	0.000	MT	1.376	.963
36900	IL	.872	.634	CR	0.000	0.000	HM	0.000	0.000
36900	AP	.023	.021	PY	0.000	0.000	NS	0.000	0.000
36900	KS	0.000	0.000	RU	0.000	0.000			

36900 MAGNESIUM/IRON RATIO 81.602

36900 ***** COMPUTE FE3 WITH FE2 *****

36900 WEIGHT AND MOLE PERCENTAGES

36900	Q	0.000	0.000	C	0.000	0.000	OR	0.000	0.000
36900	AB	2.853	2.998	AN	5.987	5.930	LC	0.000	0.000
36900	NE	0.000	0.000	KP	0.000	0.000	AC	0.000	0.000
36900	DI	52.958	53.904	HE	16.223	14.412	EN	8.922	9.795
36900	FS	3.134	2.618	FO	6.503	7.641	FA	2.518	2.043
36900	WO	0.000	0.000	LA	0.000	0.000	MT	0.000	0.000
36900	IL	.873	.634	CR	0.000	0.000	HM	0.000	0.000
36900	AP	.023	.021	PY	0.000	0.000	NS	0.000	0.000
36900	KS	0.000	0.000	RU	0.000	0.000			

36900 MAGNESIUM/IRON RATIO 78.903

38510 WEIGHT AND MOLE PERCENTAGES

38510	Q	.396	.357	C	0.000	0.000	OR	.238	.231
38510	AB	66.675	68.827	AN	6.501	6.326	LC	0.000	0.000
38510	NE	0.000	0.000	KP	0.000	0.000	AC	0.000	0.000
38510	DI	11.889	11.888	HE	6.861	5.988	EN	2.217	2.391
38510	FS	1.467	1.204	FO	0.000	0.000	FA	0.000	0.000
38510	WO	0.000	0.000	LA	0.000	0.000	MT	.657	.461
38510	IL	2.392	1.707	CR	0.000	0.000	HM	0.000	0.000
38510	AP	.701	.615	PY	0.000	0.000	NS	0.000	0.000
38510	KS	0.000	0.000	RU	0.000	0.000			

38510 MAGNESIUM/IRON RATIO 66.502

38510 ***** COMPUTE FE3 WITH FE2 *****

38510 WEIGHT AND MOLE PERCENTAGES

38510	Q	0.000	0.000	C	0.000	0.000	OR	.238	.231
38510	AB	66.705	68.827	AN	6.504	6.326	LC	0.000	0.000
38510	NE	0.000	0.000	KP	0.000	0.000	AC	0.000	0.000
38510	DI	11.079	11.073	HE	7.798	6.803	EN	2.357	2.541
38510	FS	1.903	1.561	FO	.167	.193	FA	.149	.118
38510	WO	0.000	0.000	LA	0.000	0.000	MT	0.000	0.000
38510	IL	2.393	1.707	CR	0.000	0.000	HM	0.000	0.000
38510	AP	.701	.615	PY	0.000	0.000	NS	0.000	0.000
38510	KS	0.000	0.000	RU	0.000	0.000			

38510 MAGNESIUM/IRON RATIO 61.943

2426 WEIGHT AND MOLE PERCENTAGES

2426	Q	0.000	0.000	C	0.000	0.000	OR	0.000	0.000
2426	AB	3.349	3.515	AN	6.615	6.544	LC	0.000	0.000
2426	NE	0.000	0.000	KP	0.000	0.000	AC	0.000	0.000
2426	DI	55.593	56.513	HE	12.091	10.728	EN	10.936	11.989
2426	FS	2.728	2.276	FO	4.566	5.358	FA	1.255	1.017
2426	WO	0.000	0.000	LA	0.000	0.000	MT	1.972	1.406

2426	IL	.867	.629	CR	0.000	0.000	HM	0.000	0.000
2426	AP	.023	.021	PY	0.000	0.000	NS	0.000	0.000
2426	KS	0.000	0.000	RU	0.000	0.000			

2426 MAGNESIUM/IRON RATIO 84.045

2413 ****COMPUTE FE3 WITH FE2 ***

2413 WEIGHT AND MOLE PERCENTAGES

2413	Q	0.000	0.000	C	0.000	0.000	OR	.181	.179
2413	AB	6.835	7.183	AN	8.031	7.955	LC	0.000	0.000
2413	NE	0.000	0.000	KP	0.000	0.000	AC	0.000	0.000
2413	DI	44.073	44.865	HE	16.037	14.249	EN	7.666	8.417
2413	FS	3.199	2.673	FO	8.863	10.413	FA	4.076	3.307
2413	WO	0.000	0.000	LA	0.000	0.000	MT	0.000	0.000
2413	IL	1.009	.733	CR	0.000	0.000	HM	0.000	0.000
2413	AP	.023	.021	PY	0.000	0.000	NS	0.000	0.000
2413	KS	0.000	0.000	RU	0.000	0.000			

2413 MAGNESIUM/IRON RATIO 75.895

2413 WEIGHT AND MOLE PERCENTAGES

2413	Q	0.000	0.000	C	0.000	0.000	OR	.181	.179
2413	AB	6.824	7.183	AN	8.019	7.955	LC	0.000	0.000
2413	NE	0.000	0.000	KP	0.000	0.000	AC	0.000	0.000
2413	DI	46.495	47.403	HE	13.161	11.711	EN	10.389	11.423
2413	FS	3.373	2.822	FO	6.124	7.207	FA	2.191	1.780
2413	WO	0.000	0.000	LA	0.000	0.000	MT	2.205	1.577
2413	IL	1.008	.733	CR	0.000	0.000	HM	0.000	0.000
2413	AP	.023	.021	PY	0.000	0.000	NS	0.000	0.000
2413	KS	0.000	0.000	RU	0.000	0.000			

2413 MAGNESIUM/IRON RATIO 80.187

2426 ****COMPUTE FE3 WITH FE2 ***

2426 WEIGHT AND MOLE PERCENTAGES

2426	Q	0.000	0.000	C	0.000	0.000	OR	0.000	0.000
2426	AB	3.354	3.515	AN	6.624	6.544	LC	0.000	0.000
2426	NE	0.000	0.000	KP	0.000	0.000	AC	0.000	0.000
2426	DI	53.023	53.828	HE	15.138	13.413	EN	8.374	9.168
2426	FS	2.742	2.284	FO	7.238	8.481	FA	2.611	2.113
2426	WO	0.000	0.000	LA	0.000	0.000	MT	0.000	0.000
2426	IL	.868	.629	CR	0.000	0.000	HM	0.000	0.000
2426	AP	.023	.021	PY	0.000	0.000	NS	0.000	0.000
2426	KS	0.000	0.000	RU	0.000	0.000			

2426 MAGNESIUM/IRON RATIO 80.051

2433 WEIGHT AND MOLE PERCENTAGES

2433	Q	0.000	0.000	C	0.000	0.000	OR	.182	.182
2433	AB	5.481	5.813	AN	8.871	8.868	LC	0.000	0.000
2433	NE	0.000	0.000	KP	0.000	0.000	AC	0.000	0.000
2433	DI	45.510	46.753	HE	15.485	13.884	EN	9.828	10.888
2433	FS	3.835	3.233	FO	5.069	6.010	FA	2.180	1.785
2433	WO	0.000	0.000	LA	0.000	0.000	MT	2.266	1.633
2433	IL	1.289	.945	CR	0.000	0.000	HM	0.000	0.000
2433	AP	0.000	0.000	PY	0.000	0.000	NS	0.000	0.000
2433	KS	0.000	0.000	RU	0.000	0.000			

2433 MAGNESIUM/IRON RATIO 77.102

2433 ****COMPUTE FE3 WITH FE2 ***

2433 WEIGHT AND MOLE PERCENTAGES

2433	Q	0.000	0.000	C	0.000	0.000	OR	.182	.182

2433	AB	5.490	5.813	AN	8.885	8.868	LC	0.000	0.000
2433	NE	0.000	0.000	KP	0.000	0.000	AC	0.000	0.000
2433	DI	43.019	44.124	HE	18.445	16.513	EN	7.141	7.899
2433	FS	3.511	2.956	FO	7.803	9.238	FA	4.229	3.457
2433	WO	0.000	0.000	LA	0.000	0.000	MT	0.000	0.000
2433	IL	1.291	.945	CR	0.000	0.000	HM	0.000	0.000
2433	AP	0.000	0.000	PY	0.000	0.000	NS	0.000	0.000
2433	KS	0.000	0.000	RU	0.000	0.000			

2433 MAGNESIUM/IRON RATIO 72.767

2435 WEIGHT AND MOLE PERCENTAGES

2435	Q	0.000	0.000	C	0.000	0.000	OR	.602	.601
2435	AB	14.228	15.055	AN	6.223	6.207	LC	0.000	0.000
2435	NE	0.000	0.000	KP	0.000	0.000	AC	0.000	0.000
2435	DI	43.515	44.601	HE	17.863	15.981	EN	4.239	4.686
2435	FS	1.995	1.679	FO	5.836	6.904	FA	3.028	2.474
2435	WO	0.000	0.000	LA	0.000	0.000	MT	.783	.563
2435	IL	1.587	1.160	CR	0.000	0.000	HM	0.000	0.000
2435	AP	.094	.085	PY	0.000	0.000	NS	0.000	0.000
2435	KS	0.000	0.000	RU	0.000	0.000			

2435 MAGNESIUM/IRON RATIO 73.621

2435 ****COMPUTE FE3 WITH FE2 ***

2435 WEIGHT AND MOLE PERCENTAGES

2435	Q	0.000	0.000	C	0.000	0.000	OR	.603	.601
2435	AB	14.236	15.055	AN	6.226	6.207	LC	0.000	0.000
2435	NE	0.000	0.000	KP	0.000	0.000	AC	0.000	0.000
2435	DI	42.564	43.602	HE	18.990	16.980	EN	3.412	3.770
2435	FS	1.746	1.468	FO	6.737	7.966	FA	3.799	3.102
2435	WO	0.000	0.000	LA	0.000	0.000	MT	0.000	0.000
2435	IL	1.588	1.160	CR	0.000	0.000	HM	0.000	0.000
2435	AP	.094	.085	PY	0.000	0.000	NS	0.000	0.000

2435	KS	0.000	0.000	RU	0.000	0.000			
2435	MAGNESIUM/IRON RATIO				71.972				
2508	WEIGHT AND MOLE PERCENTAGES								
2508	Q	0.000	0.000	C	0.000	0.000	OR	3.192	3.276
2508	AB	20.108	21.902	AN	26.252	26.952	LC	0.000	0.000
2508	NE	0.000	0.000	KP	0.000	0.000	AC	0.000	0.000
2508	DI	5.208	5.495	HE	5.554	5.114	EN	7.930	9.023
2508	FS	9.699	8.399	FO	5.610	6.832	FA	7.562	6.359
2508	WO	0.000	0.000	LA	0.000	0.000	MT	5.718	4.232
2508	IL	2.996	2.255	CR	0.000	0.000	HM	0.000	0.000
2508	AP	.168	.156	PY	0.000	0.000	NS	0.000	0.000
2508	KS	0.000	0.000	RU	0.000	0.000			
2508	MAGNESIUM/IRON RATIO				51.791				
2508	****COMPUTE FE3 WITH FE2						***		
2508	WEIGHT AND MOLE PERCENTAGES								
2508	Q	0.000	0.000	C	0.000	0.000	OR	3.204	3.276
2508	AB	20.188	21.902	AN	26.356	26.952	LC	0.000	0.000
2508	NE	0.000	0.000	KP	0.000	0.000	AC	0.000	0.000
2508	DI	4.321	4.541	HE	6.615	6.068	EN	3.383	3.834
2508	FS	5.940	5.123	FO	9.135	11.081	FA	17.676	14.807
2508	WO	0.000	0.000	LA	0.000	0.000	MT	0.000	0.000
2508	IL	3.007	2.255	CR	0.000	0.000	HM	0.000	0.000
2508	AP	.169	.156	PY	0.000	0.000	NS	0.000	0.000
2508	KS	0.000	0.000	RU	0.000	0.000			
2508	MAGNESIUM/IRON RATIO				42.804				
2512	WEIGHT AND MOLE PERCENTAGES								
2512	Q	4.427	4.202	C	0.000	0.000	OR	1.381	1.415
2512	AB	44.153	48.012	AN	11.903	12.200	LC	0.000	0.000
2512	NE	0.000	0.000	KP	0.000	0.000	AC	0.000	0.000
2512	DI	3.525	3.713	HE	10.604	9.749	EN	3.422	3.887

2512	FS	11.805	10.206	FO	0.000	0.000	FA	0.000	0.000
2512	WO	0.000	0.000	LA	0.000	0.000	MT	5.446	4.024
2512	IL	2.834	2.130	CR	0.000	0.000	HM	0.000	0.000
2512	AP	.494	.457	PY	0.000	0.000	NS	0.000	0.000
2512	KS	0.000	0.000	RU	0.000	0.000			

2512 MAGNESIUM/IRON RATIO 27.583

2512 ****COMPUTE FE3 WITH FE2 ***

2512 WEIGHT AND MOLE PERCENTAGES

2512	Q	.188	.177	C	0.000	0.000	OR	1.386	1.415
2512	AB	44.319	48.012	AN	11.948	12.200	LC	0.000	0.000
2512	NE	0.000	0.000	KP	0.000	0.000	AC	0.000	0.000
2512	DI	2.552	2.678	HE	11.774	10.784	EN	3.892	4.405
2512	FS	20.595	17.738	FO	0.000	0.000	FA	0.000	0.000
2512	WO	0.000	0.000	LA	0.000	0.000	MT	0.000	0.000
2512	IL	2.845	2.130	CR	0.000	0.000	HM	0.000	0.000
2512	AP	.496	.457	PY	0.000	0.000	NS	0.000	0.000
2512	KS	0.000	0.000	RU	0.000	0.000			

2512 MAGNESIUM/IRON RATIO 19.894

2515 WEIGHT AND MOLE PERCENTAGES

2515	Q	0.000	0.000	C	0.000	0.000	OR	.907	.919
2515	AB	37.047	39.817	AN	17.581	17.810	LC	0.000	0.000
2515	NE	0.000	0.000	KP	0.000	0.000	AC	0.000	0.000
2515	DI	9.124	9.499	HE	10.448	9.493	EN	4.340	4.873
2515	FS	5.700	4.870	FO	2.921	3.509	FA	4.227	3.508
2515	WO	0.000	0.000	LA	0.000	0.000	MT	4.746	3.466
2515	IL	2.739	2.035	CR	0.000	0.000	HM	0.000	0.000
2515	AP	.213	.195	PY	0.000	0.000	NS	0.000	0.000
2515	KS	0.000	0.000	RU	0.000	0.000			

2515 MAGNESIUM/IRON RATIO 50.013

2515 ****COMPUTE FE3 WITH FE2 ***

2515 WEIGHT AND MOLE PERCENTAGES

2515	Q	0.000	0.000	C	0.000	0.000	OR	.910	.919
2515	AB	37.169	39.817	AN	17.639	17.810	LC	0.000	0.000
2515	NE	0.000	0.000	KP	0.000	0.000	AC	0.000	0.000
2515	DI	7.368	7.645	HE	12.529	11.347	EN	1.011	1.131
2515	FS	1.972	1.679	FO	5.854	7.011	FA	12.582	10.406
2515	WO	0.000	0.000	LA	0.000	0.000	MT	0.000	0.000
2515	IL	2.748	2.035	CR	0.000	0.000	HM	0.000	0.000
2515	AP	.214	.195	PY	0.000	0.000	NS	0.000	0.000
2515	KS	0.000	0.000	RU	0.000	0.000			

2515 MAGNESIUM/IRON RATIO 40.254

2517 WEIGHT AND MOLE PERCENTAGES

2517	Q	0.000	0.000	C	0.000	0.000	OR	2.285	2.319
2517	AB	29.338	31.596	AN	20.344	20.651	LC	0.000	0.000
2517	NE	0.000	0.000	KP	0.000	0.000	AC	0.000	0.000
2517	DI	5.678	5.924	HE	6.103	5.557	EN	10.420	11.723
2517	FS	12.845	10.998	FO	2.700	3.251	FA	3.668	3.050
2517	WO	0.000	0.000	LA	0.000	0.000	MT	3.331	2.438
2517	IL	3.015	2.244	CR	0.000	0.000	HM	0.000	0.000
2517	AP	.266	.244	PY	0.000	0.000	NS	0.000	0.000
2517	KS	0.000	0.000	RU	0.000	0.000			

2517 MAGNESIUM/IRON RATIO 51.596

2517 ****COMPUTE FE3 WITH FE2 ***

2517 WEIGHT AND MOLE PERCENTAGES

2517	Q	0.000	0.000	C	0.000	0.000	OR	2.291	2.319
2517	AB	29.406	31.596	AN	20.391	20.651	LC	0.000	0.000
2517	NE	0.000	0.000	KP	0.000	0.000	AC	0.000	0.000
2517	DI	5.027	5.232	HE	6.879	6.249	EN	7.244	8.132
2517	FS	11.371	9.713	FO	5.164	6.204	FA	8.933	7.411
2517	WO	0.000	0.000	LA	0.000	0.000	MT	0.000	0.000

2517	IL	3.022	2.244	CR	0.000	0.000	HM	0.000	0.000
2517	AP	.267	.244	PY	0.000	0.000	NS	0.000	0.000
2517	KS	0.000	0.000	RU	0.000	0.000			

2517 MAGNESIUM/IRON RATIO 45.568

Q	quartz	C	calcite	OR	orthoclase
AB	albite	AN	anorthite	LC	leucite
NE	nepheline	KP	kaliophylite	AC	acmite
DI	diopside	HE	hypersthene	EN	enstatite
FS	ferrosilite	FO	forsterite	FA	fayalite
WO	wollastonite	LA	larnite	MT	magnetite
IL	ilmenite	CR	chromite	HM	hematite
AP	apatite	PY	pyrite	NS	nosean
KS	kalsilite	RU	rutile		

APPENDIX 7

Rock Type Classification

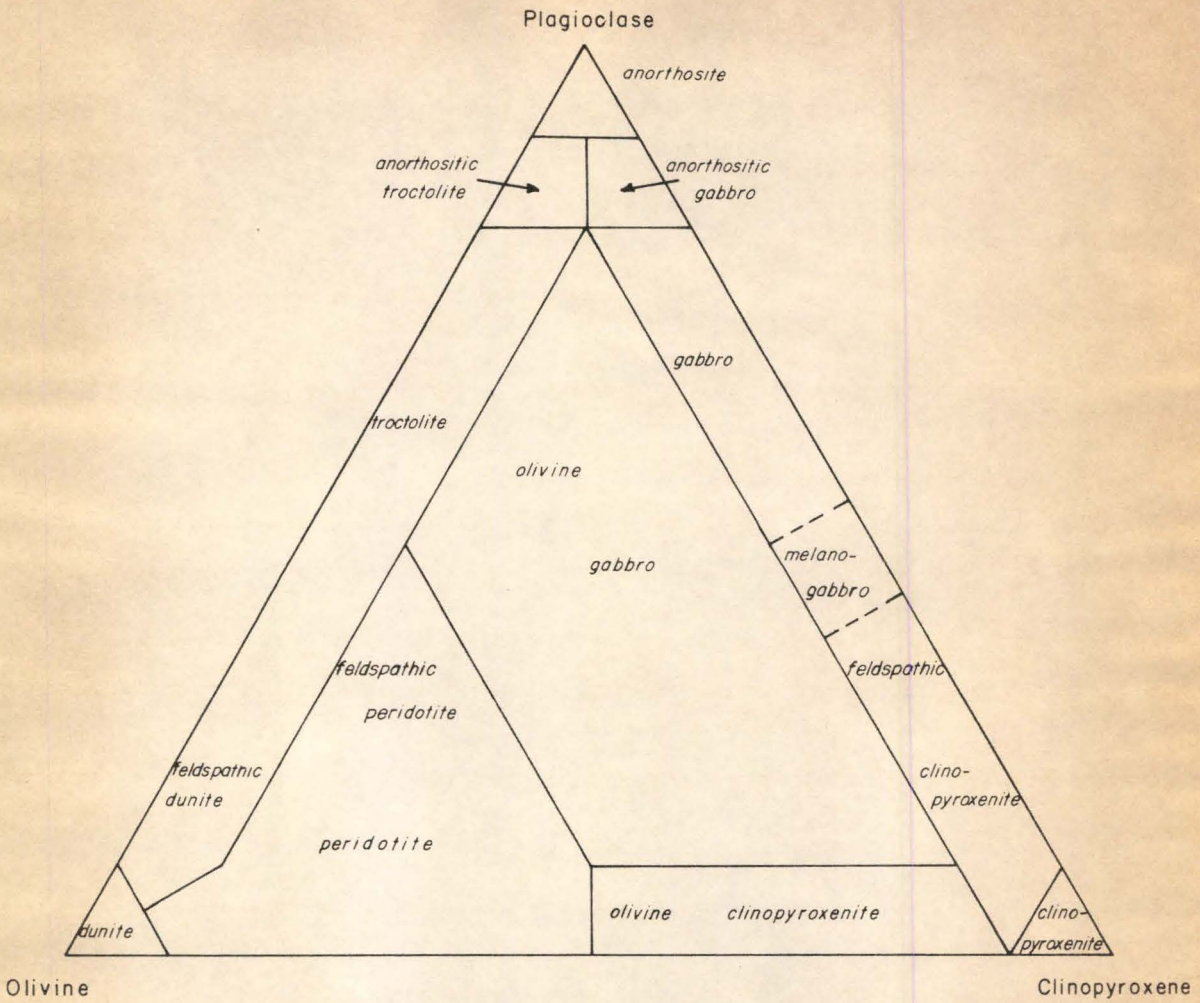

SCHEMATIC CROSS SECTION
OF MUNRO LAKE SILL

scale approx. 1"=1000'

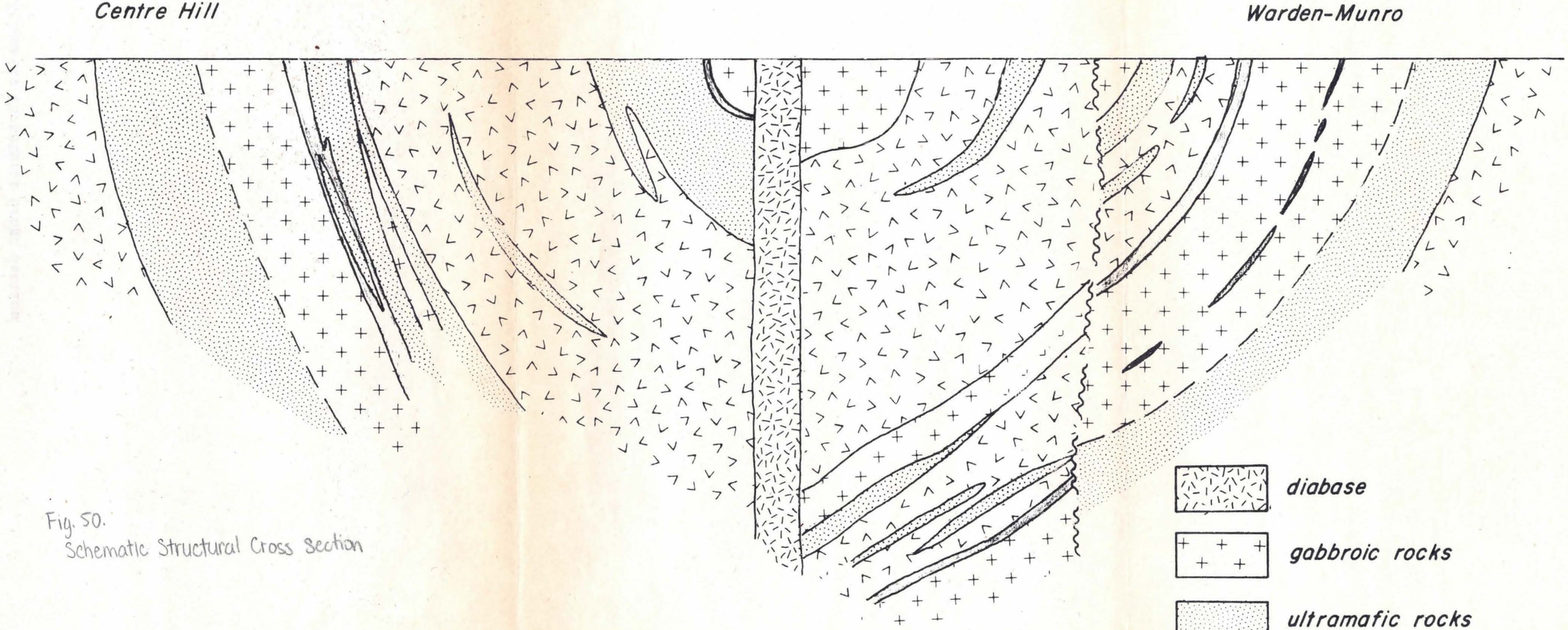

Fig. 50.
Schematic Structural Cross Section

LEGEND

PRECAMBRIAN

KEWEENAWAN

Kq — quartz diabase

MATACHEWAN

Mq — quartz diabase, diabase

ALGOMAN

Aq — quartz diorite, granite

MAFIC and ULTRAMAFIC ROCKS

du,pd — dunite, peridotite

cpx — clinopyroxenite

gb — gabbro

VOLCANIC ROCKS

Vb — basalt, andesite

Va — rhyolitic rocks

SEDIMENTARY ROCKS

Sc — chert

Sg — greywacke, argillite

SYMBOLS

- outcrop area
- contact: defined, assumed
- fault
- high ground
- glacial striae
- swamp
- anticlinal axis
- synclinal axis
- 65 / 70 — attitude of bedding
- attitude of schistosity
- attitude of flow
- attitude of pillowed lava
- trail
- tractor road
- highway
- drill hole projection

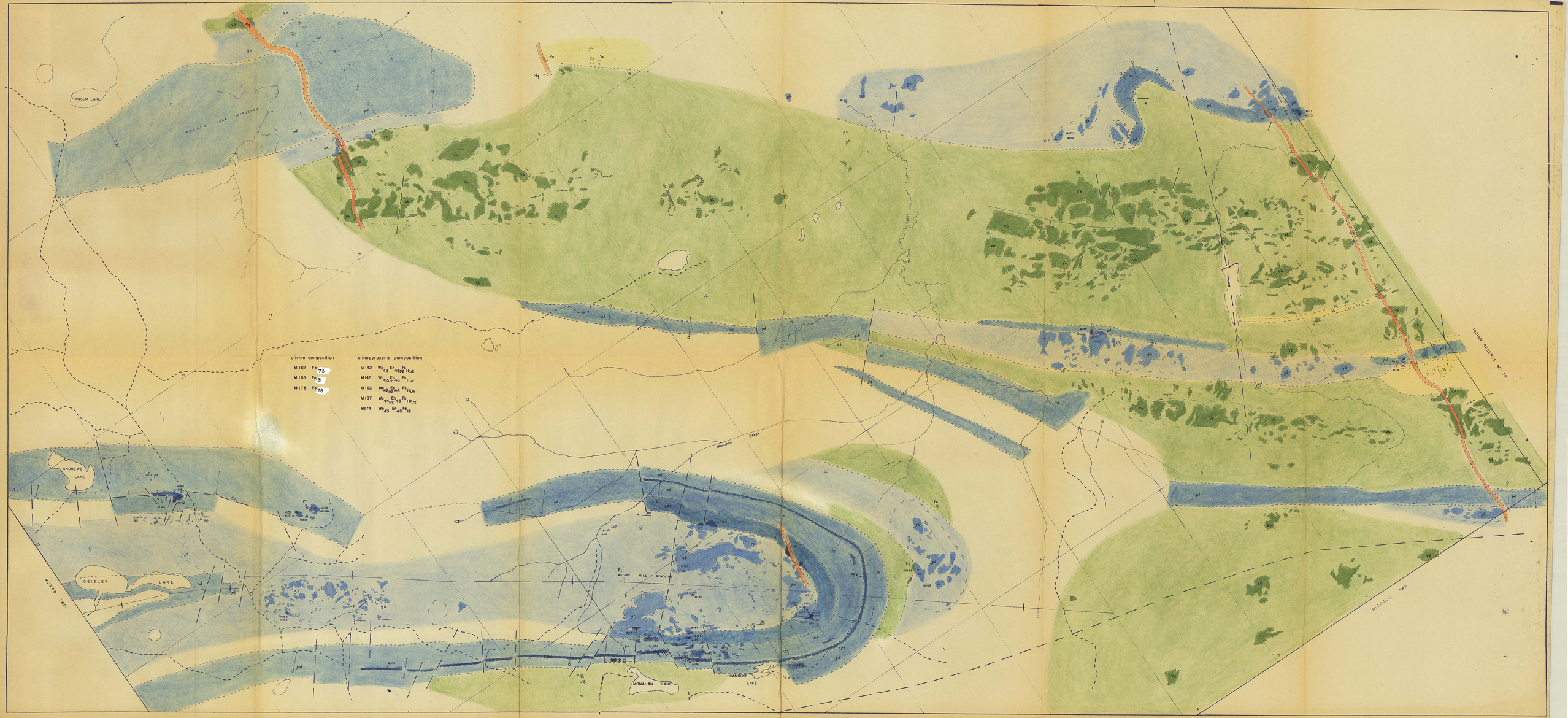
RANSOM LAKE
RANSOM LAKE INTRUSION
ANDREWS LAKE
GEISLER LAKE
MUNRO TWP.
MONAHAN LAKE
CAMROSE LAKE
MICHAUD TWP.
INDIAN RESERVE NO 70
Monahan Creek
Michaud Creek
olivine composition
M 162 Fo 73
M 165 Fo 81
M 175 Fo 78
clinopyroxene composition
M 142 Wo43 En40½ Fs11½
M 143 Wo42½ En46 Fs11½
M 162 Wo42½ En46 Fs11½
M 167 Wo44½ En45 Fs10½
M 174 Wo43 En45 Fs12

WARDEN- MUNRO SECTION

Hedmon Mine

WARDEN TWP.

MUNRO TWP.

WARDEN HILL

Centre Hill Mine

CENTRE HILL SECTION

CLASSICAL OUTCROP ULTRAMAFIC FLOWS WITH BRECCIA TOPS & QUENCH TEXTURE

CAMP LAKE

INDIAN RESERVE NO. 70

RAND TWP

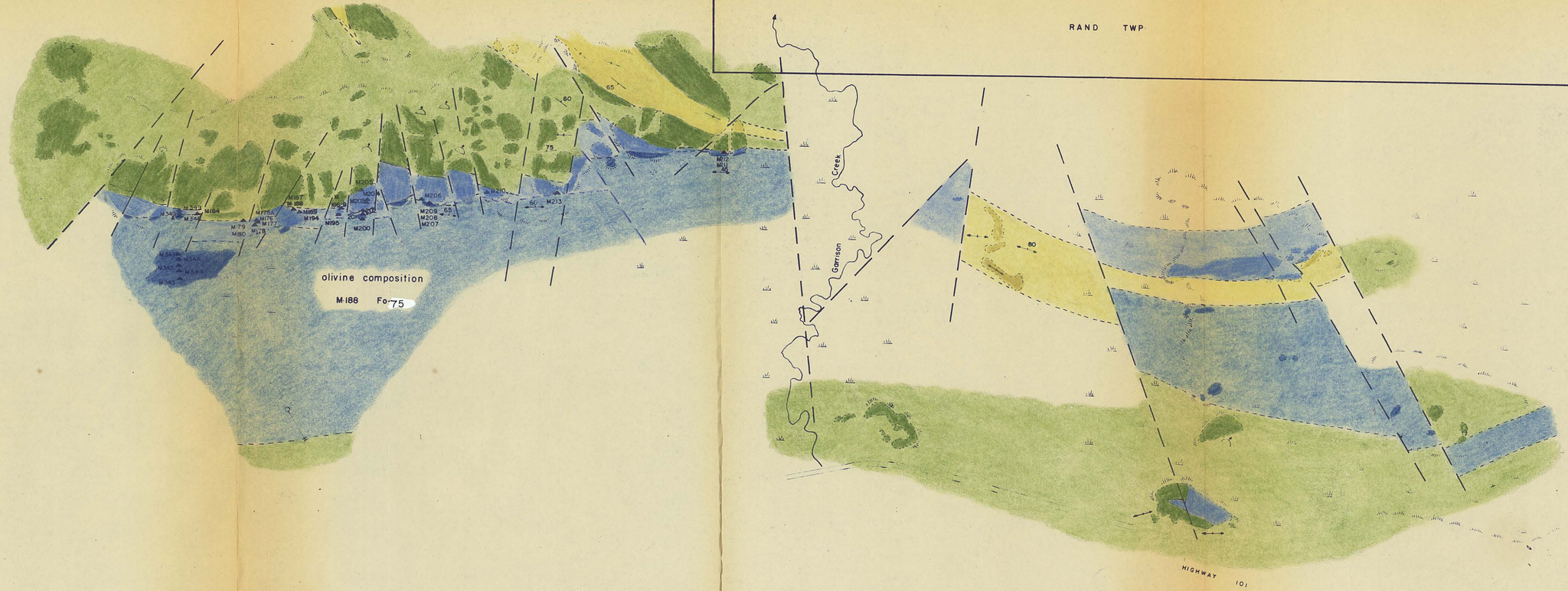

olivine composition

M233 Fo_{82}

M234 Fo_{84}

clinopyroxene composition

M235 $Wo_{44}\ En_{46}\ Fs_{10}$

M236 $Wo_{44}\ En_{48}\ Fs_{8}$